

**Neuronal migration and differentiation in the
developing locust enteric nervous system**

Von der naturwissenschaftlichen Fakultät
der Gottfried Wilhelm Leibniz Universität Hannover
zur Erlangung des Grades
Doktorin der Naturwissenschaften
Dr. rer. nat.
genehmigte Dissertation

von

Dipl.-Biol. Sabine Knipp

geboren am 14.11.1972 in Siegen

Referent:	Prof. Dr. Gerd Bicker
Korreferent:	Prof. Dr. Marcus Pröpsting
Tag der Promotion:	07. August 2009

Für Papa.

Schlagwörter

Neuronale Entwicklung; Zellmigration; gasförmige Modulatoren

Key words

Neuronal development; cell migration; gaseous modulators

Contents

Schlagwörter/Key words.....	ii
Contents.....	iii
Zusammenfassung.....	1
Abstract.....	2
1. Introduction.....	3
1.1 Structure and development of the locust enteric nervous system.....	4
1.2 The insect ENS as a model system for neuronal migration.....	8
1.3 Thesis outline.....	10
2. Publications.....	12
2.1 Contributions to publications.....	12
2.2 Regulation of enteric neuron migration by the gaseous messenger molecules CO and NO.....	13
2.3 Embryonic Differentiation of Serotonin-Containing Neurons in the Enteric Nervous System of the Locust (<i>Locusta migratoria</i>).....	39
2.4 A developmental study of enteric neuron migration in the grasshopper using immunological probes.....	68
4. Discussion.....	100
4.1 Localization of biosynthetic enzymes releasing gaseous modulators.....	100
4.2 Regulation and guidance of enteric neuron migration.....	102
4.3 Conclusions and Outlook.....	104
5. References.....	106
Abbreviations.....	121
Appendix.....	123
Acknowledgement.....	132
Lebenslauf.....	133
Eidesstattliche Erklärung.....	135

Zusammenfassung

Meine Forschung befasste sich mit der neuronalen Migration im enterischen Nervensystem (ENS) der Heuschrecke. Das Heuschrecken ENS besteht aus vier Ganglien auf dem Vorderdarm und zwei Nervenplexus, die Vorder- und Mitteldarm innervieren. Die enterischen Neurone werden in neurogenen Zonen des Vorderdarms geboren und migrieren erhebliche Strecken bis zum Aufbau der enterischen Ganglien und Nervengeflechte. Neurone wandern von den Ingluvial Ganglien auf vier definierten Migrationsrouten über den Mitteldarm und formen den Mitteldarmplexus. Diese Migration hängt kritisch von der NO/sGC/cGMP Signalkaskade ab. Ich konnte zeigen, daß embryonale Darmzellen NO synthetisierende Enzyme beinhalten und ein diffusibles NO-Signal freisetzen können. Außerdem konnte ich Hämoxygenase (HO), ein Enzym welches den gasförmigen Botenstoff Kohlenmonoxid (CO) freisetzt, in migrierenden enterischen Neuronen nachweisen. Manipulation der HO Aktivität und Gabe von exogenem CO, läßt auf eine Modulation der NO/cGMP abhängigen neuronalen Migration durch Kohlenmonoxid schließen.

Die anatomische Entwicklung eines der zentralen Neurotransmitter im ENS der Heuschrecke, Serotonin, ermöglichte weitere Einsichten in die Differenzierung und die neurochemischen Eigenschaften des sich entwickelnden ENS. Untersuchungen über das Auswachsen von serotonergen Neuriten auf dem Mitteldarm nach Inhibierung der NOS zeigten eine Überlagerung mit dem NO/cGMP Signalweg. Weitere Untersuchungen der frühen Entwicklung von NO sensitiver sGC deckte eine Doppelfunktion der NO bedingten cGMP Synthese auf. Während migrierende enterische Neurone bereits während der beginnenden Plexusausbildung auf Vorder- und Mitteldarm eine deutliche cGMP IR aufweisen, wird die sGC Aktivität in den enterischen Ganglien erst nach der Ganglienbildung sichtbar. Diese cGMP Färbung bleibt bis zum Larvenstadium erhalten, was eine neuromodulatorische Rolle für den NO/cGMP Signalweg nahe legt.

Das zelladhäsions Molekül Fasciclin I schließlich, ermöglicht eher die Faszikulierung und Wegfindung der folgenden enterischen Mitteldarmneurone, als daß es die führenden Neurone leitet. Zeitrafferaufnahmen von migrierenden Neuronen zeigten, daß möglicherweise die Mitteldarmmuskulatur Wegfindungsfaktoren enthält.

Abstract

I have used the embryonic enteric nervous system (ENS) of grasshoppers as a model system to study neuronal migration. The locust ENS consists of four ganglia located on the foregut and two nerve plexus innervating fore- and midgut. Enteric neurons are born in neurogenic zones on the foregut and migrate substantial distances to build up the enteric ganglia and nerve plexus. The midgut plexus in particular is established from neurons of the ingluvial ganglia, that travel in a mode of chain migration on four defined pathways. This migration depends critically on the NO/sGC/cGMP signalling pathway. I was able to provide evidences, that embryonic gut cells contain NO synthesising enzymes and release NO as extra-cellular diffusing signal. Moreover, I found that the biosynthetic enzyme heme oxygenase (HO), that releases the gaseous messenger carbon monoxide, is present in migrating enteric neurons. Using bioactive compounds to manipulate HO activity, and application of exogenous CO in whole embryo culture, suggest CO as a modulator of NO/cGMP driven enteric neuron migration.

The anatomical development of serotonin, one of the major neurotransmitters of the ENS, provided insights into differentiation and neurochemical properties of the developing ENS. Analysis of serotonergic neurite outgrowth on the midgut after inhibition of NOS suggests a crosstalk of the NO/cGMP signalling pathway to developmental mechanisms that are primary not responsive to NO. Moreover, by analysing the early development of NO sensitive sGC on the embryonic gut, I was able to show a possible bifunctionality for NO dependent cGMP synthesis. While migrating enteric neurons of the future nerve plexus of fore- and midgut start expressing cGMP-IR at the onset of migration, sGC activity becomes visible in the enteric ganglia only after ganglion aggregation is finished. The cGMP labelling is still present in ganglionic neurons of the larval grasshopper, suggesting a neuromodulatory function of the NO/cGMP pathway in these neurons.

Finally, the cell adhesion molecule Fasciclin I was found to enable fasciculation and guidance of following enteric midgut neurons, rather than guiding leading enteric neurons during posterior migration and branching. Time lapse videos of migrating enteric neurons revealed, that putative guidance cues may be found on the midgut musculature.

1. Introduction

Studying developmental neurobiology is to study change. Cell proliferation and morphogenetic cell movements transform a simple epithelium into a functional nervous system (Lichtman and Fraser, 2001). Neuronal cell migration is a basic feature of nervous systems development, as neurons are frequently born in certain proliferative zones apart from their ultimate target areas. For instance, precursor cells of the cerebral cortex migrate along the surface of radial glia fibres from the ventricular zone to the superficial region of the cortical plate (Hatten, 1999). Precursor cells of interneurons migrate from ganglionic eminences to the cortex via tangential migratory routes (Golden et al., 1997; Kriegstein and Noctor, 2004; Zheng and Poo, 2007). Neural crest cells migrate from the dorsal neural tube along specific routes to form sensory, autonomic, and enteric neurons in the peripheral nervous system (Song and Poo, 2001; Young et al., 2004; Burns, 2005; Anderson et al., 2006). Some neuronal precursors use a somewhat special mode of migration. Premature olfactory interneurons from the subventricular zone, travel along the rostral migratory stream towards the olfactory bulb one over the other in a process named "chain migration" (Lois et al., 1996; Wichterle et al., 1997). These examples show, that directed cell migration is essential for establishing the highly ordered cellular organisation in nervous systems (Lauffenburger and Horwitz, 1996; Hatten, 1999; Song and Poo, 2001; Marin et al., 2006). Evidences have emerged that extracellular (chemotactic) guidance cues such as Netrins, Semaphorins, Slits, Ephrins, and also certain morphogens and neurotrophic factors, do influence navigatory decisions made by an elongating axon as well as by an entire moving neuron (Tessier-Lavigne and Goodman, 1996; Wu et al., 1999; Song and Poo, 2001; Dickson, 2002; Park et al., 2002; Dormann and Weijer, 2003; Tamagnone and Comoglio, 2004; Mortimer et al., 2008).

This thesis addresses the development of a rather simple nervous system, the grasshopper enteric nervous system (ENS). Due to its good accessibility and manageable number of neurons it is a useful model to study neuronal physiology and development. To enable a better understanding of the developing enteric nervous system, I have also addressed questions regarding the differentiation of the locust gut and its adjacent ENS, e.g. its neurochemical properties. Therefore I carried out

pharmacological experiments using whole embryo *in vivo* cultures, live-imaging experiments, and used immunological and histochemical methods to analyse the components of the developing enteric nervous system.

1.1 Structure and development of the locust enteric nervous system

As in vertebrates, the insect gut consists of foregut, midgut, and hindgut divisions with corresponding specializations in their innervation. Caeca are localized at the midgut-foregut boundary and numerous malpighian tubules terminate at the midgut-hindgut boundary. The locust enteric nervous system (ENS) consists of four interconnected ganglia located on the foregut, the frontal- and hypocerebral ganglion and the paired ingluvial ganglia, and two nerve plexus innervating the foregut- and midgut musculature (Fig. 1.1). The ENS innervates the gut musculature, provides secretory and sensory neurons to control for instance gut motility, food uptake and digestion, and moulting behaviour. The foregut ganglion is connected bidirectional via the tritocerebrum to the insect central nervous system (CNS), while the hypocerebral ganglion is associated with the retrocerebral complex, thus the endocrine system. The hindgut and posterior midgut is primarily innervated by the proctodeal and rectal nerves originating from the terminal ganglion of the ventral nerve cord (Ganfornina et al., 1996; Hartenstein, 1997; Copenhaver, 2007; Bräunig, 2008).

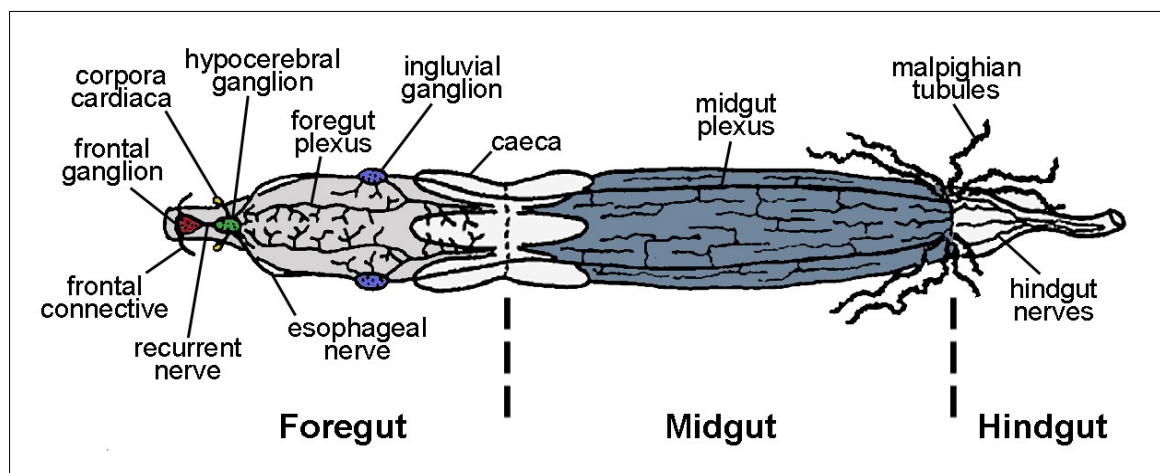


Figure 1.1: Dorsal view of a late embryonic grasshopper gut and ENS.

Semi-schematic overview of the premature alimentary canal of *Schistocerca americana* (image modified after Ganfornina et al., 1996).

Besides the term “enteric nervous system” for the arthropod gut nervous system, one can also find “stomatogastric nervous system” (SNS) in the literature (e.g. Hartenstein, 1997). But this term is often exclusively referred to the nerve ganglia on the rostral part of the alimentary canal, especially in neurophysiological studies in arthropods (e.g. Scholz, 2001; Ayali, 2009). Thus, to avoid confusions I will further on use the term enteric nervous system, that is also used for the analogous nervous system of the vertebrate gastrointestinal tract.

The development of the insect alimentary canal and adjacent enteric nervous system has been well studied on cellular and molecular levels in several insect orders (Ganforina et al., 1996; Hartenstein, 1997; Copenhaver, 2007). Formation of the locust gut starts at around 20% of embryonic development (% E) with the invagination of the stomodeum near the cephalic end of the embryo (Figure 1.2A). Invagination of the posterior proctodeum, the future hindgut, occurs slightly later at 25% E (Bentley et al., 1979). These invaginations comprise cell layers of ectodermal and mesodermal origin, that will give rise to the foregut and hindgut epithelium and musculature, respectively (Ganforina et al., 1996). Like in other insects, the locust enteric nervous system is derived from three proliferative (or neurogenic) zones in a neuroectodermal placode along the dorsal midline of the stomodeum (Z1, Z2, and Z3, Figure 1.2B) (Copenhaver and Taghert, 1990; Copenhaver and Taghert, 1991; Ganforina et al., 1996; Hartenstein et al., 1997). All cells within the stomodeal neurogenic ectoderm give rise to neural cells, similar to the neural crest and sensory placodes in vertebrates (Figure 1.3A) (reviewed in Hartenstein et al., 1997). This is in contrast to the neurogenic ectoderm of the insect brain and ventral nerve cord, where individual neuronal progenitors delaminate as individual neuroblasts from the surrounding epidermal progenitors. The neuroblasts undergo asymmetric cell divisions to produce invariant lineages of neurons (Figure 1.3B) (Goodman and Bate, 1981; Hartenstein, 1997).

After the future enteric neurons have finished their transformation from epithelial cells to individually migratory cells, most enteric neuron precursors subsequently migrate away from the neurogenic zones, while some cells dorsal to the neurogenic zones still undergo symmetrical cell divisions (Ganforina et al., 1996; Copenhaver, 2007). The patterning of foregut ganglia, foregut- and midgut plexus

results from directed cell migration of the future enteric neurons that is described in detail for the locust *Schistocerca americana* (Ganfornina et al., 1996) and can be adopted for *Locusta migratoria*. Neuronal migration on the locust stomodeum can be divided into three main phases (summarised in upper panel of figure 1B, chapter 2.4), a first anterior directed and then two lateral directed, that give rise to the nerve fibres and ganglia of the foregut. The formation of the foregut plexus takes place in the second half of embryonic development. At 60% E enteric neurons from the hypocerebral and ingluvial ganglia migrate over the foregut epithelium and the caeca and form the foregut plexus.

The formation of the midgut initiates at around 50% E (Bentley et al., 1979; Ganfornina et al., 1996). The primordium of the midgut is formed by the provisional dorsal closure growing around the yolk. The surrounding mesoderm differentiates into muscle cells, whereas expansions of the ectoderm of the stomodeum and proctodeum generate the midgut epithelium. Formation of the midgut portion of the enteric nervous system starts with the closure of the midgut and posterior foregut at 60% E. Midgut enteric neurons are born in the posterior neurogenic zone Z3 during the second main migratory phase on the foregut. Between 40 and 55% E the future enteric midgut neurons migrate bilaterally and aggregate at the caudal region of the prospective ingluvial ganglia. Just before the closure of the gut, these neurons leave in four groups, one dorsal and one ventral per ingluvial ganglia, across the caeca to the foregut-midgut boundary. Here, the enteric neurons aggregate once more in four groups, before they migrate posteriorly over the midgut epithelium on four distinct pathways. The neurons migrate in a loose chain with a short leading process, leaving behind neurites that keep connected to the ingluvial ganglion, thus building the midgut nerves. After the chain of neurons has reached the caudal end of the midgut, enteric neurons branch of the main pathways, leaving behind their axons as well, thereby establishing the orthogonal midgut plexus.

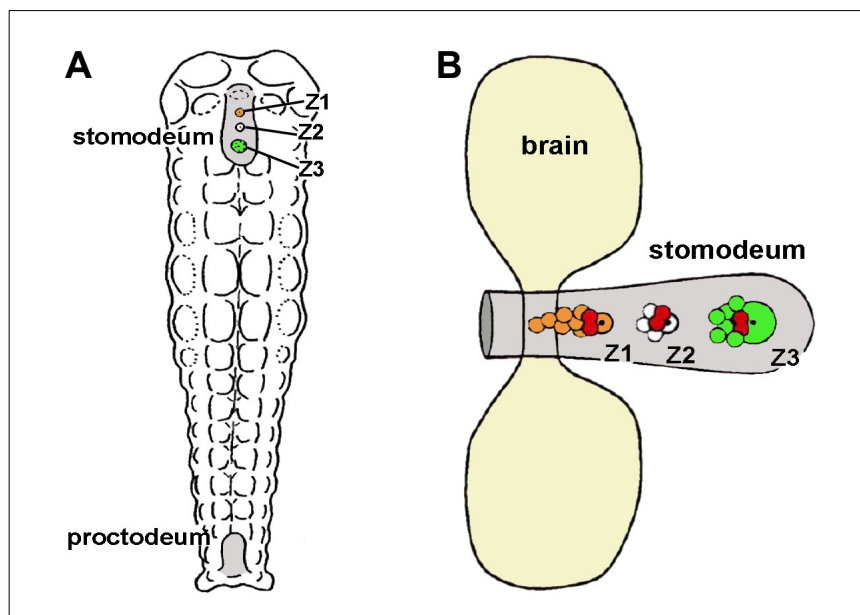


Figure 1.2: Early embryonic development of the locust ENS.

(A) Semi-schematic overview from dorsal of a grasshopper embryo at 35% E. The stomodeum (with the neurogenic zones 1-3) and the proctodeum are shaded light grey. (B) Schematic drawing of the stomodeum at the same age like (A) with the three neurogenic zones. Postmitotic neurons are coloured according to the neurogenic zone of their origin. Proliferating precursor cells are depicted in red. (Both panels are modified after Ganfornina et al., 1996).

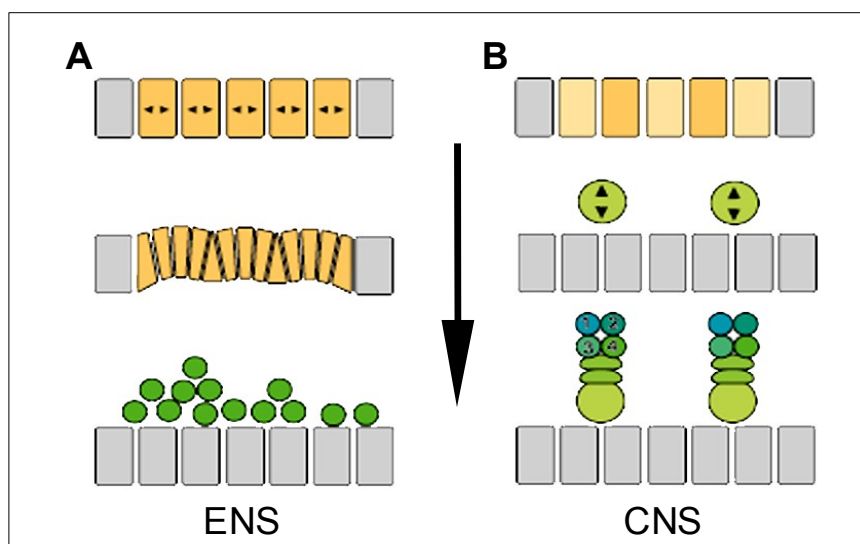


Figure 1.3: Proliferation of precursor cells of the insect ENS and CNS

(A) In the ENS neuronal precursors (green) are the result of several rounds of symmetric cell divisions in a homogeneous neuroectodermal placode (orange). (B) In the CNS individual neuroblasts (green) delaminate from the neuroectoderm (orange). The neuroblasts divide asymmetrical to give rise to distinct neural lineages. Arrow indicates progress of development. (Images modified from Hartenstein, 1997).

1.2 The insect ENS as a model system for neuronal migration

The genetic and cellular bases of neuronal specification, guidance cues for directed cell migration, and differentiation towards neuronal phenotypes during the ENS development in insects has been particularly well investigated in *Drosophila* and *Manduca* as well as in the grasshopper (Gonzales-Gaitan, 1995; Ganfornina et al., 1996; Hartenstein, 1997; Copenhaver, 2007). The grasshopper embryo in particular is quite large with identifiable neurons, robust and accessible to whole-embryo tissue culture. Thus it enables researchers to explore the rules that govern developmental events within the intact organism (Van Vactor and Lorenz, 1999). In contrast to vertebrate nervous systems, the number of neurons is limited in invertebrates – for example each hemisegment of the *Drosophila* ventral nerve cord contains about 300 neurons – and single neurons can be easily followed (Araujo and Tear, 2003).

Invertebrate model organisms have revealed new mechanisms that participate in axonal guidance, such as regulation of receptor availability, the use of many different isoforms, and crosstalk between signalling pathways (reviewed in Araujo and Tear, 2003; Clarac and Pearlstein, 2007). Moreover, many guidance molecules have been proven to be evolutionary well conserved between vertebrate and invertebrate groups. For instance, the UNC-6 molecule, which was first identified in *C. elegans* and was subsequently found to be conserved from worm to man (where it is named netrin) (Tessier-Lavigne and Goodman, 1996; Araujo and Tear, 2003). During the last decades, homologous of many of the genes involved in early neurogenesis in invertebrates have been identified in vertebrates, e.g. the proneural genes, neurogenic genes and Hox genes (Brooke et al., 1998; Arendt and Nübler-Jung, 1999; Chitnis, 1999; Araujo and Tear, 2003). However, it has often been quite difficult to draw parallels between vertebrate and insect neurodevelopment by analysing phenotypes caused through mutations. Early neurogenesis of the CNS appears to be quite different from vertebrates with a homogeneous neuroepithelium, to invertebrate groups with discrete stem cells that produce determined cell lineages (reviewed in Hartenstein, 1997; Arendt and Nübler-Jung, 1999). In contrast to the CNS, precursors forming the insect enteric nervous system present many parallels to vertebrate neural precursors, in

particular to the neural crest and sensory placodes (see figure 1.3). In vertebrates the vast majority of enteric neurons and glia cells derive from neural crest cells. Emigrated neural crest cells enter the foregut and then migrate caudally within the gut wall to colonize the entire gut. In most regions of the mature gastrointestinal tract, neurons are found in two ganglionated plexus – an outer myenteric plexus between the circular and longitudinal muscle layers, and an inner submucosal plexus at the inner margin of the circular muscle (Young et al., 2004; Burns, 2005; Hao et al., 2008). Comparable to this vertebrate neural crest cell migration, future insect enteric neurons migrate over extensive distances before they reaggregate and differentiate in peripheral ganglia. Thereby, insect enteric neurons show a considerable variability in their pattern of migration and projection, indicating that extrinsic factors may play an important role during the specification of the ENS (Hartenstein et al., 1994; Ganfornina et al., 1996; Copenhaver et al., 1996; Wildemann et al., 1997; Haase and Bicker, 2003; Coate et al., 2008). In vivo studies have begun to decipher the mechanisms for guidance and regulation of enteric neuron migration, as well in insects as in vertebrates (Copenhaver et al., 1996; Wright et al., 1999; Dormann and Weijer, 2003; Haase and Bicker, 2003; Burns, 2005; Anderson et al., 2006; Coate et al., 2007). Although the components of the insect ENS should not be considered directly homologous to vertebrate structures, the general organisation and functions of the ENS in both phyla are clearly analogous (Copenhaver, 2007). However, the insect ENS lies superficially on the gut musculature and its component cells can be individually imaged and manipulated within cultured embryos (Wright et al., 1998; Haase and Bicker, 2003; Copenhaver, 2007; see also chapter 2.2 and 2.4). Thus, concepts developed by studying the impact of neurogenesis, migration, and differentiation in the relatively simple insect enteric nervous systems may provide insights into similar developmental processes in more complex (vertebrate) systems (Hartenstein, 1997; Bicker, 2005; Copenhaver, 2007).

1.3 Thesis outline

The embryonic enteric nervous system of grasshoppers was used as a model system to study neuronal migration. I applied whole embryo in vivo culturing for pharmacological manipulation of enteric neuron migration, imaging of cell migration, protein-biochemical, immunocytochemical, and histochemical methods. The thesis is structured as a cumulative dissertation, with the publications sorted in respect to their logical structure rather than following their chronological publication.

The first publication (chapter 2.2) is based on former studies done in our lab on nitric oxide/cyclic GMP dependent enteric neuron migration (Haase and Bicker, 2003). It was shown, that locust enteric neuron migration depends critically on the presence of the gaseous neuromodulator nitric oxide (NO) and its main downstream target, the soluble guanylate cyclase (sGC). Enteric neuron migration is impaired if either the action of NO synthesising enzyme NOS or sGC is inhibited. The same effect of a diminished migration is seen if a downstream target cyclic GMP (cGMP), the protein kinase G (PKG) is inhibited. On the other hand, the negative effects resulting from enzyme inhibitions could be rescued by adding for instance membrane permeable cGMP compounds. Now, I was able to prove, that embryonic gut cells contain NO synthesising enzymes and release NO as extracellular diffusing signal. Moreover, I found that another gaseous molecule, namely carbon monoxide, is not only released from the enteric neurons themselves, but that it regulates the NO/cGMP driven migration. Pharmacological manipulation of carbon monoxide (CO) releasing heme oxygenase enzymes (HO) revealed a negative regulatory effect of CO on enteric neuron migration. Thus, I was able to show for the first time a developmental function of the messenger molecule carbon monoxide.

For a better understanding of the development of the locust ENS, I also studied the differentiation and neurochemical properties of the developing gut. This resulted in the second publication (chapter 2.3) that was developed in close cooperation with Dr. Michael Stern. In this paper we describe the anatomical development of one of the major neurotransmitters of the ENS, serotonin, throughout the embryonic and freshly hatched locust. Serotonergic neurons are

generated in the anterior neurogenic zones (Z1 and Z2) of the foregut. They migrate rostrally to contribute first to the frontal ganglion, and later on also to the other foregut ganglia. Enteric neurons on the midgut do not gain a serotonergic phenotype, although neurites of both nerve plexus become serotonergic. Pharmacological inhibition of migration of cGMP-immunoreactive midgut neurons, did not result in a moving up of the serotonergic neurites from foregut neurons. This suggests a crosstalk of the NO/cGMP signalling pathway to other developmental mechanisms that are not responsive to nitric oxide.

The last paper (chapter 2.4) deals again with enteric neuron migration, the analysis of possible guidance factors, but also with neuronal differentiation. By analysing the development of nitric oxide sensitive soluble guanylate cyclase on the embryonic gut, I was able to show a possible bifunctionality for NO dependent cGMP synthesis. Pre-mature neurons of both enteric plexus showed high levels of cGMP at the onset of migration, indicating a possible function for NO-/cGMP signalling as well for foregut plexus neuron migration as it was shown for the midgut enteric neurons. However, neurons of the foregut ganglia become cGMP positive only after the aggregation of ganglia and onset of differentiation. Time lapse microscopy displays the migratory behaviour of migrating enteric midgut neurons. The neurons are influenced in their pathfinding decisions by the parallel running longitudinal gut musculature. A cell adhesion molecule, Fasciclin I (Fas-I), may not influence pathfinding of leading enteric neurons, as revealed by its cellular distribution and blocking experiments. However, it may enable fasciculation and guidance of following enteric neurons during posterior migration and branching.

2. Publications

2.1 Contributions to publications

Regulation of enteric neuron migration by the gaseous messenger molecules CO and NO (Chapter 2.2).

Sabine Knipp and Gerd Bicker.

I carried out all the experiments, including immunocytochemical, protein biochemical and additional practical work, documentation and statistical analysis. I also wrote the paper under the supervision and with input from Prof. G. Bicker, who helped to interpret and discuss the results of the work.

Embryonic Differentiation of Serotonin-Containing Neurons in the Enteric Nervous System of the Locust (*Locusta migratoria*) (Chapter 2.3)

Michael Stern, Sabine Knipp and Gerd Bicker. (equal contribution of MS and SK)

Experimental work and preparations on midgut and late foregut development, including in vivo culture experiments and immunocytochemistry, were carried out by me. Michael Stern focused on early foregut development, carried out the serotonin uptake experiments, and prepared semi-schematic and schematic drawings. Results were discussed by all authors and the paper was written by Michael Stern with contributions and comments from all authors.

A developmental study of enteric neuron migration in the grasshopper using immunological probes. (Chapter 2.4)

Sabine Knipp and Gerd Bicker.

Just as for the first listed paper I carried out all the experiments, practical work, documentation and statistical analysis. I also wrote the paper under the supervision and with input from Prof. G. Bicker, who helped to interpret and discuss the results of the work.

2.2 Regulation of enteric neuron migration by the gaseous messenger molecules CO and NO.

Sabine Knipp and Gerd Bicker

Published in: *Development*, **136**: 85-93 (2009).

Summary

The enteric nervous system (ENS) of insects is a useful model to study cell motility. Using small molecule compounds to activate or inactivate biosynthetic enzymes, we demonstrate that the gaseous messenger molecules carbon monoxide (CO) and nitric oxide (NO) regulate neuron migration in the locust ENS. CO is produced by heme oxygenase (HO) enzymes and has the potential to signal via the sGC/cGMP pathway. While migrating on the midgut, the enteric neurons express immunoreactivity for HO. Here we show that inhibition of HO by metalloporphyrins promotes enteric neuron migration in intact locust embryos. Thus the blocking of enzyme activity results in a gain of function. The suppression of migratory behaviour by activation of HO or application of a CO-donor strongly implicates the release of CO as an inhibitory signal for neuron migration *in vivo*. Conversely, inhibition of nitric oxide synthase or application of the extracellular gaseous molecule scavenger hemoglobin reduce cell migration. The cellular distribution of NO and CO biosynthetic enzymes, together with the results of the chemical manipulations in whole embryo culture suggest CO as a modulator of transcellular NO signals during neuronal migration. Thus we provide the first evidence that CO regulates embryonic nervous system development in a rather simple invertebrate model.

Key words

carbon monoxide, nitric oxide, insect nervous system, development, stomatogastric, grasshopper embryo, cyclic GMP

Introduction

The formation of the insect enteric nervous system (ENS) provides a useful model to study the cell biology of neuronal migration. Neuronal precursors emerge from proliferative zones in the foregut epithelium and perform quite extensive cell migrations before they assemble into discrete peripheral ganglia and gastric nerve plexus. The genetic and cellular bases of neuronal specification, guidance cues for directed cell migration, and differentiation towards neuronal phenotypes have been particularly well investigated in the two holometabolous insects *Drosophila* and *Manduca* (Hartenstein, 1997; Copenhaver, 2007). In the hemimetabolous grasshopper *Schistocerca*, the enteric midgut neurons of the grasshopper embryo migrate posteriorly from caudal pockets of the ingluvial ganglia towards the foregut-midgut boundary of the embryo (Ganfornina et al., 1996). Subsequently, they undergo a rapid phase of migration and move in four migratory pathways posteriorly on the midgut surface. At the completion of migration, the enteric neurons invade the space between the four migratory pathways and extend terminal branches on the midgut musculature (Ganfornina et al., 1996). Neuronal motility along the migratory pathways of the grasshopper midgut depends critically on the nitric oxide/cyclic GMP (NO/cGMP) signalling cascade including nitric oxide synthase (NOS) and the target receptor protein soluble guanylyl cyclase (sGC) (Haase and Bicker, 2003).

NO has been reported to be a key signalling molecule during nervous system development (Peunova et al., 2001, Chen et al., 2004; Bicker, 2005; Krumenacker and Murad, 2006; Godfrey et al., 2007). In particular, the downstream acting cyclic nucleotide cGMP is implicated as intracellular mediator of growth cone behaviour both in vertebrate and invertebrate nervous systems (Gibbs and Truman, 1998; Polleux et al., 2000; Seidel and Bicker, 2000; Song and Poo, 2001; Van Wagenen and Rehder, 2001; Schmidt et al., 2002; Demyanenko et al., 2005; Welshhans and Rehder, 2005; Gutierrez-Mecinas et al., 2007; Stern and Bicker, 2008).

In addition to NO, there is also increasing evidence for carbon monoxide (CO) as another gaseous messenger of neural tissues (Boehning and Snyder, 2003). CO is generated by heme oxygenase enzymes (HO) during oxidative degradation of heme to biliverdin-IX and ferrous iron (Tenhunen et al., 1968; Maines, 1997).

Similar to NO, CO is able to activate the cGMP-synthesising enzyme sGC, albeit about 100-fold less effective (Kharitonov et al., 1995; Denninger and Marletta, 1999; Baranano and Snyder, 2001; Koesling et al., 2004). In vertebrate nervous systems, the constitutive isoform HO-2 is the predominant heme oxygenase (Sun et al., 1990; Verma et al., 1993). In the majority of brain regions, HO-2 mRNA appears to be co-localised with that of sGC, while NOS and sGC transcripts show hardly any overlap (Verma et al., 1993). While NO is the major activator of sGC, CO seems to reduce cGMP levels by modulating the effect of NO on sGC (Ingi et al., 1996a). At the mechanistic level, CO has been suggested to mediate long term adaptation in amphibian olfactory receptor neurons (Zufall and Leinders-Zufall, 1997), to serve as a neurotransmitter in nonadrenergic/noncholinergic (NANC)-dependent smooth muscle relaxation (Boehning and Snyder, 2003), and to increase field potential oscillations in an invertebrate olfactory system (Gelperin et al., 2000). Exogenous CO application or administration of hemin influences human neutrophil migration and platelet aggregation via cGMP (Brüne and Ullrich, 1987; VanUffelen et al., 1996; Andersson et al., 2002; Freitas et al., 2006). In the vertebrate enteric nervous system, NOS and HO-2 are either co-expressed in a subset of myenteric neurons, or localised in separate, but nearby positioned cells. NO and CO may function here as co-neurotransmitters, with CO modulating the NO-signalling pathway (Maines, 1997; Xue et al., 2000; Miller et al., 2001; Colpaert et al., 2002; Boehning and Snyder, 2003).

There are comparatively few studies about the distribution of HO enzymes and the functions of CO as messenger molecule in invertebrate nervous systems. Immunoreactivity to HO-2 has been described in the olfactory system of a mollusc (Gelperin et al., 2000) and the stomatogastric system of crayfish (Christie et al., 2003). A HO gene is expressed in the honeybee brain (Watanabe et al., 2007) and the catalytic properties of a recombinant *Drosophila* HO protein have been analysed (Zhang et al., 2004). Unlike for NO signalling in arthropods, which could be linked to discrete developmental processes such as cell proliferation (Kuzin et al., 1996; Champlin and Truman, 2000; Benton et al., 2007), neurite outgrowth (Seidel and Bicker, 2000), patterning of synaptic connectivity (Ball and Truman, 1998;

Gibbs and Truman, 1998, Wright et al., 1998), and axonal regeneration (Stern and Bicker, 2008), no neurodevelopmental functions of CO have so far emerged.

To investigate whether CO is a cellular messenger molecule in insect development, we use immunochemical techniques for the localization of HO in comparison to NOS during the formation of the grasshopper enteric nervous system. With the concept in mind that CO may interact with NO/cGMP-signalling (Ingi et al., 1996a; Artinian et al., 2001), we focus on the NO-dependent cell migration of the midgut plexus neurons. Application of enzyme substrates, chemical inhibitors, activators, messenger releasing compounds, and scavengers in whole embryo culture implicate CO as an intracellular messenger molecule that modulates transcellular NO signalling during neuronal migration.

Materials and Methods

Locust eggs (*Locusta migratoria*) were collected from our crowded animal culture, reared under standard conditions and kept in moist Petri dishes at 30°C prior to use. Embryos were staged by percentage of development (% E) according to Bentley et al. (1979) with additional criteria for later embryos (Ball and Truman, 1998). All chemicals were purchased from Sigma (St. Louis, MO, USA) unless stated otherwise.

Immunocytochemistry

All steps of immunocytochemistry were performed at room temperature and with smooth agitation unless stated otherwise. Embryonic guts were dissected and collected as whole mount preparations in cooled Leibowitz 15 medium (L15, Gibco, Life Technologies, Paisley, UK). To reduce the background caused by the yolk inside guts, some whole guts were dissected and transferred to a Petri-dish containing a poly-D-lysine coated coverslip with L15 culture medium. Subsequently guts were carefully rolled over the coverslips. During this „tissue blotting“ procedure cells on the gut surface including neurons of the plexus, muscle fibres, and ganglia of the ENS adhered to the coated surface while the intact epithelium and yolk could be removed. To ensure sufficient adherence of the nerve cells, preparations were allowed to settle for about 30 minutes at room temperature ahead of fixation.

Preincubation for NO-dependent cGMP immunocytochemistry was carried out as already described (De Vente et al., 1987; Haase and Bicker, 2003) but with adding YC-1 (3-(5'-hydroxymethyl-2'-furyl)-1-benzyl Indazole, 25 µM), a sensitiser of sGC, immediately after preparation (Ott et al., 2004). Omitting the NO-source from the cGMP-preincubation solution or adding sGC inhibitors, revealed no cGMP-IR at all. All specimens were fixed in 4% paraformaldehyde (PFA) dissolved in phosphate-buffered saline (PBS, 10 mM sodium phosphate, 150 mM NaCl, pH 7.4) overnight at 4°C. Preparations were permeabilised in 0.3% Saponin in PBS for one hour, rinsed in PBS containing 0.5% Triton X-100 (PBS-T) and blocked for at least one hour in 5% normal serum/PBS-T (serum of animal in which secondary antibody was raised). The primary antibody was diluted in blocking solution and

applied overnight at 4°C. Used primary antibodies and concentrations were: sheep anti-cGMP (1:10.000 – 1:20.000, Tanaka et al., 1997), monoclonal mouse anti-acetylated α -tubulin (1:500 – 1:1000), and polyclonal rabbit anti-heme oxygenase-2 (1:400 – 1:1000, Stressgen, Victoria, BC, Canada). After rinsing in PBS-T, guts were exposed for at least two hours at room temperature or overnight at 4°C to biotinylated (Vector, Burlingame, CA, USA) or AlexaFluor488-coupled (Molecular Probes, Eugene, OR, USA) secondary antibodies in blocking solution. Biotinylated secondary antibodies were visualised using fluorescent streptavidin coupled dyes (Sigma, Molecular Probes). After washing in PBS-T and PBS, preparations were cleared in 50% glycerol (Roth, Karlsruhe, Germany)/PBS and mounted in 90% glycerol/PBS with 4% n-propyl-gallate. Control preparations incubated with 5% normal serum instead of primary antibodies and subsequent detection system revealed absolutely no staining. For double-labelling, ENSs were stained first for cGMP followed by acetylated α -tubulin immunocytochemistry.

Western blotting

To obtain tissue homogenates of embryonic CNS, whole brains and ventral nerve cords were dissected. For homogenates of the ENS, we used complete gut tissue with the yolk removed. Tissue was dissected in cooled PBS, collected, and homogenised in ice cold 0.3% Saponin-PBS containing 1% protease inhibitor cocktail (HALT, Pierce, Rockford, IL, USA). Samples of 20 (ENS) or 10 (CNS) embryos were collected per 200 μ l lysis buffer. Homogenisation was done using a Kontes Duall tissue grinder with PTFE pestle (Landgraf Laborsysteme, Langenhagen, Germany). Homogenates were centrifuged for 10 minutes at 6000x g to allow a crude separation of cytosolic soluble proteins from membrane bound protein fractions and cellular debris. For HO-2 immunoblots proteins were precipitated with acetone for 16-48 hours at -20°C. Protein pellets were re-dissolved in 2x Laemmli-buffer (100 mM Tris-HCl, pH 6.8 with 4% SDS, 20% glycerol, 0.02% bromphenol blue) after centrifugation and ethanol washing. For universal NO synthase (uNOS) immunoblots, homogenates were used without any precipitation. Prior to SDS-PAGE, samples were denaturated at 95°C for three minutes in loading buffer (2x Laemmli buffer with 2% SDS, 10% 1 M DTT).

Proteins were separated either on 8% (NOS) or 15% (HO-2) PAGE and transferred to a PVDF-membrane (Roth). Membranes were equilibrated in PBS, blocked for at least one hour at room temperature and incubated overnight at 4°C with the antibody dissolved in blocking solution. Following antibodies and blocking solutions were used: polyclonal rabbit anti-uNOS (1:400, Affinity Bioreagents, Golden, CO, USA), in 5% low fat milk powder (Humana, Herford, Germany) in PBS containing 0.05% TWEEN (PBS-TW); polyclonal rabbit anti-HO-2 (1:400 – 1:1000), blocked with 1% bovine serum albumin (BSA) in PBS-TW. Membranes were then rinsed with PBS-TW and incubated with biotinylated secondary antibody in the appropriate blocking solution for two hours at room temperature. After washing with PBS-TW, bound antibodies were visualized by standard peroxidase staining techniques using the Vectastain ABC kit (Vector). To estimate total cell mass in immunoblots from different tissues, some blots were stained additionally for α -tubulin. Stained membranes were dried, scanned, and after reactivation of the membrane with methanol, the blot was probed but with anti-acetylated α -tubulin diluted 1:10000 in PBS-TW containing 5% low fat milk powder.

For a specificity control of the HO-2 antiserum, purified recombinant rat HO-2 (rHO-2, Stressgen) was applied to a 15% SDS-PAGE in parallel with locust homogenates. Homogenates were divided in two aliquots and separated on the identical gel. After blotting, half of the membrane was incubated with antibody while a pre-adsorbed antibody was applied to the other half. For pre-adsorption, recombinant rat HO-2 was added to the anti-HO-2 solution (75 μ g protein/ml) and pre-incubated overnight at 4°C. Western blot analysis was repeated at least three times for each protein with homogenates from several preparations and developmental stages.

In vivo culture experiments

Embryos were staged between 60 and 65% E. An optimal stage for *in vivo* chemical manipulation of cell migration on the midgut is 63% E. At this stage, which is indicated by the first appearance of brownish pigmentation at the tips of the antennae, midgut neurons have just started their cell migration (Fig. 1A).

Eggs of one clutch were sterilised in 70% ethanol and dissected in sterile L15 medium. Subsequently embryos were randomly divided into groups that were exposed to the pharmacological compounds or the control media respectively. Embryos were immobilised in Sylgard embedded Petri dishes and covered with cell culture medium, supplemented with 1% penicillin-streptomycin solution. A small incision in the dorsal epidermis above the foregut allowed access of pharmacological agents to the developing ENS during the *in vivo* culturing period. Following an incubation for 24 hours at 30°C, guts were dissected and prepared for anti-cGMP and anti-acetylated α -tubulin double staining.

To quantify the cell migration on the midgut surface, we measured the distance from the foregut-midgut boundary to the position of the leading enteric neuron (Fig. 1A, indicated by double arrow; Wright et al., 1998) using NIH ImageJ (v. 1.35 – 1.39). The obtained values were normalised with respect to the mean distance of migration of the control group. A Wilcoxon Mann-Whitney test was employed for statistical comparisons of experimental and control groups using KyPlot (version 2.0 beta15). All significance levels are two-sided. Bar-graphs display mean values \pm standard error of the mean (s.e.m.) as percentage of the matched control values of each experiment.

Fig. 1B displays the mode of action of chemical agents we used to manipulate NO and CO signal transduction cascades. L-arginine and hemoglobin were predissolved in L15. Hemin and zinc protoporphyrin-IX (ZnPP-IX, Alexis, San Diego, CA, USA) were predissolved in 0.1 M NaOH resulting in a final concentration less than 0.5% NaOH in the culture medium. 7-nitroindazole (7-NI), YC-1, tricarbonyldichlororuthenium (II) dimer (CORM II), and zinc deuteroporphyrin-IX 2,4 bis glycol (ZnBG, Alexis) were predissolved in DMSO resulting in less than 0.5% DMSO in the culture medium.

Cell viability and cytotoxicity test

To exclude neurotoxic side effects of hemin and CO-donor applications, a cell viability assay (Live/Dead Viability/Cytotoxicity Kit for animal cells, Molecular Probes) was carried out. This assay allows for a clear simultaneous discrimination between living and dead cells using two different fluorescent probes that indicate distinct parameters of cell viability: intracellular esterase activity and plasma membrane integrity. Immediately after *in vivo* culturing, guts were dissected and the tissue was blotted on poly-D-lysine coated coverslips. Subsequently tissue blots were incubated in the assay reagents for 30 minutes at room temperature in the dark, followed by image acquisition. After counting of living and dead enteric neurons, the percentage of living neurons was calculated.

Image acquisition and processing

Preparations were analysed and photographed using a Zeiss Axioscope equipped with an AxioCam3900 digital camera linked to a Zeiss image acquisition system (Zeiss Axiovision) or a Zeiss Axiovert 200 equipped with a Photometrics Cool Snap digital camera and associated MetaFluor Imaging software. Confocal images of selected preparations were taken with a Leica TCS SP2 confocal microscope using Leica LCS software. Image processing, including arrangement, conversion to grayscale, inversion and contrast enhancement, were carried out using Adobe Photoshop or NIH ImageJ (Rasband, W.S., ImageJ, U.S. National Institutes of Health, Bethesda, MD, <http://rsb.info.nih.gov/ij/>).

Results

Localisation of NOS and cGMP on the developing midgut

During the phase of directed cell movement along the four midgut migratory pathways (Fig. 1A; Ganfornina et al., 1996), the enteric neurons express NO-induced cGMP immunoreactivity (Haase and Bicker, 2003). To obtain a high resolution image of the cellular distribution of cGMP, we probed tissue blots of the midgut for acetylated α -tubulin and cGMP. Confocal microscopy showed an evenly distributed cGMP-IR throughout the entire cell bodies of enteric neurons, growth cones, and the trailing neurites (Fig. 2A, C). Neither the underlying gut epithelium nor the developing musculature show any cGMP-IR, whereas these tissues are clearly stained with an antibody against α -tubulin, indicative for stable microtubules (Fig. 2B, C). Whereas filopodia and thinner cell processes of the migratory neurons typically are lacking immunoreactivity for acetylated α -tubulin, these cell structures show strong cGMP-IR (Fig. 2B, C). This NO-dependent cGMP synthesis suggests a source of NO in the adjoining tissue, that might stimulate the formation of cGMP in the enteric neurons including their highly motile filopodia. Since cytochemical markers for NOS did not label the motile neurons but indicated staining in the midgut epithelium (Haase and Bicker, 2003), we used an additional biochemical approach. Immunoblots of CNS homogenates from 65% E locust embryos revealed a protein of about 135-140 kDa that was clearly recognised by the universal NOS antibody (Fig. 2D, CNS). This immunostained protein is also present in homogenates of the embryonic foregut (FG) as well as of the midgut (MG, MG-M, midgut homogenates do also include the adjacent hindgut) (Fig. 2D). An additional, somewhat smaller protein of approximately 128 kDa was labelled that is missing in the membrane fraction of midgut (MG-M) and is only very faintly visible in the CNS lane by the uNOS antibody. This double band appearance of NOS may be due to post translational modifications, with the smaller one representing pre-processed or degraded proteins. To normalise for total protein content, some immunoblots were additionally marked for α -tubulin (Fig. 2D, bottom lane). We estimate from the ratio of the loading control to the NOS band, that the midgut contains in average a two times higher NOS concentration than the CNS probe (midgut cytosol 0.30 and midgut membrane 0.33 versus 0.18, n=4).

Transcellular NO signalling regulates enteric neuron migration

Since NO/cGMP signal transduction is a positive regulator of enteric neuron migration, pharmacological inhibition of NOS leads to a reduction of cell motility (Haase and Bicker, 2003). We could confirm that bath application of the NOS inhibitor 7-NI results in a significant reduction of enteric neuron migration (Fig. 3A). Moreover, in vivo incubation of 63% E embryos with the extracellular NO scavenger hemoglobin, revealed a similarly strong reduction in the migrated distance (Fig. 3A). Most likely, NO released by cells of the gut (Fig. 2D) serves as a transcellular regulator of neuronal cell migration.

To test whether enteric neuron migration could be enhanced by a stimulation of NO/cGMP signal transduction, embryos of 63- to 65% E were allowed to develop in culture with an excess of the NOS substrate L-arginine (2 mM). The substrate activation of NOS did not result in any significant increase of migrated distance (Fig. 3B). NO-donors, such as sodium nitroprusside or S-nitroso-N-acetyl-L, l-penicillamine failed also to enhance enteric neuron migration (data not shown). Stimulation of sGC by application of 65 μ M YC-1 (Ko et al., 1994; Evgenov et al., 2006) appeared to slightly increase the migrated distance, however, this result was not statistically significant (Fig. 3B).

Carbon monoxide acts antagonistical to nitric oxide in enteric neuron migration

Heme oxygenase activity can be inhibited with low concentrations of metalloporphyrins like ZnBG or ZnPP-IX (Maines, 1981; Verma et al., 1993; Ingi et al., 1996a,b; Appelton et al., 1999; Labbe et al., 1999). Embryos at stages 63-65% E were exposed in culture to 5 μ M ZnBG, leading to a highly significant increase of the average migrated distance up to 131% (Fig. 3C). Figs 4A, B, illustrate that HO inhibition by ZnBG enhances enteric neuron migration without affecting the precision of pathfinding on the migratory routes. Using ZnPP-IX (10 μ M) as another HO inhibitor, we obtained a similar gain of function result (Fig. 3C).

By stimulating the production of CO, we performed a complementary experiment and applied 100 μ M hemin as a substrate analogue for HO to the cell culture medium. Activation of HO resulted indeed in an opposite effect, as enteric

neuron migration was significantly reduced (Figs 3C, 4A, C). Moreover, exogenous application of carbon monoxide by using the CO releasing compound CORM-II (Motterlini et al., 2002) reduced enteric neuron migration similar to stimulation of HO enzymes (Figs 3C, 4A, D). In an additional control experiment, we tested whether the carbon monoxide exhausted compound might account for the slowing down of enteric neuron migration. Therefore, CORM-II was dissolved in DMSO and kept for 24 – 48 h at room temperature and used afterwards. This exhausted CORM-II (iCORM) did not affect enteric neuron migration (Fig. 3C). Neither hemin nor the CO-donor caused any decrease in cell viability at used (hemin) or even higher (CORM-II) concentrations (Fig. 3D). All of these findings are in line with a negative regulatory role of HO activity and CO signalling on enteric neuron migration.

Localisation of HO-positive neurons in the developing ENS

We used homogenates of whole guts, including ENS, gut epithelium, and musculature (ENS in Fig. 5), or central nervous systems (CNS in Fig. 5) of 65% embryos for immunoblot analysis of HO. An antibody to HO-2 strongly recognised proteins of approximately 30-35 kDa (Fig. 5A). These proteins are of comparable size to recombinant rat HO-2 (rHO-2), labelled with the same antibody (Fig. 5B, first two lanes). Remarkably, anti-HO-2 labelled proteins are mainly present in the membrane fraction of homogenates of gut and CNS (Fig. 5A, left lanes). This is in line with reports about an association of vertebrate HO-2 with the endoplasmic reticulum and nuclear outer membrane (Maines, 1988; Ma et al., 2004). The multiple band appearance and the slightly heavier proteins between 35-45 kDa that is visible in cytosolic portions may be a result of post translational modifications. Diverse cleavage of the C-terminus of the protein has also been often observed during separation of HOs on SDS gels (Ding et al., 1999).

To test the specificity of the antibody against vertebrate HO-2 on invertebrate tissues, we used pre-adsorbed antibody-solution (75 µg rHO-2/ml). Pre-adsorption leads to a complete loss of labelling of the 30-35 kDa protein bands from locust homogenates (Fig. 5B, arrowhead). Additional labelled proteins around 60 kDa become visible, when rHO-2 is applied in high quantity (1 µg) to the gel (Fig. 5B).

left side/HO-2). Since they are not recognised by the pre-adsorbed antibody, these bands are likely due to aggregates of HO-2 (Fig. 5B right side/HO-2). Such high protein concentrations may also account for some of the larger molecular weight protein bands in homogenates. However, since pre-adsorption abolished both the labelling of 30-35 kDa protein bands derived from recombinant HO-2 and embryonic locust, we can safely infer the presence of HO in the developing CNS and gut tissue.

We also performed immunocytochemical stainings for HO-positive cells on the midgut. At the onset of neuronal migration at 63-65% E, virtually all migrating enteric neurons on the midgut exhibit a clear immunoreactivity to HO (Fig. 6A, B). HO-IR can be detected in soma and main neurites. Although underlying tissues of the gut show mild background staining, it is easily possible to discern the signal intensity between enteric neurons and non-neuronal cells. The gut musculature (m) is only faintly stained in whole mount (Fig. 6A) and also in tissue blot preparations (Fig. 6B). When enteric neurons start to form the midgut plexus by leaving the anterior-posterior migratory pathways around 80% E, HO-IR is still apparent (data not shown). At a later embryonic stage around 95% E, the staining intensity of neuronal HO-IR approaches the level of the underlying tissues (Fig. 6C). However, the enteric neurons of the nearly established midgut remain clearly identifiable by their α -tubulin-IR (Fig. 6D). In summary, the results of western blotting and immunocytochemistry indicate the presence of HO in embryonic guts and the migrating enteric neurons.

Discussion

In this study, we show that inhibition of HO with metalloporphyrins promotes enteric neuron migration in an intact locust embryo. This gain of function in conjunction with the suppression of migratory behavior by chemical activation of HO or application of exogenous CO strongly implicates the release of the messenger CO as inhibitory signal for neuron migration (Figs 3C, 4). Further support for this concept comes from the immunoblotting of HO in dissected gut preparations (Fig. 5A) and the direct immunocytochemical localization of HO in the enteric neurons (Fig. 6A-C). All these data point towards an autoregulatory role of CO signalling during enteric neuron migration. The application of small molecule compounds to activate or inactivate proteins in real time is a powerful approach for the study of complex signal transduction systems (Yeh and Crews, 2003). While a genetic approach would be very useful to reveal additional downstream molecular pathways of NO and CO signalling during insect embryonic development, the application of chemical agents at precise time intervals is more suited to detect subtle modulatory influences of the gaseous messengers.

NOS expression provides for a transcellular NO signal during formation of enteric midgut plexus

The uNOS antibody stains NADPH-diaphorase positive interneurons in the adult locust antennal lobe (Bicker, 2001) which express Ca^{2+} /calmodulin sensitive NOS (Müller and Bicker, 1994, Elphick et al., 1995). In the absence of molecular sequence data for the NOS of locusts, we used a universal NOS antibody that recognises a highly conserved sequence of the three mammalian NOS isoforms and also detects arthropod NOS (Bicker, 2001; Bullerjahn and Pflüger, 2003; Christie et al. 2003; Settembrini et al., 2007). Western blotting of homogenates from embryonic fore- and midguts revealed the presence of NOS-like proteins with a size of 135-140 kDa at the onset of enteric neuron migration (Fig. 2D). The approximate size of NOS has been independently determined as 135 kDa in the locust brain (Elphick et al., 1995), between 116 to 180 kDa in the locust abdominal nervous system (Bullerjahn and Pflüger, 2003), and between 130-150 kDa in other insects (Gibson and Nighorn, 2000; Watanabe et al., 2007; Settembrini et al.,

2007). The genome of *Drosophila* contains only a single NOS gene (Regulsky and Tully, 1995; Enikopolov et al., 1999) and immunoblotting showed a band of the corresponding protein at about 150 kD (Regulski et al., 2004). Our results indicate highly enriched NOS proteins in the midgut, compared to the CNS (Fig. 2D). Most likely, this is caused by high levels of NOS expression in a substantial fraction of the epithelial gut cells. Using quantitative PCR, NOS expression has also been found in the midgut epithelium of *Anopheles* (Akman-Anderson et al., 2007). NADPHd-diaphorase histochemistry detected staining in a subset of the locust embryonic midgut cells (Haase and Bicker, 2003) and hemocytes (data not shown) as potential endogenous NO-producing cells. However, since the diaphorase reaction depends on fixation conditions (Ott and Burrows, 1999), it may quite often not completely resolve the expression pattern of NOS. Since application of hemoglobin as an extracellular scavenger of gaseous molecules suppressed enteric neuron migration a transcellularly diffusing NO signal derived from the gut cells may stimulate cGMP-mediated enteric neuron migration. This concept is in line with the immunocytochemical localization of cGMP in the cell bodies and filopodia after exogenous application of NO and the sGC sensitizer YC-1 (Figs 1B, 2A, C; Haase and Bicker, 2003).

NOS proteins are present in an even higher amount in the particulate fraction than in the cytosolic fraction of embryonic midgut homogenates (Fig. 2D, MG-M), suggesting, that they may be partly membrane associated. In vertebrates a significant amount of NOS isoforms is present in the particulate cell fraction (Hiki et al., 1992; Watanabe et al., 1998; Oess et al., 2006). Therefore, the double band appearance of NOS proteins that we observed in homogenates of locust embryos (Fig. 2D), might be due to posttranslational modifications similar to vertebrate NOS modifications accompanying protein membrane association.

CO is an inhibitor of enteric neuron migration

In a gain of function experiment we could show, that inhibition of HO with low concentrations of ZnBG and ZnPP-IX resulted in a significant acceleration of migration on the midgut (Figs 3C, 4A, B). Conversely, we could significantly delay enteric neuron migration by stimulating CO production with the HO substrate analogue hemin or with exogenous CO application (Figs 3C, 4A, C and D). This confirms CO as a likely effector molecule of HO activation on the regulation of enteric neuron migration.

Unlike to the locust, application of 10 μ M ZnPP-IX to the developing *Manduca* ENS caused no significant enhancement of enteric neuron motility (Wright et al., 1998). However, despite the common developmental origin from neuroepithelial parts of the foregut, enteric nervous systems of insects exhibit quite extensive variations in the detailed pattern of cell migration and underlying molecular guidance cues (Hartenstein, 1997; Ganfornina et al., 1996; Copenhaver, 2007). For example, whereas in *Manduca* specific sets of visceral muscle bands support migration of the enteric neurons on the midgut (Copenhaver and Taghert, 1989b; Copenhaver et al., 1996; Wright et al., 1999) no morphologically distinct muscle bands can be recognised along the migratory pathways in the grasshopper embryo (Ganfornina et al., 1996). Instead, the migratory neurons move parallel to the longitudinal muscle bands directly on the surface of the midgut.

Specificity of chemical manipulations

At high concentrations, some metalloporphyrins have been reported not only to block HOs but also to inhibit sGC or NOS activity (Luo and Vincent, 1994; Grundemar and Ny, 1997; Serfass and Burstyn, 1998). An example is the potent inhibitor of HOs ZnPP-IX (Maines, 1981), which was shown to cause such unspecific side effects later on. However, the low concentrations of ZnBG (5 μ M) or ZnPP-IX (10 μ M) that we applied have been demonstrated to be highly effective for the inhibition of HO enzyme activity without influencing NOS or sGC (Ingi et al., 1996a; Appleton et al., 1999). Moreover, the direction of observed motility changes, rules out an additional inhibitory effect on sGC or NOS. As shown by Fig. 3A, a direct inhibition of NOS with 7-NI or sGC with ODQ (Haase and Bicker, 2003)

revealed a significant retardation in enteric neuron migration. Thus, an additional inhibition of NOS/sGC enzymes by ZnBG or ZnPP-IX would have slowed down neuronal migration. Since the application of metalloporphyrins caused a significant acceleration of migration (Fig. 3C), our results provide no evidence for unspecific side effects.

Application of the extracellular scavenger hemoglobin delayed migration (Fig. 3A). Since hemoglobin binds both NO and CO, the net effect of a reduced motility can therefore be caused by a reduced concentration of both compounds in the extracellular space. Surprisingly, the reduced motility after incubation with hemoglobin matches the reduction after inhibition of NOS, whereas a lack of CO leads to an opposite effect of accelerating neuron migration (Fig. 3A, C). This result would suggest that the net effect of hemoglobin could be mainly due to scavenging extracellular NO. Moreover, the presence of the HO enzyme in enteric neurons and the lack of NOS (Figs 2D, 6A-C) argue for an intracellular CO and transcellular NO signal transduction mechanism. However, in the absence of real concentration measurements of intra- and extracellular CO/NO levels before and after hemoglobin application, it is difficult to draw any firm conclusions. It remains a distinct possibility that CO produced in an enteric neuron may not only act intracellularly but that some of the CO escaping in the extracellular space may also downregulate the motility of neighbouring cells.

Regulation of cell motility by gaseous messengers

The most straightforward functional explanation for all our reported data is a scenario in which the gut cells provide a transcellular NO signal (Figs 2D, 3A) for stimulating sGC in the enteric midgut neurons (Fig. 2A-C). NO-induced cGMP synthesis is in turn a permissive, but essential prerequisite for enteric neuron migration (Haase and Bicker, 2003). An additional CO pathway within and between the HO-positive midgut neurons provides for an auto-/paracrine signal that downregulates neuronal motility along the chain of migrating enteric neurons (Figs 3C, 4). We propose that both gaseous messenger molecules interact via sGC to organise the timing of the posterior directed cell migration along the midgut. Since NO and CO can both bind to sGC, but CO with less efficiency to stimulate cGMP

formation (Kharitonov et al., 1995; Denninger and Marletta, 1999; Baranano and Snyder, 2001; Koesling et al., 2004), a simple competition mechanism between the two messengers may regulate cGMP levels in the migratory neurons (Fig. 1B). In the presence of NO and CO, part of sGC enzymes would bind CO resulting in a suboptimal cGMP production. By decreasing CO concentrations, an increasing number of sGC enzymes would be available for efficient NO activation. A decrease in CO concentration by blocking HO (Fig. 1B) would thus be reflected by the increased cellular motility (Fig. 3C). It is also conceivable that CO binding causes conformational changes of sGC affecting its efficiency (Hernandez-Viadel et al., 2004) or perhaps induces allosteric effects arising from interactions among sGCs or their regulatory proteins (Ingi et al., 1996a) that cause a downregulation of the NO stimulated cGMP production. Currently, we cannot exclude an sGC/cGMP independent pathway for the effect of HO/CO signalling on enteric neuron migration, since CO can have other cellular effects apart from modulating cGMP levels (Boehning and Snyder, 2003; Kim et al., 2006).

Even though the filopodial tips of migrating enteric neurons can upregulate cGMP (Fig. 2A, C), neither the chemical manipulations of NO/cGMP- nor CO dependent signalling pathways causes misrouting of enteric neurons. Thus, a permissive effect of gaseous messengers on motility appears to be independent from growth cone steering. A quantitative evaluation of pathfinding errors (data not shown) provided no evidence for enhanced misrouting of migrating enteric neurons after the application of metalloporphyrins, hemin, or CORM-II. This result is illustrated in examples of migratory pathways under the chemical manipulation of HO (Fig. 4).

To fully appreciate the role of HO/CO signalling in cell migration, it remains insufficient to define the cellular sources and targets of CO. Technology has yet to be developed to resolve the temporal pattern of CO production. While neuronal production of NO is a tightly Ca^{2+} /calmodulin regulated process in locusts and vertebrates (Müller and Bicker, 1994; Elphick et al., 1995; Boehning and Snyder, 2003), regulation of HO activity is thought to depend mainly on the availability of heme. However, in response to neuronal stimulation a modest regulation of HO-2 has been demonstrated by casein kinase-2 (CK-2) (Boehning et al., 2003) and *in*

vitro studies have uncovered an additional mode of activation by binding of Ca^{2+} /calmodulin (Boehning et al., 2004). Thus, there is increasing evidence for an activity dependent release of CO, one of the necessary criteria for a role as neural messenger molecule.

Using a rather simple invertebrate model, we have uncovered an antagonistic role of CO versus NO as gaseous messenger molecules regulating nerve cell migration. Since many signalling mechanisms of neuronal and cellular guidance are strikingly conserved among vertebrate and invertebrate animals, it will be interesting to examine whether CO signalling plays also a vital role during vertebrate brain development.

Acknowledgements

We thank Dr. J. de Vente for his gift of the cGMP antiserum, the Department of Microbiology, University of Hannover, for access to their confocal microscope, Dr. I. Fischer for initial help with western blotting, and Dr. M. Stern for helpful comments on a previous version of the manuscript. This work was supported by a grant from the Deutsche Forschungsgemeinschaft BI 262/10-5.

Figures

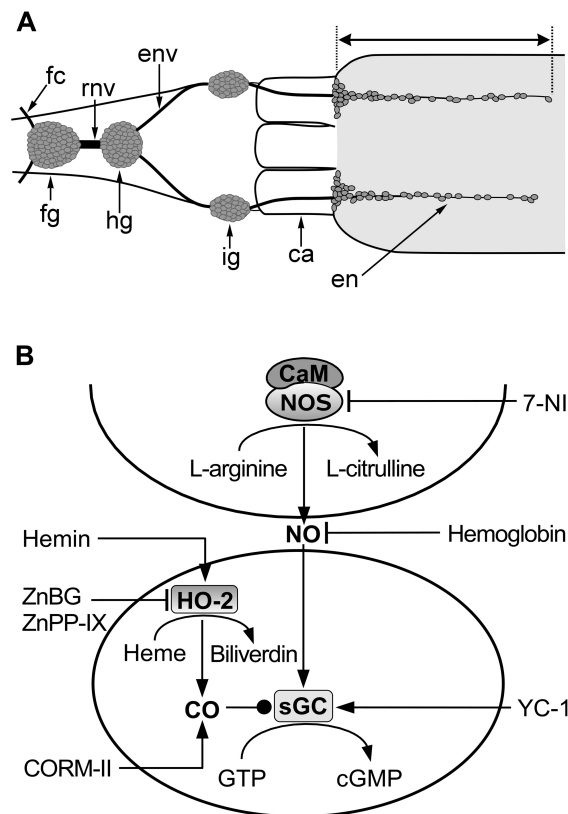


Figure 1: Cellular organisation of embryonic enteric nervous system and proposed signal transduction cascades regulating neuronal motility.

(A) Schematic drawing of locust embryonic fore- and anterior midgut at 65% E in dorsal view. Midgut is shaded light gray, enteric ganglia and neurons dark gray. Two of the four migratory pathways are visible on the dorsal midgut. Already developing foregut plexus is left out for sake of clarity. Double headed arrow indicates measured distance of enteric neuron migration after 24 hours in vivo culture incubation. ca, caecum; en, enteric neuron; env, esophageal nerve; fc, frontal connective; fg, frontal ganglion; hg, hypocerebral ganglion; ig, ingluvial ganglion; rnv, recurrent nerve. Anterior is to the left as in following figures. **(B)** Schematic diagram of CO and NO/cGMP signalling transduction influencing enteric neuron migration. Ca^{2+} -calmodulin (CaM) activated NOS catalyses the conversion of L-arginine into L-citrulline, thereby releasing NO. NOS activity can be stimulated by applying an excess of arginine or blocked by the inhibitor 7-NI. The diffusible NO binds to the heme moiety in soluble guanylyl cyclase (sGC) thus stimulating synthesis of cGMP. Intercellular diffusing NO can be trapped by the extracellularly acting scavenger hemoglobin. The stimulation of sGC with YC-1 artificially amplifies cGMP production. Heme oxygenase enzymes (HO), such as the HO-2-immunoreactive constitutive isoform release CO as a byproduct during heme degradation. The enzyme activity can be manipulated by its substrate analog hemin or metalloporphyrin inhibitors like ZnBG and ZnPP-IX. CORM-II is an exogenous CO donor. CO competes with NO for binding to sGC (blunt tip), leading only to a rather modest increase of the cGMP level.

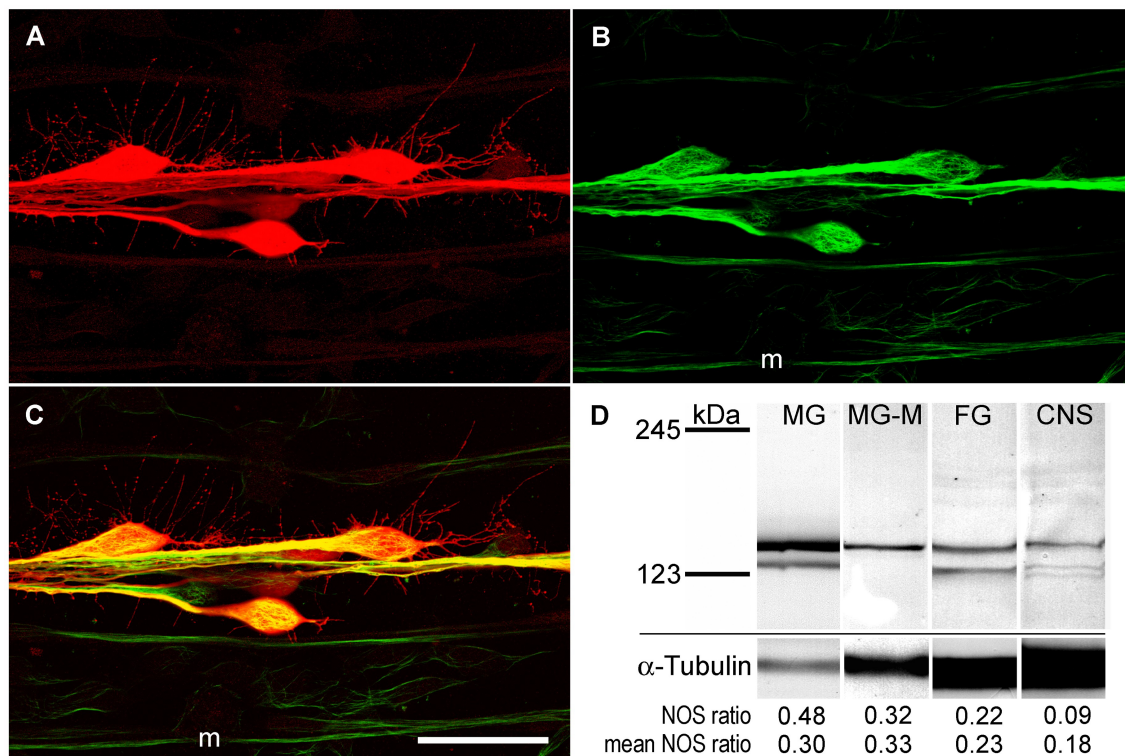


Figure 2: Immunochemical investigation of cGMP formation and the expression of NOS in the embryonic enteric nervous system.

(A) and (B) Confocal fluorescence images of migrating enteric neurons on the midgut at 65% E in a so-called „tissue blot“ preparation. Neurons were marked immunocytochemically for anti-cGMP (red) and anti-acetylated α -tubulin (green). (C) Merged image of (A) and (B). m, gut musculature. Scale bar in (C) indicates 50 μ m. (D) Immunoblot analysis with an antibody against universal NOS in homogenates of different parts of embryonic gut and in the CNS (65-70% E). The antibody recognises a protein of approximately 135-140 kDa and a second, somewhat lighter protein band in the fore- and midgut cytosolic fraction. Bottom lanes provide an acetylated α -tubulin band as loading control. For quantification, the ratio of the NOS signal to the α -tubulin signal was calculated and averaged for all probed blots (mean NOS ratios, n=4, s.e.m. of the ratios are: +/- 0.07 MG, +/- 0.04 MG-M, +/- 0.01 FG, +/- 0.08 CNS). The NOS ratio directly below the lanes corresponds to the actual signals of the shown Western blot. MG, midgut; MG-M, membranous part of midgut (both midgut homogenates included adjacent hindgut); FG, foregut; CNS, central nervous system including ventral nerve cord.

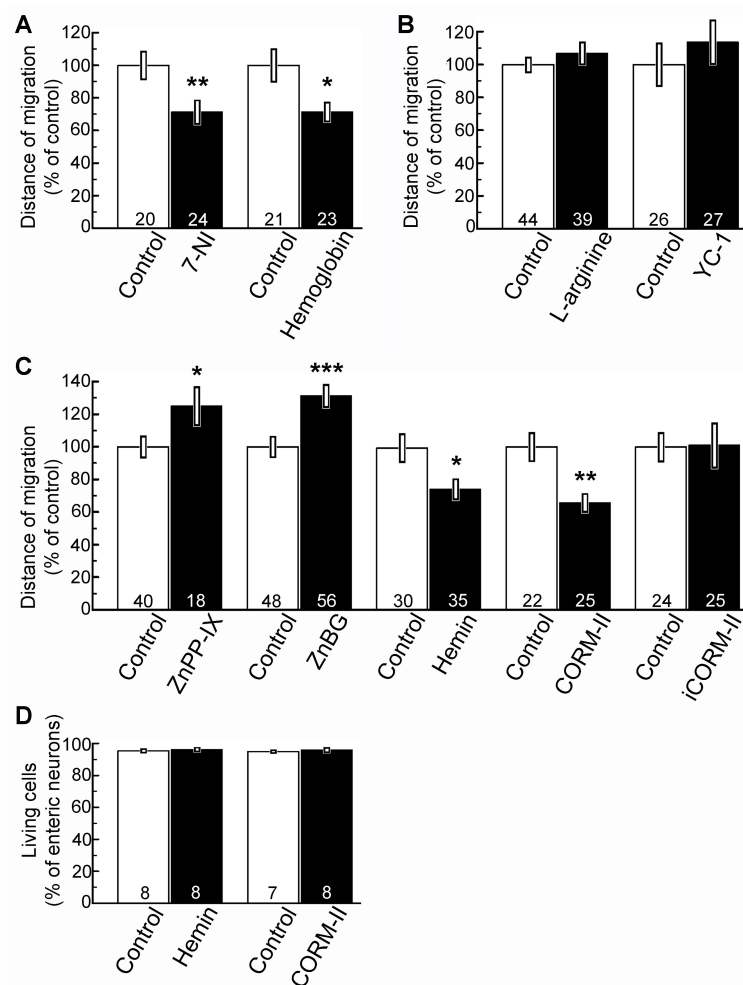


Figure 3: Quantitative evaluation of enteric neuron migration after chemical manipulation of the NO/cGMP pathway and HO enzymes.

Bar plots show average migration distance covered by the leading enteric neurons during 24 hours of in vivo culture. Data result from at least two independent experiments, each normalised to the mean of the corresponding control. **(A)** Inhibition of NOS with 500 μ M 7-NI or scavenging NO with 500 μ M hemoglobin result in a significant reduction of migration on dorsal migratory pathways. **(B)** Excess of NOS substrate L-arginine (2 mM) or stimulation of sGC with 65 μ M YC-1 revealed no difference of migration compared to the control. **(C)** Inhibition of CO releasing HO enzymes with 10 μ M ZnPP-IX or 5 μ M ZnBG lead to a significant acceleration of enteric neuron migration. Activating HO with 100 μ M hemin or applying CORM-II (20 μ M) resulted in a significant reduction of average migrated distance. Application of inactivated CORM-II (iCORM-II, 20 μ M) did not affect migration. **(D)** Enteric neuron viability after 24 hours of in vivo culture with 100 μ M hemin or 200 μ M CORM-II. 100% represents total number of counted enteric neurons. Error bars are \pm standard errors of the mean (s.e.m.). The numbers of experimental gut preparations are indicated in the bars. A Wilcoxon Mann-Whitney test was employed for statistical comparisons. *** $p < 0.001$; ** $p < 0.005$; * $p < 0.05$.

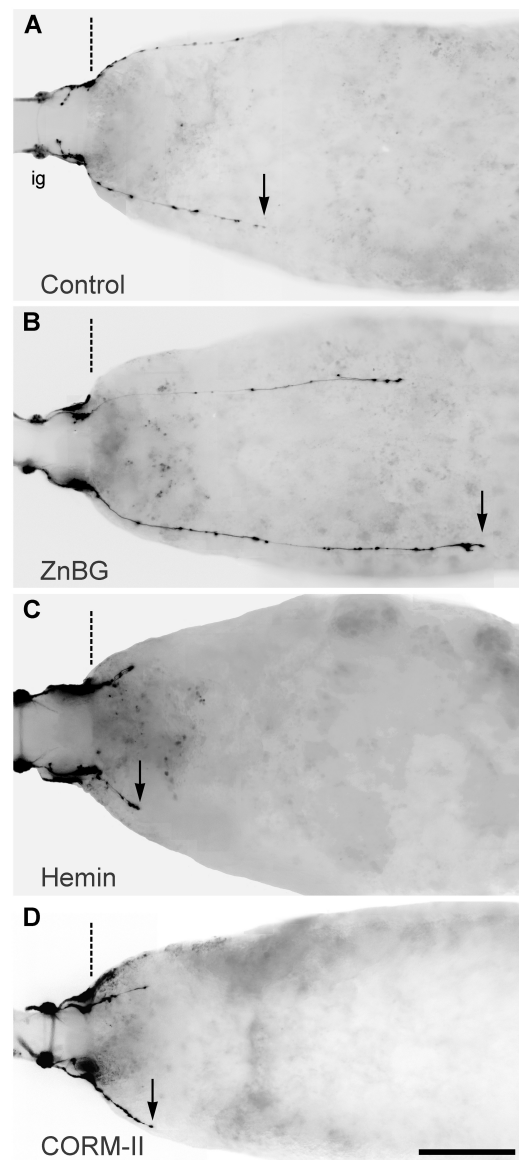


Figure 4: Enteric neuron migration under influence of neurochemicals affecting heme oxygenase catalysed CO production.

Immunofluorescence images of enteric neuron migration on individual guts after 24 hours in vivo culture. Dissected guts were stained with cGMP antiserum. Composed images are resulting from microphotographs of several focal planes, that were converted to gray scale, inverted for fluorescence intensity, and arranged in Adobe Photoshop. **(A)** Control conditions. **(B)** Inhibition of HO enzymes by 5 μM ZnBG. **(C)** Activation of HO with excess of its substrate analogue hemin (100 μM). **(D)** Exogenous carbon monoxide (CORM-II, 20 μM). Dashed lines indicate foregut-midgut boundary. Arrows point to furthestmost migrated enteric neuron. ig, ingluvial ganglion. Scale bar indicates 500 μm .

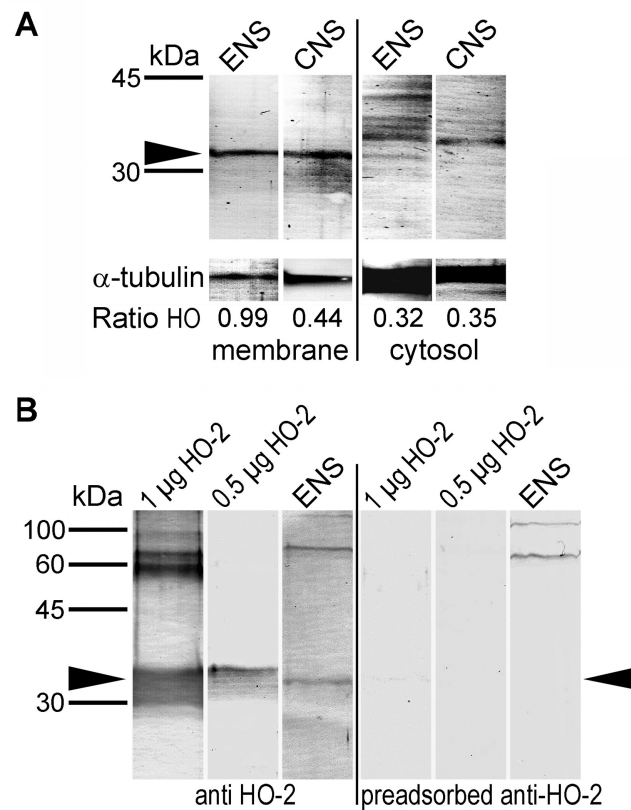


Figure 5: Western blot analysis of HO in the enteric nervous system.

(A) Immunoblots obtained from whole guts at 65% E with enteric nervous system attached (ENS) and from dissected CNS. HO-2 antibody recognises proteins of approximately 30-35 kDa. In CNS and cytosolic fractions an additional, slightly heavier protein band is enriched in the membrane fraction of homogenates. Both membrane (left) and cytosolic (right) fractions derive from the same preparation. Bottom lanes provide an acetylated α -tubulin band as loading control. For quantification, the ratio of the HO-2 signal to the α -tubulin signal was calculated for each lane ($n=3$, s.e.m. of the ratios are: ± 0.29 membrane ENS, ± 0.17 membrane CNS, ± 0.08 cytosol ENS, ± 0.03 cytosol CNS). **(B)** Immunoblotting of recombinant rat HO-2 protein and membrane fraction of ENS at 65% E. The blots were probed either with the antibody against HO-2 (left, anti-HO-2) or corresponding antibody solution pre-adsorbed with HO-2 protein (right, anti-HO-2, pre-adsorbed). Arrowheads in (A) and (B) mark distinct HO bands.

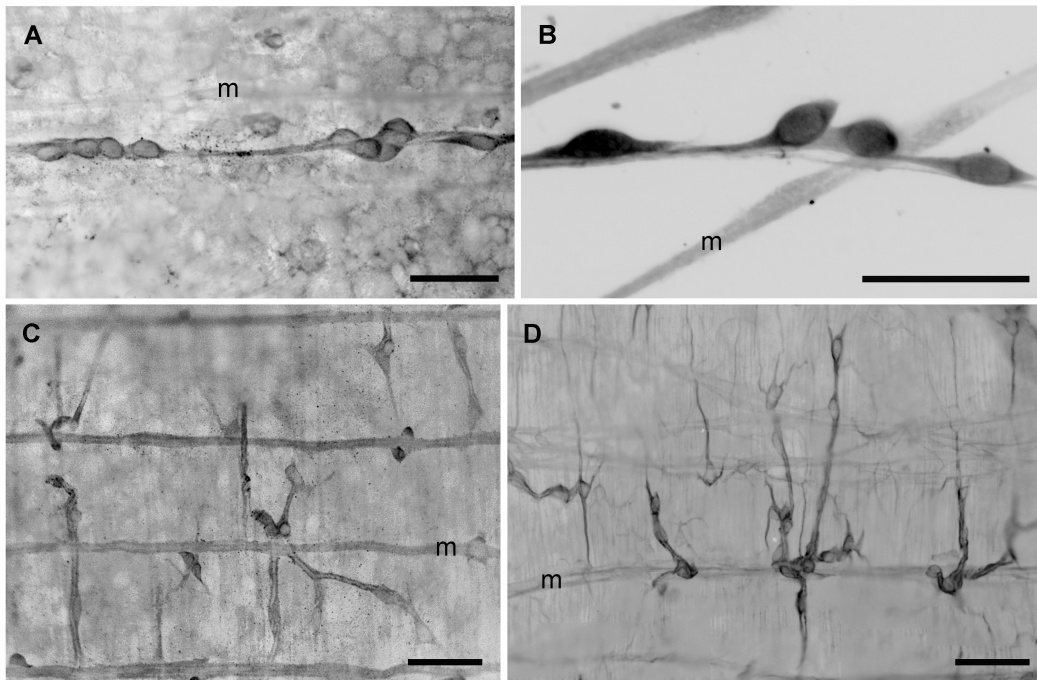


Figure 6: Immunocytochemical detection of HO in the enteric nervous system.

(A) and **(B)** Immunocytochemical labelling of the enteric neurons migrating on the midgut at 65 % E, using the antiserum in a whole mount **(A)** and tissue blot **(B)** preparation. 1% BSA was added to the blocking solution in **(B)**. **(C)** HO-2 immunocytochemistry at 95 % E on a whole mount midgut. Enteric neurons have left the four migratory pathways and established the midgut plexus. At this stage other tissues such as gut musculature show similar labelling intensity. **(D)** ENS at the same developmental stage as in **(C)** but stained for acetylated α -tubulin. **A**, **C**, and **D** are composed images from microphotographs of several focal planes. **m**, gut musculature. Scale bars indicate 50 μ m.

2.3 Embryonic Differentiation of Serotonin-Containing Neurons in the Enteric Nervous System of the Locust (*Locusta migratoria*).

Michael Stern*, Sabine Knipp* and Gerd Bicker

Published in: The Journal of Comparative Neurology, **501**: 38-51 (2007).

* *M.S. and S.K. contributed equally to this work.*

Abstract

The enteric nervous system (ENS) of the locust consists of four ganglia (frontal and hypocerebral ganglion, and the paired ingluvial ganglia) located on the foregut, and nerve plexus innervating fore- and midgut. One of the major neurotransmitters of the ENS, serotonin, is known to play a vital role for gut motility and feeding. We have followed the anatomy of the serotonergic system throughout the embryonic development. Serotonergic neurons are generated in the anterior neurogenic zones of the foregut and migrate rostrally along the developing recurrent nerve to contribute to the frontal ganglion. They grow descending neurites, which arborise in all enteric ganglia and both nerve plexus. On the midgut, the neurites closely follow the leading migrating midgut neurons. The onset of serotonin synthesis occurs around 50% development – the time of beginning midgut closure. Cells developing to serotonergic phenotype express the serotonin uptake transporter (SERT) significantly earlier, beginning at 40% development. The neurons begin SERT expression during migration along the recurrent nerve, indicating that they are committed to a serotonergic phenotype before reaching their final destination. After completion of the layout of the enteric ganglia (at 60%) a maturational phase follows, during which serotonin-immunoreactive cell bodies increase in size and the fine arborisations in the nerve plexus develop varicosities, putative sites of serotonin release (at 80%). This study provides the initial step for future investigation of potential morphoregulatory functions of serotonin during ENS development.

Key words

development, stomatogastric, 5-HT, SERT, migration, insect

Introduction

In both vertebrates and invertebrates, there exists a system of nerve fibres and ganglia which innervate the alimentary canal commonly referred to as the stomatogastric or enteric nervous system (ENS). It is connected to the brain and the endocrine system and controls food intake, digestion, and molting behaviour by generation of rhythmic motor patterns. These rhythmic motor patterns and their modulation have been studied for decades in crustaceans (Harris-Warrick and Marder, 1991), and more recently in insects (reviewed by Ayali, 2004). In addition to its use as a model system to study the physiology of neuronal networks, the ENS is also very interesting from a developmental point of view. Within the insect nervous system, the ENS is somewhat special because neuronal migration is an essential part of its formation (reviewed by Hartenstein, 1997), as compared to the relatively fixed locations of precursor cells and their progeny in the CNS or PNS (Goodman and Bate, 1981). Thus, it bears some similarities to the vertebrate ENS, which develops from migrating neural crest cells (Burns, 2005), and to the vertebrate CNS where neurons are born in the ventricular zones and migrate to their destinations in the cortex (Hatten, 1999). Thus, the insect ENS, because of its accessibility and ease of manipulation, is a useful model system for studying cellular mechanisms of neuronal migration and development.

Insect enteric nervous systems develop from neurogenic zones or placodes on the stomodaeum to form a network of ganglia and an enteric plexus associated with the entire gut (reviewed by Hartenstein, 1997). The neurons of both ganglia and plexus migrate from their places of birth to their final destinations in all insect species that have been investigated. Despite the common ground plan shared by ENS of all insect groups, there is a great amount of variability (Ganfornina et al., 1996; Hartenstein, 1997), indicating considerable differences in the developmental regulation of ENS formation. The pattern of migration on the midgut of the hawk moth *Manduca* has been described in detail (Copenhaver and Taghert, 1989b). Migration of enteric plexus neurons takes place in two steps, an initial phase of slow migration of neurons to form packets of cells accumulating at the foregut-midgut boundary, and a subsequent phase of fast migration along stereotyped migration pathways on the midgut. A similar pattern of two waves of migration has

been observed in the locust (Ganfornina et al., 1996). Mechanisms of neuronal migration on the midgut and formation of the midgut plexus have been studied in both species. In *Locusta*, the initiation and maintenance of migration depends on the presence of nitric oxide/cGMP signalling (Haase and Bicker, 2003), whereas in *Manduca* not the migration itself depends on nitric oxide, but lateral branching and synapse formation on the midgut plexus does (Wright et al., 1998). Taken together, a considerable amount of insight has been achieved about the formation of the ganglia and the generation of the neuronal plexus. Far less is known about the further differentiation steps of ENS development, the forming of the connections between ganglia and the gut epithelia, and the acquisition of neurotransmitter phenotypes.

A broad variety of neurotransmitters has been found in insect enteric nervous system, e.g. various peptides (Copenhaver and Taghert, 1989a; Clark et al., 2006; Duve and Thorpe, 2003; Hill and Orchard, 2003), GABA (Luffy and Dorn, 1992; Trumm and Dorn, 2000), acetylcholine (Bicker et al., 2004), and serotonin (Davis, 1985; Klemm et al., 1986; Radwan et al., 1989; Luffy and Dorn, 1992; Molaei and Lange, 2003). Serotonergic neurons form a large group among ENS neurons. In particular, the frontal ganglion, the motor control centre for the digestive tract (Ayali, 2004), contains up to 40% serotonergic neurons (Klemm et al., 1986). Serotonergic neurons are also found in significant numbers in the vertebrate ENS. Serotonin is necessary for peristaltic intestinal motility in both vertebrates (Gershon, 2004) and invertebrates (Luffy and Dorn, 1992), and depletion of serotonin in locusts results in disturbance of food propagation through the gut (Trumm and Dorn, 2000). A dual role of serotonin on midgut motility has been demonstrated in the stick insect: an activating modulatory role on rhythm generation in the enteric ganglia, and a direct stimulation of contraction of the gut itself (Luffy and Dorn, 1992). In the locust, however, serotonin applied to the isolated midgut leads to a reduced tonus, and counteracts proctolin-induced contraction (Molaei and Lange, 2003).

In addition to its well-known role as a - mainly modulatory - neurotransmitter, a second important role for serotonin is the regulation of neuronal development. There is quite detailed evidence for the involvement of serotonin in embryonic

development of both vertebrates and invertebrates. In vertebrates, serotonin has been shown to be involved in synaptogenesis (Mazer et al., 1997) and mouse neural crest cell migration (Moiseiwitsch and Lauder, 1995). Among invertebrates, possible roles for serotonin in developmental processes have been investigated most thoroughly in molluscs. In the snail *Tritonia*, serotonin has been shown to regulate cell divisions in prenervous stages (Buznikov et al., 2003). From other mollusc species there is evidence that in the developing nervous system, serotonin regulates neurite growth and branching during development (Goldberg and Kater, 1989; Diefenbach et al., 1995) and regeneration (Koert et al., 2001). In olfactory interneurons of the lobster, serotonin depletion has been shown to compromise proliferation and survival (Benton and Beltz, 2001), and inhibit branching in the deutocerebrum (Sullivan et al., 2000).

In insect embryos, development of a single well-defined group of serotonergic CNS neurons has been extensively studied in both grasshoppers (Taghert and Goodman, 1984; Condrón, 1999) and *Drosophila* (Valles and White, 1988; Lundell and Hirsh, 1998; Sykes and Condrón, 2005). In the insect ENS, the embryonic development of the serotonergic system has been described in the frontal ganglion of *Manduca* (Radwan et al., 1989). In *Drosophila*, Budnik et al. (1989) have described the postembryonic development of serotonergic midgut arborisations and its dependence on the presence of serotonin. In locusts, however, the development of the serotonergic system in the ENS has not yet been examined, despite the extensive work on ENS physiology in this animal (Ayali, 2004).

In the present study, we describe the embryonic development of the serotonin-containing neurons of the enteric nervous system. Using a pharmacological approach, we investigate when neurons begin to express a serotonin-uptake system. Then, we follow the outgrowth and branching in the enteric ganglia and on the enteric plexus during embryonic and early postembryonic development. We manipulate cell migration on the midgut and examine how this affects outgrowth of the serotonergic fibres.

Material and methods

Locust eggs (*Locusta migratoria*) were collected from our crowded culture reared under standard conditions. Embryos were staged by percentage of development according to Bentley et al. (1979) and Ball and Truman (1998). All chemicals were purchased from Sigma, unless stated otherwise.

Enteric nervous systems (ENS) were dissected in Leibowitz L15 culture media (Gibco Life Technologies). For immunocytochemistry of serotonin and tubulin, preparations were fixed in 4% Paraformaldehyde dissolved in phosphate buffered saline (PBS, 10 mM sodium phosphate, 150 mM NaCl, pH 7.4) for 1-2 hours at room temperature or overnight at 4° C. For cytochemistry of cyclic guanosine monophosphate (cGMP), guts were preincubated for 20 minutes at room temperature in L15 containing the NO-donor sodium nitroprusside (SNP, 100 µM), the phosphodiesterase inhibitor IBMX (1 mM), and YC-1 ([3-(5'-hydroxymethyl-2'-furyl)-1-benzyl indazole], 25 µM), an NO-sensitiser of soluble guanylyl-cyclase (De Vente et al., 1987; Haase and Bicker, 2003). IBMX and YC-1 were dissolved in DMSO, SNP in L15.

Serotonin uptake experiments

Preparations were incubated for 10 minutes in 5 µM Serotonin (5-HT) in Leibowitz L15 culture media made from a freshly prepared 1 mM stock solution in water, washed briefly in PBS, and fixed in paraformaldehyde for immunocytochemistry as described above. In some experiments, the serotonin-uptake blocker Fluoxetine (Prozac®) was added at a final concentration of 200 µM. After a 10 min preincubation with Fluoxetine alone, preparations were incubated in 5µM 5-HT + 200 µM Fluoxetine for 10 min before a brief wash in PBS and fixation.

Immunocytochemistry

After fixation, preparations were permeabilised for 1 hour in 0.3% Saponin in PBS, washed three times in PBS with 0,5% Triton X100 (PBS-T) and incubated for 1 hour in blocking solution (5% normal serum of the animal in which the secondary antisera had been raised in PBS-T) and incubated in primary antibody dissolved in

blocking solution overnight at 4°C. The following primary antibodies were used: polyclonal rabbit-anti-serotonin (1:5000 - 1:10000), monoclonal anti-acetylated α -tubulin (1:500), sheep-anti-cyclic GMP (1:20000, De Vente et al., 1987, a kind gift from Dr. J. De Vente), a FITC-coupled goat-anti HRP antiserum as a general neuronal marker (1:200, Jackson Immunoresearch). After several washes in PBS-T, secondary antibodies in blocking solution were applied for 1-2 h at room temperature. Secondary antibodies were CY3-coupled goat-anti-rabbit (1:200, Jackson Immunoresearch), biotinylated rabbit-anti-sheep (1:250, Vector), and biotinylated horse-anti-mouse (1:250, Vector). Biotinylated secondary antibodies were visualized using Streptavidin-CY3 (1:200) or Streptavidin-alexaFluor488 (1:250, Molecular Probes). After several washes in PBS, preparations were cleared in 50% glycerol/PBS, and mounted in 90% glycerol/PBS with the addition of 4% n-propyl-gallate as antifading agent. Preparations were viewed with a Zeiss Axioscope, equipped with an Axiocam3900 digital camera. Photographs were taken using Zeiss Axiovision software and arranged, converted to greyscale, inverted, and contrast enhanced in Adobe Photoshop. In colour illustrations the red channel (CY3) was converted to magenta in Photoshop. Confocal images of selected preparations were taken with a Leica TCS SP5 confocal microscope using Leica LCS software or NIH ImageJ, version 1.35p or 1.36 (Rasband, W.S., ImageJ, U.S. National Institutes of Health, Bethesda, Maryland, USA, <http://rsb.info.nih.gov/ij/>, 1997-2006, (Plugin: BIG - Extended Depth of Field)).

Specificity of the antisera

The antiserum against serotonin (Sigma cat. no. S5545, lot no. 013K4840) is a polyclonal rabbit antiserum raised against a serotonin creatinine sulphate complex conjugated to BSA as the immunogen. In ventral nerve cords of the same locust embryos in which we examined the ENS, it consistently stained the serotonergic neurons S1 and S2 in the same way as reported by Taghert and Goodman (1984) and Condron (1999). In serotonin-uptake experiments, it specifically stained S1 and S2 neurons in the ventral nerve cord of 45% embryos and putatively serotonergic neurons in the frontal ganglion when preincubated with 5 μ M 5-HT, but not without 5-HT-preincubation or when co-preincubated with 5-HT and the

specific serotonin-uptake blocker Fluoxetine (see results). In control experiments, we preadsorbed the diluted antiserum with either 500 μ M 5-HT or 1 mg/ml BSA for four hours at room temperature. When the antiserum was preadsorbed with 5HT, staining was completely absent both in the CNS and ENS; when preadsorbed with BSA, staining was identical to staining achieved without preadsorption, thus excluding that the antibody recognises a BSA-epitope instead of serotonin.

The antibody against cyclic GMP was a gift from Dr. J. de Vente, Maastricht, Netherlands. Its specificity has been described in detail by Tanaka et al. (1997). In brief: the antiserum was raised in sheep immunised with a conjugate of cGMP-formaldehyde-thyroglobulin. It recognises formaldehyde-fixed cGMP in oligodendrocytes in the developing rat brain (Tanaka et al., 1997) as well as BSA-coupled 3'5'cGMP blotted on nitrocellulose membranes, but not BSA-coupled 2'3'cGMP, GMP, guanosine, cAMP, AMP, or adenosine. Immunoreactivity to cGMP both on blots and in tissue can be blocked by preadsorption of the diluted antiserum with BSA-coupled cGMP at very low concentrations, but not by preadsorption with BSA-conjugates of other nucleotides even at very high concentrations. In our preparations of locust embryos it labels the same neurons in the CNS as reported by Ball and Truman (1998) and in the ENS as reported by Haase and Bicker (2003). In control experiments, when either IBMX or SNP were omitted during the preincubation before fixation, or where the specific blocker of soluble guanylyl-cyclase, ODQ (1H-[1,2,4]-oxadiazolo[4,3-a]quinoxalin-1-one), was applied (200 μ M) before fixation, cGMP-immunoreactivity was absent.

The antibody against acetylated α -tubulin (Sigma clone 6-11b-1, lot no. 103K4819) was raised against acetylated tubulin from *Strongylocentrotus purpuratus*. It labels microtubules in various tissues and species. In Western blots of locust CNS and gut tissue, it labels a single band of \sim 50 kD. Since it labels enteric neurons much stronger than midgut epithelium, we use it as a general marker for neurons on the midgut.

The antibody against HRP (Jackson Immunoresearch, code no. 123-095-021, lot no. 65876) was raised against peroxidase from horseradish. It recognises a neural-specific carbohydrate moiety on a large group of glycoproteins expressed on the surface of insect nervous systems, including the cell adhesion molecules

Fas I and Fas II (Snow et al., 1987). In our preparations of locust embryos, it stains the developing ENS in the same way as described by Ganformina et al. (1986).

In control experiments for possible unspecific binding of secondary antisera, we omitted the primary antiserum, replaced it with blocking solution, and followed the labelling protocol as above. In these cases, staining was absent.

Migration experiments

Embryos used for *in vivo* culture experiments were carefully staged between 60% and 65%. An optimal stage for *in vivo* culturing and pharmacological manipulation is 63% indicated by the first appearance of brownish pigmentation at the tips of the antennae. Eggs of one clutch were sterilised in 70% ethanol and dissected in sterile L15 medium. Embryos were randomly divided into two groups that were exposed to pharmacological substances or control media, respectively. Embryos were immobilised in Sylgard-lined petri-dishes and covered with sterile cell culture medium, supplemented with 1% penicillin-streptomycin solution. A small incision in the dorsal epidermis above the foregut allowed sufficient access of drugs to the developing ENS during the whole culturing period. The NO-synthase inhibitor 7-nitroindazole (7-NI) was dissolved in DMSO and applied at a final concentration of 500 μ M providing not more than 0.1% DMSO in the culture medium. For a control culture 0.1% DMSO was added to the cell culture medium. Following 24 h incubation at 30 °C, guts were dissected out of the embryos and prepared for anti-cGMP or anti-tubulin double immunohistochemistry with anti-serotonin.

To quantify cell migration on the midgut surface, the distance from the foregut-midgut boundary to the position of the leading migrating midgut neuron and to the end of serotonin-IR was measured. A Mann-Whitney U-test was employed for statistical comparisons of the means of the experimental and the control groups. Numbers are given as mean \pm S.E.M. throughout the text.

Results

Structure of the enteric nervous system

Our observations are based on examination of 223 embryonic and 24 postembryonic enteric nervous systems. In Fig. 1A, we illustrate the structure of the enteric nervous system (ENS) of a newly hatched *Locusta* nymph and indicate the distribution of serotonin immunoreactivity.

The alimentary canal of the locust comprises the foregut with the esophagus, pharynx, and the large, expandable crop, the midgut with six blind sacks or caeca, and the hindgut (Fig.1). With the exception of the most anterior section of the esophagus, the digestive tract is innervated by two neural plexus and four enteric ganglia, together forming the enteric nervous system (ENS). The most anterior enteric ganglion, the frontal ganglion, is connected to the brain via the frontal connectives – the only major connection of the ENS to the central nervous system. The recurrent nerve connects the frontal ganglion with the hypocerebral ganglion, which is connected to the paired ingluvial ganglia via the esophageal nerves. From each ingluvial ganglion, two main nerves project posterior along the midgut and give rise to the midgut plexus. Five other nerves leave the ingluvial ganglia to innervate the foregut, the caeca, and connect to the other ingluvial ganglion via a ventral commissure (Fig. 1A, B).

Serotonin and SERT in the ENS

In postembryonic locusts, serotonin-immunoreactivity is observed in the entire ENS with exception of the most anterior part of the esophagus (Fig. 1A). The neuropil cores of all four enteric ganglia contain a dense meshwork of varicose fibres. Serotonergic fibres with marked varicosities appear to be evenly distributed throughout the entire meshworks of both foregut and midgut plexus, and on the caeca. There are very few (2-4) serotonin-immunoreactive fibres originating in the tritocerebrum that reach the frontal ganglion via the frontal connectives - the vast majority of serotonin-immunoreactivity arises from neurons in the ENS itself. The frontal ganglion contains about 40 serotonergic cells, only occasionally 1-3 serotonin-like immunoreactive neurons were seen in the ingluvial ganglia, and

none at all in the hypocerebral ganglion. In some preparations, several immunopositive cells were detected in the region of the hypocerebral ganglion, but confocal analysis showed that they belonged to the retrocerebral complex, which is in close apposition with the hypocerebral ganglion but has no direct connection to it. In the postembryonic ENS, serotonergic cell bodies are quite big (20-40 μm diameter), with a large cytoplasmic compartment.

In the embryo, the first few serotonin-immunoreactive cell bodies are detectable at, or just before, 50% of development. Then, immunoreactivity is very weak and hardly discernable from background. In order to improve the staining quality, we utilized the fact that in most animals, serotonergic neurons express a specific serotonin-reuptake transporter (SERT), which is well characterized in mammals and *Drosophila* (Barker et al., 1998) and which is also present in the locust (Condrón, 1999). We incubated guts and nervous systems of 50% embryos with 5 μM serotonin in L15 media for 10 minutes prior to fixation. To our surprise, not only the morphology of the serotonergic neurons was now clearly revealed, but a lot more cells were stained in preincubated preparations (at 50%: 30.35 ± 0.75 , $n=14$, as opposed to 3.13 ± 1.26 , $n=8$, in preparations without 5-HT preincubation, Fig. 2). It appears as if, at this stage, many cells that do not yet synthesise serotonin already express the serotonin transporter. We then went back to earlier stages and tested for SERT expression. The first stage where serotonin-immunoreactivity was observed after 5-HT preincubation was at 40% of embryonic development (Fig. 2, 3B, C). At this stage we saw 2.4 ± 0.43 immunoreactive cell bodies in the frontal ganglion ($n=20$). No positive cells were observed in control preparations without preincubation ($n=8$) (Fig. 3D, E). To exclude the possibility of unspecific uptake of serotonin, we blocked SERT activity with the specific antagonist Fluoxetine, also known as Prozac[®]. When incubated in 200 μM Fluoxetine together with 5 μM 5-HT, serotonin-immunoreactivity was completely abolished (Fig 3F, G). At lower concentrations of Fluoxetine (20 μM), some residual immunoreactivity remained (not shown). The same concentration of Fluoxetine (200 μM) that was needed for complete block of SERT in the ENS proved to be necessary and sufficient to block SERT in the serotonergic neurons S1 and S2 of the ventral ganglion chain (data not shown), in which SERT has

been extensively studied (Condrón, 1999). Thus, we assume that the cells expressing SERT are those committed to a serotonergic phenotype. When this experiment was repeated in later stages, serotonin-immunoreactivity was only partially abolished – to the amount of cells that synthesise serotonin at this stage. For instance, at 65%, 19.00 ± 1.61 ($n=5$) frontal ganglion cells showed serotonin-immunoreactivity after treatment with Fluoxetine and 5-HT, which does not differ from 22.5 ± 0.98 ($n=10$) somata counted in untreated preparations ($p>0.05$, Mann-Whitney U-test). For comparison, at the same stage, when incubated with 5-HT alone, 32.85 ± 1.95 ($n=7$) frontal ganglion somata were serotonin-immunoreactive (Fig. 2).

Serotonin in the enteric ganglia

At about 40% embryogenesis, the first few neurons start expressing SERT. Expression is very weak at the beginning, but becomes stronger as the cells migrate from the neurogenic zones on the posterior stomodaeum to the anterior end of the developing frontal ganglion (Fig. 4C, D, F; Fig. 5). The number of SERT-expressing cell bodies increases rapidly to reach a plateau value of 35-40 cells between 55% and 60% development (Fig. 2, 3). Without 5-HT preincubation, the number of serotonin-immunoreactive cell bodies raised from a few cells at 50% (Fig. 2, 5B) to the same plateau around 35 cell bodies, at 80% (Fig. 2). This number persists into adulthood (37 ± 0.57 , $n=3$). Since there are about 100 neurons in the *Locusta* frontal ganglion (Ayali, 2004), roughly 40% of the frontal ganglion cells are serotonergic. Initially, the neurons have a small diameter ($10.5 \pm 0.45 \mu\text{m}$ at 40%, $11.45 \pm 0.37 \mu\text{m}$ at 50%, $n=10$ for all size measurements). At 80%, when all cells have reached their destination and begun serotonin synthesis, a maturational phase begins during which the cells gain size (Fig. 4G, H). At completion of embryogenesis (100%), two clusters of serotonergic neurons could be distinguished by their size and position: a dorsal-anterior group of large diameter cells ($20.2 \pm 0.54 \mu\text{m}$) and a posterior group of smaller cells ($15.1 \pm 0.61 \mu\text{m}$). In adult frontal ganglia, the cells grow even further to a diameter of $39.8 \pm 0.7 \mu\text{m}$ (anterior cells) and $18.9 \pm 0.54 \mu\text{m}$ (posterior cells). It is this differential growth of the cell bodies, together with expansion of the neuropil that transforms the

initially oval ganglion into its characteristic pear-shape in the adult. Unlike the serotonergic neurons in the frontal ganglion of *Manduca*, the size of which decreases after an initial phase of increase (Radwan et al., 1989) serotonergic ENS neurons of *Locusta* never reduce their diameter.

Between 40% and 45%, the SERT-expressing cells send an axon along the midline through the developing recurrent nerve, which reaches the hypocerebral ganglion at or shortly before 45% (Fig. 4B, C). Many SERT-expressing axons bifurcate in the hypocerebral ganglion, before they leave the ganglion through one or both of the esophageal nerves, around 50%. Between 45% and 50%, an extensive meshwork of immunoreactive fibres is elaborated in the neuropil. Numerous fibres cross the midline through the single posterior commissure of the hypocerebral ganglion which starts to form shortly before 50%. Serotonin-immunoreactive fibres are most abundant in this commissure and the bifurcating tracts, which eventually leave the ganglion through the esophageal nerves, whereas the most central part of the ganglion is innervated by relatively few serotonergic fibres (Fig. 4E, F).

In the ingluvial ganglia, no consistent serotonin-immunoreactive cell bodies were found. Only occasionally (in 6 out of 42 preparations), 1-3 cell bodies per ganglion showed faint SERT activity in 50-80% embryos (see Fig. 6C, open arrow, for a rare example of a positive neuron without 5-HT-preincubation). No immunoreactive cells were found in ingluvial ganglia of later stages. The first serotonin-immunoreactive fibres reached the region of the developing ingluvial ganglion at 50% (Fig. 6A; 5B) to immediately bifurcate into a dorsal and a ventral branch. Those branches grow in size, leave the ingluvial ganglion between 50% and 60% (Fig. 6B), and will eventually give rise to the four main nerves that run along the entire midgut (Fig. 1). Other branches follow and leave the ingluvial ganglion through nerves that innervate the crop and the caeca. Later, the serotonergic axons ramify and form a dense meshwork of arborisations in the neuropil of the ingluvial ganglia, which appears mature at 80% (Fig. 6C) and only slightly grows until hatching (Fig. 6D). In all four ganglia, the serotonergic arborisations acquire varicosities, which appear to be evenly distributed throughout the neuropil areas by 80% (Figs. 4G, H; 6C, D).

Serotonin in the foregut and midgut plexus

The mature foregut plexus consists of an irregular meshwork surrounding the crop (Fig. 1A, 7C), originating from the ingluvial ganglia and the esophageal nerves, and a less extensive network on the esophagus and pharynx, originating from the frontal ganglion and in some cases from nerve roots emerging out of the recurrent nerve directly posterior to the frontal ganglion. One or two ventral commissure-like connections connect the ingluvial ganglia (Ganforina et al., 1996), which appear to be quite variable and can be fused in some preparations. Serotonergic neurites can be found in all major branches of the foregut plexus (Fig. 1A; 7B, C). The foregut plexus begins to develop between 55% and 60% (Ganforina et al., 1996). Whereas the scaffold of the nerve plexus is laid out relatively quickly, displaying all major branches at 65% (Fig. 7A), serotonin-immunoreactive processes follow more slowly. At 65%, serotonergic fibres were only seen in the ventral, commissure-like connection between the ingluvial ganglia (Fig. 7A). At 75%, most major branches of the foregut plexus were innervated by several serotonergic fibres (Fig. 7B). Between 80% and 100%, followed a phase of maturation and the serotonergic fibres acquired numerous varicosities (Fig. 7C).

On the midgut, the serotonergic axons follow the migratory routes of the midgut neurons (Fig. 8). Midgut neurons are born in a neurogenic zone on the stomodaeum and initially migrate to a position just posterior of the developing ingluvial ganglia, where they form four “tongues” from which they would rapidly migrate along four pathways on the midgut that later form the main midgut nerves (Ganforina et al., 1996, Fig. 5B). At 50%, the first growth cones of the serotonergic neurons have just passed the developing ingluvial ganglion and make contact with the migratory tongues (Fig. 6A). Already within the ingluvial ganglion, there is a main bifurcation into the dorsal and ventral midgut nerve roots. At 60%, the serotonergic neurites had followed the migrating midgut neurons to the foregut-midgut boundary, between the budding caeca (Fig. 1B; 6B). During the following phase of midgut neuron migration, serotonergic neurites closely followed along the main midgut nerves without branching (Fig. 8B, D). They started branching at 80% development (Fig. 8E), when the midgut cells ceased longitudinal migration and left the main nerves to form the meshwork of the midgut

plexus. Until hatching, the serotonin-immunoreactive axons followed the meshwork of the plexus (Fig. 8F) and acquired varicosities (Fig. 8G). During the migration of the midgut neurons, serotonergic fibres always stayed in close apposition to the leading cells. This is strikingly different to the situation on the foregut, where serotonergic processes do not arrive before most major branches of the plexus are already laid out (Fig. 7A).

Manipulation of midgut cell migration

It has been shown that midgut neuron migration critically depends on the presence and action of nitric oxide/cGMP (Haase and Bicker, 2003). We made use of this feature to test whether outgrowth of serotonin-containing neurites is independent of migration of midgut neurons. If this were the case, slowing down the midgut neurons by application of an inhibitor of the NO/cGMP-signalling-pathway should not affect the outgrowth of the serotonergic neurons. We visualised migrating neurons by labelling of acetylated α -tubulin (Fig. 8A) or NO-induced cGMP (Fig. 8C). An experimental group of embryos was kept in culture with addition of the NO-synthase inhibitor 7-nitro-indazole (7NI), whereas a control group was incubated in cell culture media with DMSO only. As expected, the migrating cells in the experimental group were significantly delayed – the distance between leading neuron and foregut-midgut boundary was 1.200 ± 0.195 mm, as compared to 2.102 ± 0.214 mm in the control group ($p < 0.01$, Mann-Whitney U-test). In both groups, serotonin-immunoreactive fibres stayed close behind the leading migrating neurons (Fig. 8B, D). The distance between the first serotonin-immunoreactive growth cone and the anterior edge of the first migrating neuron was 370 ± 158.6 μ m in controls and 217.6 ± 71.2 after incubation with 7NI, respectively. The difference was not significant ($p > 0.05$, Mann-Whitney U-test).

Discussion

This study set out to fill the gap between embryological studies of ENS development (Ganfornina et al., 1996; Haase and Bicker, 2003) and histochemical studies of the distribution of one of the main transmitters of the ENS, serotonin (Klemm et al., 1986; Luffy and Dorn, 1992) in orthopteroid insects. We monitored the development of serotonergic neurons in the ENS, beginning at the late stage of their migration from the proctodeal neurogenic zones into the frontal ganglion until maturity in the hatched hopper. To do so, critically depends on being able to detect the neurons during early stages of embryogenesis.

Correspondence of SERT-expressing and serotonin-synthesising neurons

Unlike the situation in the CNS, where the serotonergic neurons S1 and S2 express the homeobox gene *engrailed* throughout their development (Condrón, 1999), serotonergic neurons in the ENS do not express *engrailed* (own unpublished data), and we have no other independent marker for them that would allow us to unequivocally determine their identity before they begin to synthesise serotonin. However, the serotonin transporter SERT is expressed significantly before the beginning of serotonin synthesis in the CNS (Condrón, 1999), and can be used to identify serotonergic neurons by means of preincubation with serotonin before fixation. Here, we show that the serotonergic ENS neurons of *Locusta* share this feature. When ENS neurons were incubated in 5 μ M serotonin, it was quickly taken up from the culture medium. Uptake was completely blocked by the specific SERT inhibitor Fluoxetine at an effective concentration that could be expected from uptake inhibition studies using heterologously expressed recombinant *Drosophila* SERT protein (Barker et al., 1998). This indicates a specific serotonin uptake transporter. Only serotonergic neurons express SERT, and even if SERT is ectopically expressed in other neurons, only very few cells which employ other biogenic amines as transmitters are capable of specifically taking up serotonin (Park et al., 2006). Moreover, the number of SERT-neurons in our stainings of the frontal ganglion did not at any time exceed the maximum number of serotonergic neurons found at later stages. Instead, the number of serotonin-synthesising cells approached the number of SERT-neurons

asymptotically, reaching the plateau value between 60% and 80% development, when the phase of migration and initial neurite outgrowth was completed. This, together with the very good morphological correspondence between SERT-activity and native serotonin-immunoreactivity, points to the identity of SERT-expressing and serotonin-synthesising cells.

Possible physiological role of serotonergic neurons

There is evidence for the enteric ganglia being targets of serotonergic modulation from several preparations. In the lobster stomatogastric system, serotonin can influence the pattern of motor rhythms even in the embryo (e.g. Richards et al., 2003). In the stick insect, both frequency and amplitude of rhythmic contractions are increased by serotonin application in a midgut preparation with the ingluvial ganglia attached (Luffy and Dorn, 1992). In midgut preparations without ganglia, application of 5-HT causes a strong, tonic contraction in the stick insect (Luffy and Dorn, 1992). In the locust, on the other hand, serotonin causes relaxation in isolated midgut tissue and modulates proctolin-induced contractions (Molaei and Lange, 2003). Despite this considerable variability of serotonin action between species, these physiological data, together with the varicose appearance, indicate that the serotonergic terminals on the gut are output sites. Whether this is also the case for the varicose terminals in the enteric ganglia is less clear. Serotonin-induced changes in rhythmic contractions of stick insect midguts with attached ganglia indicate a modulatory role of the serotonergic neurons as well. Unfortunately, there is only sparse information about the physiology of insect enteric neurons on the intracellular level (Ayali, 2004), which is confined to cells of the frontal ganglion. We do not know where the input sites of the enteric neurons are, nor do we know which neurons may be presynaptic to them. There appears to be some inhibitory input from the brain, since isolated frontal ganglia show spontaneous rhythmic patterns only when the connection to the brain is severed (Ayali, 2004). Proprioceptive inhibition to the locust enteric pattern generator has been demonstrated both for feeding behaviour (Bernays and Chapman, 1973) and crop inflation during molting (Ayali, 2004). In *Manduca*, roughly one third of the -

presumably sensory - midgut neurons contain FMRFamide (Copenhaver and Taghert, 1989a). On the locust midgut however, FMRFamide is located mainly in neuroendocrine cells and in efferent fibres originating in the frontal ganglion (Hill and Orchard, 2003). How serotonergic neurons are embedded into the neuronal network controlling the gut remains unclear until further electrophysiological and pharmacological observations.

Early expression of SERT

We have shown that SERT is expressed long before the ENS neurons have acquired their final shape and even before they have finished migration into the frontal ganglion (Fig. 3, 4, 5). This contrasts to FMRFamide-containing neurons of the midgut of *Manduca*, which acquire their peptidergic phenotype only after completion of migration (Copenhaver and Taghert, 1989a). This indicates that local cues of the target tissue cannot be the only signals that determine the neurotransmitter phenotype in the serotonergic neurons of the locust ENS. In the *Drosophila* CNS, a serotonergic phenotype depends on transcription factors such as *engrailed* and *eagle* (Lundell and Hirsh, 1998). In the grasshopper CNS, an FGF2-like signal is involved in developing SERT expression (Condrón, 1999). Whether any of these factors are involved in determination of neurotransmitter phenotype in the ENS remains to be investigated.

Early expression of SERT, before the onset of serotonin synthesis, appears to be quite common among serotonergic neurons in various species. It is reported from the CNS of the grasshopper (Condrón, 1999), *Drosophila* (Valles and White, 1988), and from the ENS of the lobster (Richards et al., 2003). Whereas in the embryonic lobster ENS, serotonin taken up from the hemolymph and released by SERT-expressing neurons could play a possible physiological role (Richards et al., 2003), this is not likely in the 40% locust ENS, because at this stage the neurons do not yet have a peripheral arborisation and show only very limited branching in the enteric ganglia. More likely is a developmental role of serotonin, as a possible regulator of ENS formation.

Regulators of ENS development

Despite the common developmental origin from a neuroepithelial placode in the foregut, the insect enteric nervous system exhibits quite extensive variations in the detailed pattern of migration and design of neural connections (Hartenstein, 1997; Ganfornina et al., 1996). For example, whereas in *Manduca*, specific sets of visceral muscle bands support migration of the enteric neurons on the midgut (Copenhaver and Taghert, 1989b; Copenhaver et al., 1996; Wright et al., 1998) no morphologically distinct muscle bands can be recognized along the migratory pathways in the grasshopper embryo (Ganfornina et al., 1996). Instead, the migratory neurons move parallel to the longitudinal muscle bands directly on the surface of the midgut. In *Manduca*, different isoforms of the cell recognition molecule Fasciclin II mediate distinct aspects of the migration process, such as adhesion, fasciculation and the promotion of motility. These results can be deduced from the transient expression of Fasciclin II molecules on the muscle bands coinciding with the active period of cell migration, in vivo manipulations using blocking antibodies, antisense oligodeoxynucleotides and other types of perturbation techniques that interfere with the different isoforms (Wright and Copenhaver, 2000). Similar types of perturbation experiments have not been performed in the grasshopper embryo, but it is evident that the expression pattern of Fasciclin II on the midgut looks quite different during cell migration in the grasshopper and *Manduca* (Ganfornina et al., 1996; Wright et al., 1999; Knipp, unreported data).

Other regulators of cell migration and branching patterns appear to be NO and cGMP (Wright et al., 1998; Haase and Bicker, 2003). Midgut neuron migration is delayed by perturbing the NO/cGMP-pathway in locust embryos (Haase and Bicker, 2003). In the present study, we show that growth of serotonin-immunoreactive neurites on the midgut is also delayed by inhibiting NO-synthase. This can be explained by a *pioneering* character of the migrating neurons which lay down the pathway for the following components of the nerve plexus. Slowing down midgut neuron migration by inhibiting the NO/cGMP-pathway would then slow down the outgrowth of serotonergic fibres as well. Alternatively, NO could be a growth-promoting factor in the serotonergic fibres themselves, independent of

the migrating midgut neurons. This possibility cannot be ruled out, but it seems unlikely. The serotonin-containing cells do not show NO-stimulated cGMP-immunoreactivity. Also, in most vertebrate and invertebrate preparations, NO induces growth cone collapse (Hess et al., 1993) and slow-down and search behaviour of growth cones rather than increased growth rates (Trimm and Rehder, 2004). Since the serotonin-containing neurites always remained close to the leading edge of midgut neuron migration, we suggest that the soma migration of the midgut cells is a critical step preceding serotonergic fibre outgrowth.

Serotonin as possible modulator of ENS development

Dopa decarboxylase mutants of *Drosophila* are deficient in the synthesis of serotonin and dopamine. This defect leads to an abnormally extensive branching of serotonergic fibres on the midgut that can be partially rescued by feeding dopamine (Budnik et al., 1989). Biogenic amines, and in particular serotonin, have been shown to regulate neurite outgrowth and branching in various invertebrate preparations (Diefenbach et al., 1995, Koert et al., 2001). In most cases, such a regulative effect of serotonin has been shown to affect serotonergic neurons themselves, in an autoregulatory fashion. However, olfactory interneurons of the lobster embryo, which do not contain serotonin themselves, are affected by depletion of 5-HT from the brain in several ways: reduced proliferation and survival, and inhibition of branching.

Here, we show that serotonin is expressed early in the developing ENS of the locust. Serotonin synthesis commences at 50%, foregut motility at around 70% (own unpublished observations). On the midgut, serotonergic neurons immediately follow the migrating cells that lay down the midgut plexus (Fig. 8), whereas midgut peristalsis starts much later, after 80%. This implies that serotonin may have functions other than promoting gut motility. The close spatial relationship between serotonergic growth cones and migrating neurons would allow for mutual interactions on the midgut. A striking feature of midgut plexus development is the division in two distinct phases: (1) a phase of straight migration of midgut neurons, and following of outgrowing neurites originating in the enteric ganglia, along the four main nerve tracts, and (2) a phase of branching from those main tracts and

formation of the plexus proper (Haase and Bicker, 2003). In *Manduca*, midgut plexus branching is regulated by NO (Wright et al., 1998). In the locust, it could be possible that serotonin is involved in delaying branching during midgut plexus development. Such inhibition of neurite branching by serotonin has been shown, for instance, in the snail *Helisoma* (Diefenbach et al., 1995).

On the locust's foregut plexus, which develops in a less stereotyped fashion, serotonin-containing fibres arrive much later than the migrating neurons, and cannot contribute to regulation of the initial layout. Here, numerous branchings occur during the whole period of plexus formation, resulting in a final morphology far more variable than that of the midgut plexus. Since the development of the locust enteric plexus can be manipulated in an embryo culture system (Haase and Bicker, 2003), it will be possible to test whether biogenic amines do also regulate the morphology of enteric neurons in a simple hemimetabolous insect.

Acknowledgments

We thank Dr. J. de Vente for his gift of the anti-cGMP antiserum. We are grateful to the Department of Microbiology, University of Hannover, for access to their confocal microscope. We thank Mrs. Sandra Ammersdörfer for help with initial experiments in this study.

Grant sponsor: Deutsche Forschungsgemeinschaft, Grant number Bi262/10-4

Figures

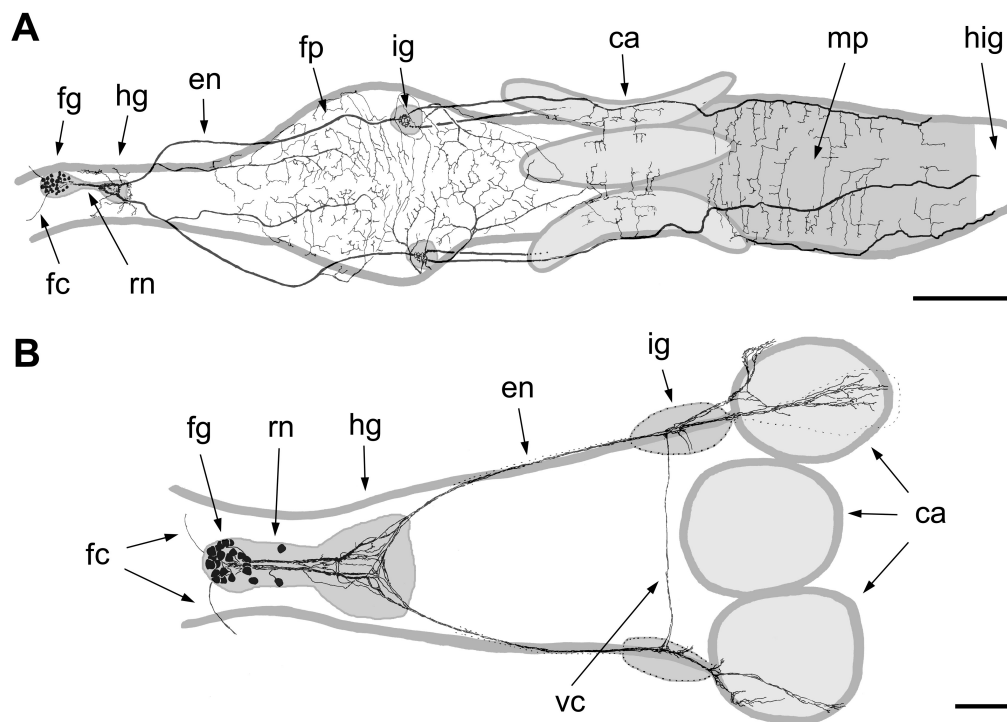


Figure 1: Layout of the serotonergic system in the ENS of *Locusta migratoria*.

A: Dorsal view of fore- and midgut of a newly hatched first instar with the major serotonergic processes indicated. Camera lucida drawing after labelling with anti-serotonin. **B:** Dorsal view of the developing serotonergic system on the foregut of a 60% *Locusta* embryo, drawn after labelling with anti-serotonin. The midgut is shaded dark grey, enteric ganglia and the caeca (in A) are shaded light grey. ca: caecum, en: esophageal nerve, fc: frontal connective, fg: frontal ganglion, fp: foregut plexus, hg: hypocerebral ganglion, hig: hindgut, ig: ingluvial ganglion, mp: midgut plexus, rn: recurrent nerve, vc: ventral commissure, scale bar 500 μm (A), 100 μm (B), anterior is to the left.

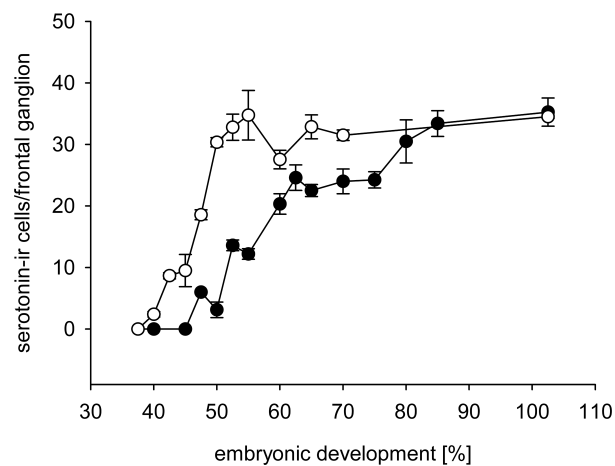


Figure 2: Embryonic development of SERT and serotonin-synthesis in the frontal ganglion.

Each data point is the average number (\pm S.E.M.) of serotonin-immunoreactive cells of at least 3 (typically 5-10) preparations either with 10 min preincubation with 5 μ M 5-HT (open circles) or without preincubation (filled circles). Freshly hatched first instars are assigned a stage of 102.5%.

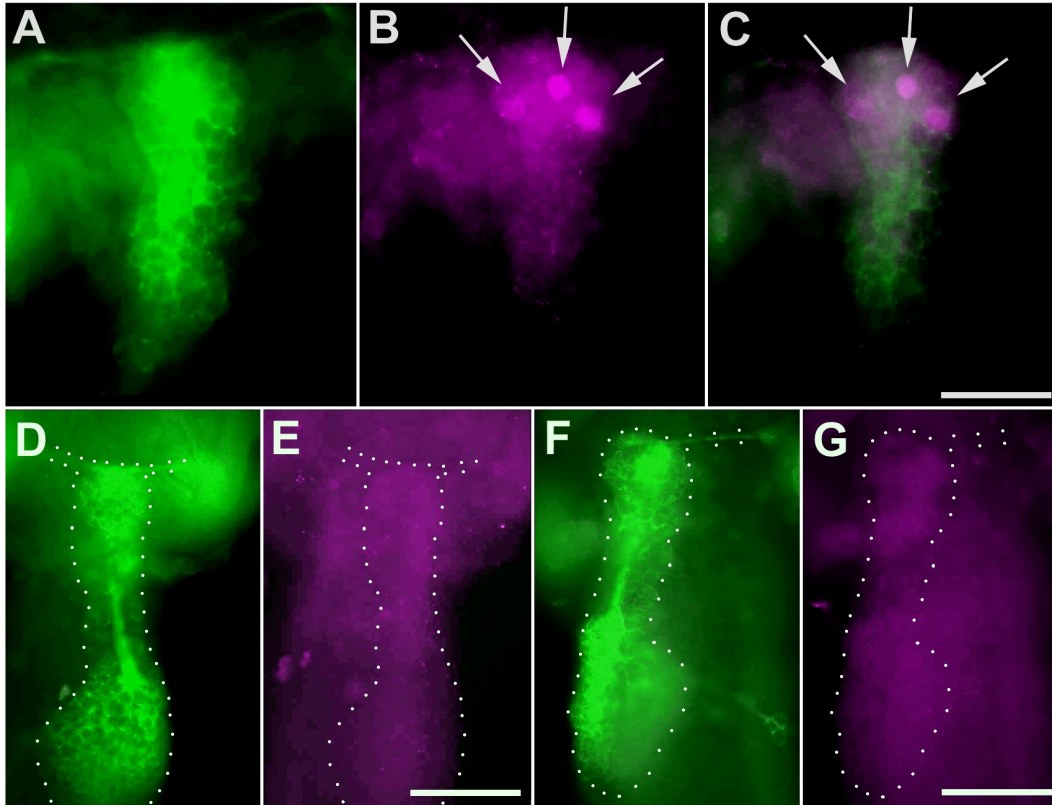


Figure 3: Serotonin uptake activity (SERT) in the 40% ENS.

Dorsal views of fluorescence images of 40% embryonic foreguts (green: anti-HRP, magenta: anti-serotonin). **A-C**: After preincubation in 5 μ M 5-HT, three serotonin-immunoreactive cell bodies are seen (arrows). C is an overlay of A and B. **D-E**: No serotonin-immunoreactive cell bodies are seen without 5-HT preincubation. **F-G**: When preincubated with 200 μ M of the SERT-blocker Fluoxetine in addition to 5 μ M 5-HT, again no serotonin-immunoreactive cell bodies are visible. Scale bar: A-C: 50 μ m, D-G: 100 μ m, anterior is to the top.

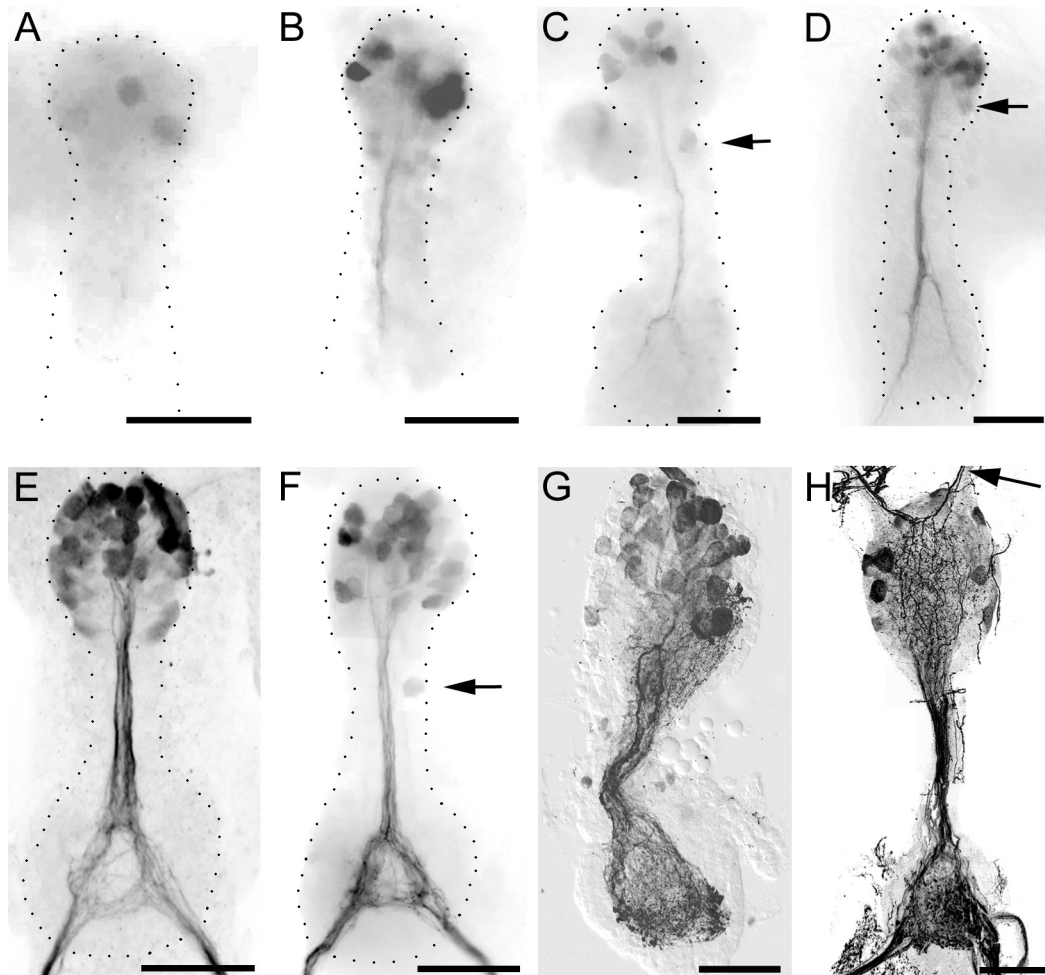


Figure 4: SERT and Serotonin in the frontal and hypocerebral ganglia during embryonic development.

A: 40%, **B:** 43%, **C:** 45%, **D:** 47%, **E:** 50%, **F:** 53%, **G:** 80%, **H:** freshly hatched first instar nymph. Dorsal views of inverted fluorescence (A-D, F) or confocal (E, G, H) images (in D and G combined with Nomarski-images) of frontal and hypocerebral ganglia stained for serotonin (after preincubation with 5 μ M 5-HT in A-F, without preincubation in G-H). Dotted outlines indicate the border of the ENS, arrows in C, D, F indicate weakly immunoreactive neurons which have not yet finished anterior migration, arrow in H indicates serotonin-immunoreactive fibres in the frontal connective. Scale bar: 50 μ m (A-D), 100 μ m (E-H), anterior is to the top.

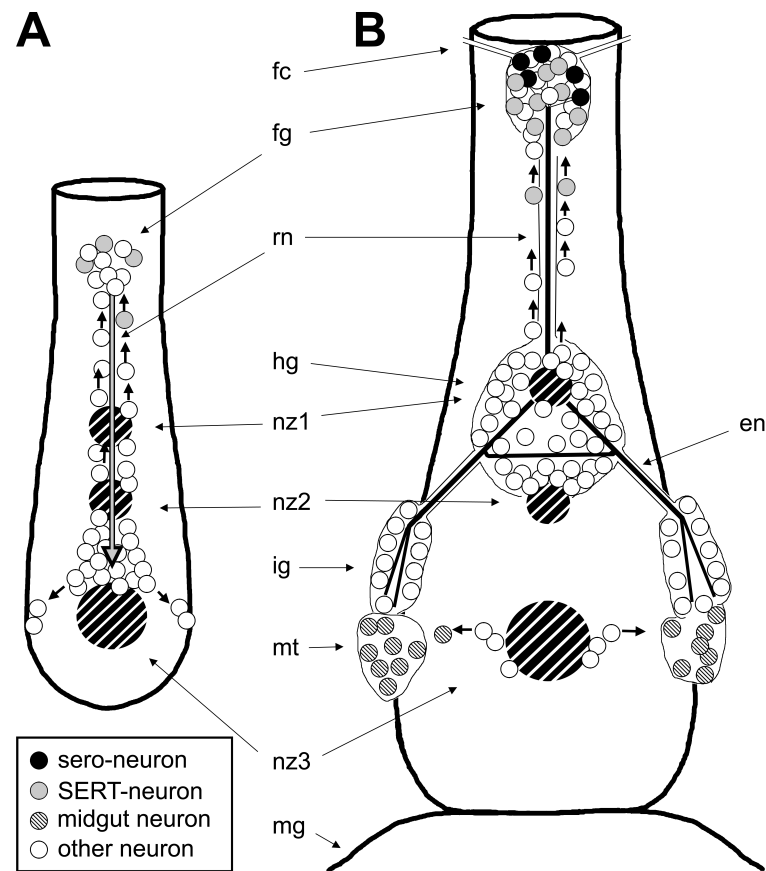


Figure 5: Schematic diagram of dorsal views onto the foregut and developing ENS at 40%.

(**A**) and 50% embryogenesis (**B**). The direction of cell migration is indicated by arrows. The large grey arrow in A indicates elongating SERT-positive axons. Black lines in B indicate serotonin-immunoreactive axons. Neurogenic zones are depicted as dark hatched circles. en: esophageal nerve, fc: frontal connective, fg: frontal ganglion, hg: hypocerebral ganglion, ig: ingluvial ganglion, mg: midgut, mt: migratory tongue, rn; recurrent nerve, z1, z2, z3: neurogenic zones (placodes), anterior is to the top.

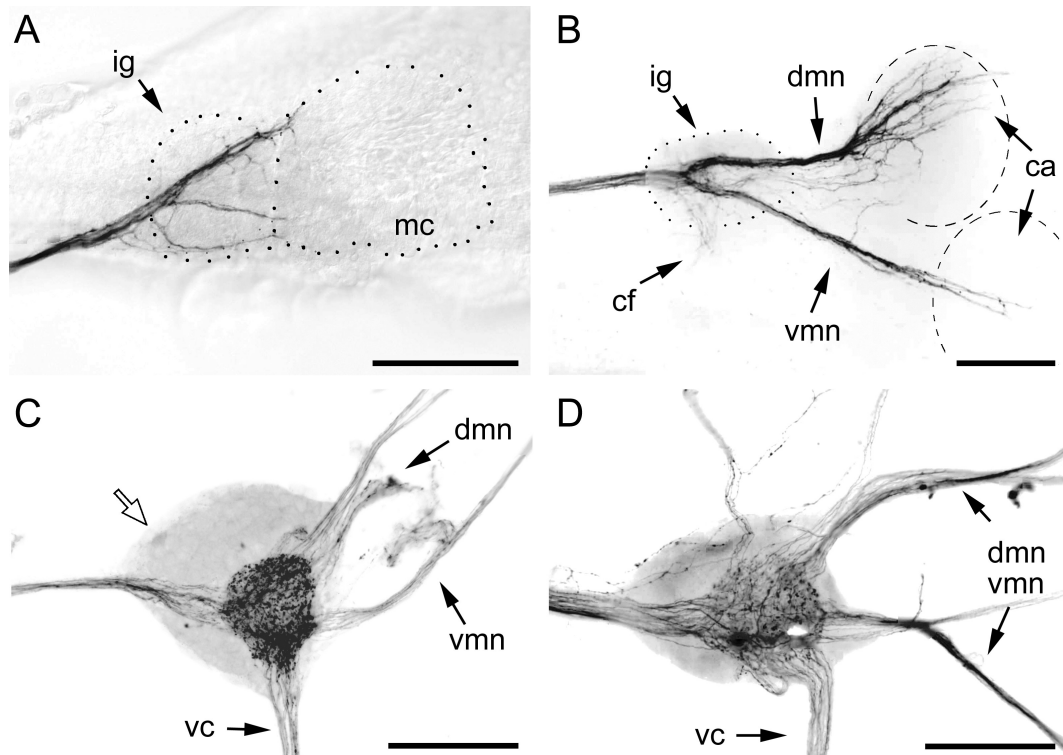


Figure 6: Development of serotonin-immunoreactivity in the ingluvial ganglia.

Lateral views of ingluvial ganglia at 50% (**A**), 60% (**B**), 80% (**C**) and in a first instar nymph (**D**), stained for serotonin (inverse immunofluorescence in A-B, confocal images in C-D, combined with Normarski images in A,C). Only the preparation in **A** was preincubated with 5 μ M 5-HT before fixation. Open arrow in **C** points to a weakly immunoreactive cell. ca: caecum, cf: commissural fibres, dmn: dorsal midgut nerve, ig: ingluvial ganglion, mc: package of migrating midgut neurons, vc: ventral commissure, vmn: ventral midgut nerve, Scale bar: 50 μ m, anterior is to the left.

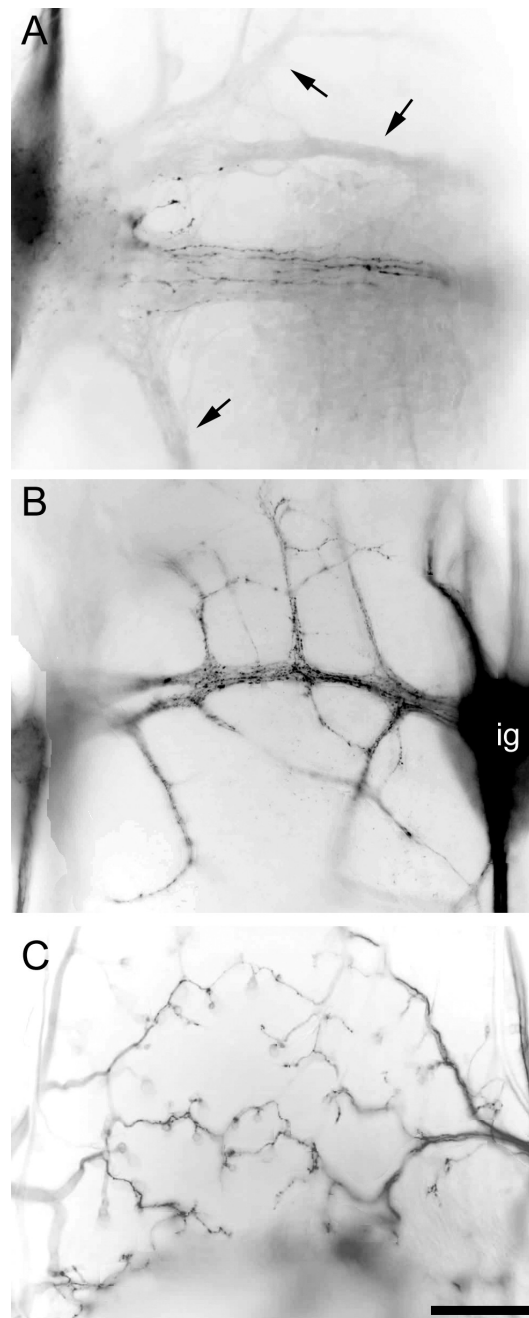


Figure 7: Development of serotonin-immunoreactivity on the foregut plexus.

All figures are inverted fluorescent images of preparations stained for serotonin without preincubation with 5-HT. **A:** 65% embryo, ventral view of the foregut. Serotonergic fibres are projecting through a ventral commissure. The background staining is an anti-HRP-labelling, revealing the extent of the midgut plexus (arrows). **B:** 75% embryo, ventral view. Serotonergic arborisations have invaded all major branches of the foregut plexus. **C:** Newly hatched first instar, dorsal view of the mature foregut plexus with numerous varicosities. ig: ingluvial ganglion, scale bar: 50 μm (A), 100 μm (B-C), anterior is to the top.

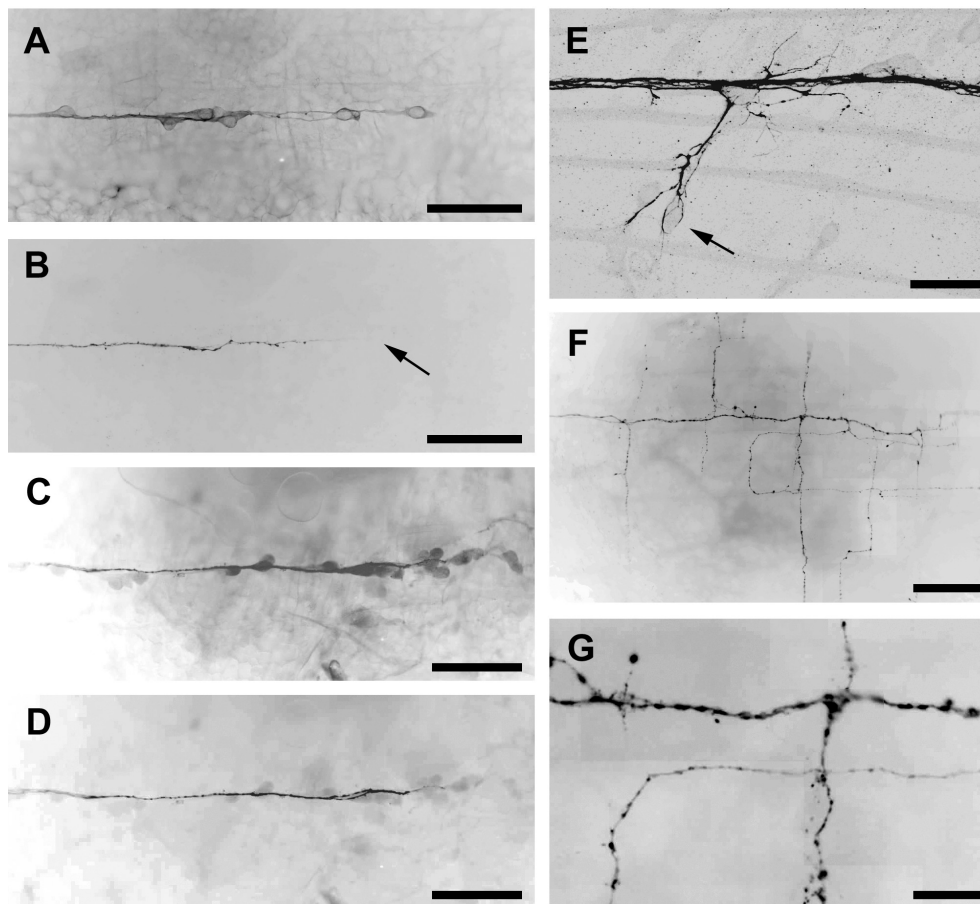


Figure 8: Development of serotonin-immunoreactivity on the midgut plexus.

Inverted fluorescent images of midguts, E is a Confocal image. **A** 65-70%, stained for acetylated α -tubulin, showing the leading edge of midgut cell migration after 24 h incubation in L15 without added drugs. **B** The same preparation as in A, stained for serotonin, arrow points to faintly visible growth cone. **C** 65-70%, stained for cGMP, after 24 h incubation with 500 μ M 7NI, showing the leading edge of midgut neuron migration. **D** The same preparation as in C, stained for serotonin. **E** 80% embryo, midgut stained for serotonin. The longitudinal structure of the developing visceral musculature is faintly visible in the background. Arrow points to a migrating midgut neuron that has left longitudinal pathway, surrounded by serotonergic processes. **F** Midgut of a freshly hatched first instar, stained for serotonin, showing the orthogonal lattice of the plexus. **G** Same preparation as in F, at higher magnification, showing numerous varicosities. Scale bars: 50 μ m (A-D, G), 20 μ m (E), 200 μ m (F).

2.4 A developmental study of enteric neuron migration in the grasshopper using immunological probes.

Sabine Knipp and Gerd Bicker

Manuscript intended for publication.

Abstract

Motility of enteric midgut neurons in the hemimetabolous grasshopper *Locusta migratoria* depends critically on the nitric oxide/cyclic GMP signalling cascade including nitric oxide synthase (NOS) and the target receptor protein soluble guanylyl cyclase (sGC) (Haase and Bicker, 2003). Here, we extend our analysis of nitric oxide (NO) dependent cyclic GMP (cGMP) to the foregut part of the enteric nervous system (ENS). We find that first cGMP immunoreactivity occurs at 45% of embryonic development in the enteric ganglia clearly after the main migratory processes have taken place. The cGMP-IR lasts in the foregut ganglia beyond hatching. Thus, expression of cGMP-IR in migrating neurons is a distinct phenomenon restricted to neurons forming midgut and foregut plexus, that does not occur during convergence of neurons to form the enteric ganglia.

For a better understanding of enteric neuron migration, it would be good to know the involved guidance cues. Therefore, we analysed the anatomical distribution of the cell adhesion molecule Fasciclin I (Fas-I) during midgut development. The cell surface molecule Fasciclin has been shown to mediate fasciculation of grasshopper peripheral nervous system pioneers (Diamond et al., 1993). Antibody blocking experiments show that the epitope recognised by an Fasciclin-I antibody plays no essential role for guidance of enteric neuron migration on the midgut, but the Fas-I molecule may enable fasciculation of the migratory chain and during branching. Analysis of time-lapse video microscopy of migrating enteric neurons together with immunocytochemical data implies that especially the anterior-posterior chain migration may be guided by the midgut musculature.

Keywords

Nitric oxide, cGMP, Fasciclin-I, enteric nervous system, migration, guidance

Introduction

Directed neuronal cell migration is essential for establishing the highly ordered cellular organisation in nervous systems, as neurons are usually born in proliferative zones located separated from their final positions in the mature nervous system (Hatten, 1999; Song and Poo, 2001). The formation of the insect enteric nervous system (ENS) resembles in certain aspects the development of vertebrate nervous systems. Neuronal precursors emerge from proliferative zones in the foregut epithelium and perform quite extensive cell migrations before they assemble into discrete peripheral ganglia and gastric nerve plexus (Hartenstein, 1997). But unlike to developing vertebrate nervous systems the number of neurons is rather limited and single neurons can be easily followed. The genetic and cellular bases of neuronal specification, guidance cues for directed cell migration, and differentiation towards neuronal phenotypes during the ENS development in insects has been particularly well investigated in *Drosophila* and *Manduca* as well as in the grasshopper (Copenhaver and Taghert, 1989a,b; Hartenstein et al., 1994; Ganformina et al., 1996). Thus, the developing insect ENS provides a useful and robust model to study the cell biology of neuronal migration (Copenhaver, 2007).

In preceding studies we focused on the enteric neuron migration during midgut plexus formation in the *Locusta migratoria* embryo (Haase and Bicker, 2003; Stern et al., 2007; Knipp and Bicker, 2009). Neuronal motility along the migratory pathways of the midgut depends critically on the nitric oxide/cyclic GMP signalling cascade including nitric oxide synthase (NOS) and the target receptor protein soluble guanylyl cyclase (sGC) (Haase and Bicker, 2003). It is negatively regulated by carbon monoxide, another gaseous bioactive molecule (Knipp and Bicker, 2009). Nitric oxide (NO) has been reported to be a key signalling molecule during nervous system development (Truman et al., 1996; Peunova et al., 2001, Chen et al., 2004; Bicker, 2005; Krumenacker and Murad, 2006; Godfrey et al., 2007). In particular, the downstream acting cyclic nucleotide cGMP is implicated as intracellular mediator of growth cone behaviour both in vertebrate and invertebrate nervous systems (Gibbs and Truman, 1998; Polleux et al., 2000; Seidel and Bicker, 2000; Song and Poo, 2001; Van Wagenen and Rehder, 2001; Schmidt et

al., 2004; Demyanenko et al., 2005; Gutierrez-Mecinas et al., 2007; Tornieri and Rehder, 2007; Stern and Bicker, 2008).

In the locust embryo virtually all migrating enteric neurons exhibit a strong NO inducible cGMP-immunoreactivity (cGMP-IR) during midgut plexus formation (Haase and Bicker, 2003). Comparatively little is known about the onset and distribution of NO sensitive sGC activity on the developing foregut of the locust embryo. Here we present data illustrating the first appearance of cGMP-IR in the frontal ganglion during the first half of locust embryonic development. Even though NO dependent sGC activity is increasing fast in additional neurons of the enteric ganglia and in foregut nerves, migrating cGMP-IR positive neurons occur only during formation of foregut and midgut plexus.

For a better understanding of enteric neuron migration, the identity of extracellular guidance cues for the accurate anterior-posterior migration or the lateral branching during midgut plexus formation would be supporting. Migratory enteric neurons have been shown to express different cell surface glycoproteins that may serve as guidance cues, including Fasciclin-I (Fas-I) and Semaphorin 1 (Sema-1) (Ganformina et al., 1996). Fasciclins are cell adhesion molecules that have been shown to mediate fasciculation of locust peripheral nervous system pioneers (Bastiani et al., 1987; Diamond et al., 1993). The analysis of the detailed regional distribution of Fas-I on migrating enteric neurons and blocking experiments of the Fas-I antigen implied a role for neuron fasciculation, rather than for a guidance molecule of pioneering enteric neurons. Using time lapse video microscopy we show that the directed migration of enteric neurons seem to be hemmed by the longitudinal muscle fibres. The lateral branching during formation of the midgut plexus at later stages occurs along circumferential muscle fibres. Thus, we propose that crucial guidance factors both for the posterior and the laterally directed cell migration may be found in the extracellular matrix of the midgut musculature.

Results

Nitric oxide dependent cGMP-immunoreactivity during early development of the locust enteric nervous system

In the first half of ENS development the active neuronal migration on the locust stomodeum can be divided into three main phases (Ganfornina et al., 1996). We have illustrated these phases schematically in figure 1A and B, upper panel. The developmental timing for the onset of each phase does not differ remarkably from *Schistocerca americana* to *L. migratoria*, thus we have adopted the classification that was already described (Ganfornina et al., 1996): A first anteriorly directed migratory phase starts at 31% E and is followed by two lateral migratory phases starting at 38 and 40% E respectively, leading to the formation of the foregut enteric ganglia and aggregation of the midgut enteric neurons.

During the first anteriorly directed migratory phase in *L. migratoria* (indicated by arrow in fig. 1A), newborn cells acquire their neuronal phenotype just after they have initiated migration (Fig. 2A). This can be visualised by labelling with the general insect neuron marker anti-HRP (Jan and Jan, 1982). While migrating on the foregut, the neurons avoid crossing the respective anterior neurogenic zones, leaving the neurogenic zones Z1 and Z2 as open areas (Fig. 2A). At this time point of development we could not detect nitric oxide induced sGC activity on the developing foregut (Fig. 2B). During the second phase of migration, neurons from the hypocerebral ganglion migrate bilaterally and form the prospective ingluvial ganglia (Fig. 1B). Again these neurons are clearly visible with anti-HRP (Fig. 2C, arrowhead), without showing cGMP-IR (Fig. 2D, arrowhead). In the last main migratory phase on the foregut, commencing at 40% E, future midgut plexus neurons detach from the highly active neurogenic zone Z3, migrate bilaterally, and aggregate at the caudal region of the prospective ingluvial ganglia (Fig. 2E). We found a distinct anti-HRP labelling in these neurons, that increase successively during departure from Z3 (arrowheads in Fig. 2E). The prospective enteric midgut neurons retain this HRP-IR during all further cell migrations and the whole midgut plexus development. Similar to the previous migratory processes during ENS development on the foregut, these neurons still do not exhibit NO dependent cGMP immunofluorescence (Fig. 2F).

The first nitric oxide induced sGC activity becomes visible at around 45% E when the embryo undergoes katarrepsis. Two adjacent neurons of the anterior frontal ganglion and their posteriorly directed (fasciculated) neurites in the prospective recurrent nerve acquire rather rapidly a cGMP-IR (Fig. 2H). Only in four preparations out of 22, a single neuron expressed cGMP-IR (insets in figure 2G, H). Axons of the two initial cGMP-IR positive neurons elongate along the recurrent nerve, bifurcate in the hypocerebral ganglion and extend along the nascent esophageal nerve towards the bilateral ingluvial ganglia (Fig. 2I). The neuropils of the ingluvial ganglia are reached between 50-55% E (Fig. 3A). During subsequent development additional cGMP positive neurons in the frontal- and from 50-55% E onwards also in the hypocerebral ganglia become visible (Fig. 2I). Some neurons migrating away from the nascent recurrent nerve exhibit now a NO dependent sGC as well and contribute to the establishment of the foregut plexus (open arrow in Fig. 2I).

At about 58% E the young enteric midgut neurons start their posterior migration from the caudal part of the ingluvial ganglia to the foregut-midgut border. At this time point roughly all enteric neurons show a NO sensitive sGC activity, while the neurons of the ingluvial ganglia do not (Fig. 3A, B). Cyclic GMP-IR becomes visible in neurons of the ingluvial ganglia at around 60% E, when the enteric neurons reach the foregut-midgut boundary (Fig. 3C, D). Finally, a majority of the cells and the neuropil in frontal-, hypocerebral-, ingluvial ganglion and associated nerves and foregut plexus are positive for NO dependent cGMP (Fig. 2J, 3E). This immunoreactivity persists in the enteric ganglia at least to the first larval stage (e.g. fig. 3F), while the number of foregut plexus neurons showing a clear NO dependent cGMP-IR decrease.

In summary, all migratory processes during neuronal aggregation for establishment of the foregut ganglia take place without detectable NO dependent cGMP-IR. Only migrating foregut neurons that take part in the establishment of the foregut plexus exhibit a distinct NO sensitive sGC during migration. However, the foregut ENS gains a virtually overall strong cGMP-IR in the ganglia, nerves and plexus during neuronal maturation in the second half of embryonic development.

Posterior chain migration on the midgut

The formation of the midgut nervous plexus starts at 60% E after closure of the gut (Bentley et al., 1979). Enteric midgut neurons aggregate in four tongue-shaped clusters at the foregut-midgut-boundary. At 62-63% E the cells migrate posteriorly on four distinct pathways parallel to the longitudinal musculature (Fig. 1B, lower panel) (Ganfornina et al., 1996; Haase and Bicker, 2003; Knipp and Bicker, 2009). To visualise the migration of enteric neurons we have used time lapse video microscopy of tissue blot preparations from embryonic midguts (Fig. 4). The migrating enteric neurons have a bipolar (lenticular to fusiform) shape with leading processes and opposing trailing neurites. The trailing neurites continuously elongate and keep connected to the ingluvial ganglia, thus giving rise to the midgut nerves.

Pioneering enteric neurons (Fig. 4, left hand panels) frequently contact the muscle fibres with their leading edge filopodia during their navigation and either retract (t0'-t16') or continue along them (t26'; t196'). The neurons usually avoid to cross the musculature while migrating posteriorly. However, if such misrouting has occurred, they continue on the new track which is confined again between two muscle fibres. Later migrating enteric neurons navigate in general along the trailing processes of the pioneering neurons (Fig. 4, right hand panels, t0' or t31') but seem to be also guided by muscle fibres (t6' to t31'). Their trailing neurites fasciculate with already present ones. Visualising the basic components of the enteric neuron cytoskeleton shows a typical growth cone structure at the leading edge (Fig. 5A-C). Actinfilaments are concentrated in filopodia and the peripheral areas of the growth cone and close to the plasmamembrane, while microtubules are abundant in the central cytoplasm, the central domain of the growth cone, and in trailing neurites. The whole posterior migration proceeds in a highly dynamic chain of cells on the midgut (Fig. 5D). Individual cell movement consists of phases of relative fast crawling interspersed with phases of stationary "searching" behaviour, thus resulting in a moderate average cell speed. The neurons travel either in elongated cell aggregates or more dispersed, associated to each other through their cell processes. Some enteric neurons are crawling alongside, overtaking each other (e.g. cell marked with asterisk in figure 4), as well

as hindering following neurons. Moreover, highly motile hemocytes can be observed to join the migratory pathways from time to time, travel along with the enteric neurons – or in the opposing direction – and leaving the pathways again.

Immunocytochemical analysis of migrating enteric neurons during midgut plexus development

Virtually all cells of the four migratory chains on the midgut are labelled for the HRP epitope, confirming their neural phenotype (data not shown). Up to 95% of the migrating enteric cells exhibit a strong NO dependent sGC activity throughout their whole posterior migration and also during most of the time of plexus establishment (Fig. 5). But although we added YC-1 as enhancer of sGC to the preincubation solution for anti-cGMP ICC, some enteric neurons showed no cGMP immunoreactivity (arrows in fig. 5F, H). However, the decrease of NO sensitive sGC activity was substantially postponed after the migratory phase. Even in the freshly hatched first instar larvae some single neurons exhibited NO dependent cGMP (Fig. 5I). Moreover, the relative amount of cGMP positive neurons at 90% E was still comparable to earlier stages in preparations if YC-1 was added. A minimum of 60% up to 80% neurons were cGMP-positive after YC-1 incubation.

To analyse the distribution of possible candidates of guidance molecules for the enteric neurons on the midgut, we focused on glycoproteins that are known to act as cell adhesion molecules, like Fasciclin-I and -II (Fas-I/-II) and Semaphorin 1 (Sema-1). These were already reported to play a role in the ENS development of *Manduca* and *Schistocerca* (Ganfornina et al., 1996; Wright et al., 1999). But neither antibodies against grasshopper Fas-II (Bastiani et al., 1987) nor Sema-1 (Kolodkin et al., 1992) revealed a specific immunocytochemical staining on the locust embryonic midgut, even though the staining pattern of the ventral nerve cord was similar to published data (data not shown). However, immunolabelling of the extracellular glycoprotein Fas-I revealed a comparable staining of neuropils and nerves to *Schistocerca americana* (Ganfornina et al., 1996) on the foregut of *Locusta* embryos (Fig. 6A, B). The migrating enteric neurons on the midgut showed a strong anti-Fas-I labelling (Fig. 6C). Especially the trailing neurites are labelled (Fig. 6D). The cell soma shows at best a faint punctate staining that is

restricted to the cell surface. Most fine cell processes like the filopodia exhibit no Fas-I as additional visualising of the F-actin cytoskeleton shows (Fig. 6E). This becomes even more apparent at the posterior end of a migratory chain. The growth cones of pioneering neurons exhibit no Fas-I at all (compare fig. 6F and G), while the future enteric midgut nerve is brightly stained. However, Fas-I is not necessarily restricted to trailing neurites, as cell in the migratory chain extend Fas-I positive advancing processes. Thus, leading neurons are enwrapped with Fas-I positive neurites from more following neurons (see arrow in fig. 6F and G). To test for a potential physiological role for enteric neuron migration, we have carried out additional *in vivo* culture experiments. Whole embryos were incubated with an excess of the hybridoma 3B11-antibody directed against the Fas-I epitope during enteric neuron posterior migration on the midgut. After 24 hours of *in vivo* culture, treated embryos showed no significant delay of enteric neuron migration on the midgut (Fig. 7A). Quantification of migration errors during posterior migration of enteric neurons on the midgut showed also no difference between control and 3B11-treated animals (Fig. 7B).

Lateral branching and midgut plexus formation

Around 80% E enteric neurons leave the main migratory routes and spread out on the midgut (Haase and Bicker, 2003), thereby forming the almost rectangular midgut plexus. The enteric neuron turning from an anterior-posterior migration to a lateral migration exhibit no Fas-I labelling on their cell soma or leading processes (Fig. 8A, B). However, established lateral branches turn gradually Fas-I positive (arrowhead fig. 8C, D, arrows point to still unlabelled enteric neurons). During on going migration and lateral branching cell somata become visible with the Fas-I staining (arrow in fig. 8E, F), as well as secondary longitudinal branches (data not shown).

Intriguingly, lateral migrating enteric neurons are often found moving along the developing circular muscle fibres (Fig. 9A-C). The branching neurons often keep closer contact with the lateral muscle fibres, either during lateral turning from the main migratory pathway (Fig. 9A), or during lateral migration (Fig. 9B, C). During the formation of terminal processes highly arborised neurites are send out from

enteric neurons and contact the midgut musculature (Fig. 9D, E). At this late stages of midgut plexus maturation the orthogonal meshwork of enteric midgut neurons and their neurites clearly exhibit NO dependent sGC activity. Almost all enteric neurites have acquired a dense chain of varicosities (Fig. 9F, G). Counterstaining with anti-HRP visualises the gridlike structure of muscle fibres on the midgut surface, since the polyclonal HRP antibody does not only produce a specific punctate staining of neuronal extracellular glycoproteins but also an unspecific faint but even staining of muscle fibres. Thus, it becomes obvious that most enteric neurites have grown on or in close vicinity to longitudinal muscle fibres (Fig. 9G).

Discussion

Nitric oxide dependent sGC activity in the developing enteric nervous system.

Migrating enteric midgut neurons have already been shown to exhibit strong NO induced cGMP-staining. Moreover, NO-/cGMP signalling is required for proper enteric neuron migration during midgut plexus formation (Haase and Bicker, 2003; Knipp and Bicker, 2009). Thus, we asked the question, whether NO-/cGMP-signalling may also play a role for enteric neuron migration on the foregut. To answer this issue we have analysed the developmental distribution of NO dependent cyclic GMP in the locust alimentary canal, from the assigned time point of the first occurrence of anti-cGMP staining to the freshly hatched first instar larvae.

The first neurons that have acquired a nitric oxide sensitive sGC can be found in the anterior frontal ganglion (Fig. 2H) at 45% E. In more than 80% of the preparations cGMP labelling appears almost seamless simultaneously in the cell somata and in the posterior axonal elongations of two neighbouring neurons, thus indicating a short term expression of sGC. This time point correlates with the onset of cGMP staining in the ventral nerve cord at 45-50% E (Truman et al., 1996). In the embryonic brain first cGMP neurons can be determined slightly earlier at around 38% E (R. Eickhoff, personal communication). On the locust foregut the development of NO dependent cGMP-IR proceeds posteriorly. The hypocerebral ganglion as well as the ingluvial ganglia are traversed first by cGMP-positive axons, bifurcating in the neuropil, before neurons in the ganglia can be labelled with cGMP antiserum (Fig. 2H-G, 3). This may reflect the anterior-posterior directed maturation delay as it is typical for the developing locust ventral nerve cord (e.g. Truman et al., 1996). The only migrating neurons on the foregut that show a NO dependent cGMP-IR are neurons forming fore- and midgut plexus (Fig. 2I, 3B). Thus, NO/cGMP-signalling is quite unlikely to affect the neuronal convergence leading to foregut ganglia. However, the cGMP-IR in the enteric ganglia does not disappear after hatching, thus it may not be restricted to a developmental function in the enteric ganglia. A NO/cGMP pathway may be active as a neuromodulatory pathway necessary for larval and adult feeding behaviour

comparable to the stomatogastric system of a crab in which the NO-/cGMP cascade is responsible for timing of pyloric- and gastric mill rhythm (Scholz et al., 2001).

The midgut enteric neurons are actually born in the most posterior neurogenic zone (Z3) on the stomodeum beginning at 40% E, migrate bilaterally, and congregate at the caudal part of the ingluvial ganglion (Fig. 1B upper panel, Fig. 2E). In *Schistocerca americana* the (prospective) midgut neurons are not labelled with the general neuronal marker anti-HRP, neither during their lateral migration from Z3 nor while migrating on the midgut (Ganfornina, et al., 1996). In contrast, we find in the *Locusta migratoria* embryo a strong increase in HRP-staining intensity correlating with the distance from Z3 to their caudal ingluvial ganglia assembly area (arrowheads in Fig. 2E). The future midgut neurons do not leave any processes behind (Ganfornina et al., 1996), thus they can be safely discerned from neurons forming the ingluvial ganglia. Furthermore, in tissue blot preparations of the midgut all enteric neurons including the leading neurons can be labelled with anti-HRP until the end of midgut plexus formation (Fig. 5, 9D-G).

We had intensified the cGMP-IR by adding the sGC sensitiser YC-1 to the preincubation solution (Friebe and Koesling, 1998). To rule out, that this compound produces additional cGMP staining patterns, we examined also the cGMP-IR during midgut plexus development. The pattern of sGC activity can be compared with data published by Haase and Bicker (2003), where no YC-1 was used. During the main phase of plexus formation, caudal migration and lateral branching of enteric neurons on the midgut, no apparent difference in cGMP-IR was detected. Staining was restricted to neurons and their processes. Up to 95% HRP positive cells exhibited sGC activity, as was the case after preincubation without YC-1 (Fig. 5E-H). However, additional YC-1 in the preincubation solution shifted the margins of cGMP-IR onset and decrease in the enteric midgut neurons markedly. Anti-cGMP staining could be detected immediately with the onset of enteric neuron migration from the caudal ingluvial ganglion to the foregut midgut boundary at 58% E (Fig. 3B). In contrast, first cGMP-IR became visible only between 60-62% E, when the enteric neurons have already reached the midgut, if the compound was not used (Haase and Bicker, 2003). On the other hand, the decrease of NO

dependent cGMP-IR was delayed from the formation of terminal processes at around 90% E beyond hatching (Fig. 5G-I, 9D-G). This is in contrast to a drastical reduction to less than 30% cGMP positive cells if the sGC sensitising compound was left out (compare fig. 1 in: Haase and Bicker, 2003). Thus, addition of YC-1 expands the time of sGC sensitivity to NO in midgut neurons, rather than arises sGC activity in additional cells. For instance, concentration of soluble guanylate cyclase may be low at the onset of enteric midgut neuron migration, so that stimulation with nitric oxide alone is not sufficient to rise cGMP levels to a detectable concentration.

The topical immunocytological data and the preceding pharmacological manipulation of midgut enteric neuron migration together suggest an additional purpose of the NO/sGC/cGMP pathway on the foregut than on the midgut. The timing and duration of NO induced cGMP-IR suggests a neuromodulatory function of this signalling cascade. Intriguingly, nitric oxide sensitive sGC appears on the foregut clearly after convergence of neurons forming the enteric ganglia, while it is present from the onset of migration in neurons spreading out to establish the nerve plexus on the midgut and on the foregut.

Chain migration and lateral branching on the midgut.

To visualize midgut enteric neuron migration without movement artefacts from the gut, we used time-lapse video microscopy from living tissue blot preparations. In this method the surrounding musculature and at least parts of the extracellular matrix of the midgut epithelium adhere together with the enteric neurons on the coated cover-slip. This allows microscopic visualisation in one focal plane. What is more, this arrangement appears to preserve posterior migration. The highly motile chain of neurons migrate on the midgut surface between two longitudinal muscle fibres (Fig. 4). Enteric neurons show a saltatory pattern of migration with periods of fast movement (not necessarily in posterior direction) interspersed from periods with a static cell nucleus and highly motile processes, indicating a stop and search behaviour. The neurons are arranged along the longitudinal chain in small groups or just as well isolated (Fig. 5D, 6C). This mode of migration resembles the chain migration of neuronal precursors along the rostral migratory stream (RMS) from

the subventricular zone (SVZ) to the olfactory bulb in rodents (Lois et al., 1996; Wichterle et al., 1997). Interestingly, migrating neuroblasts of the RMS seem to possess a NO sensitive sGC (Gutierrez-Mecinas et al., 2007). Moreover, in vitro data from SVZ tissue explants of eNOS knockout mice suggest that NO could influence neuroblast migration (Chen et al., 2004).

To achieve a better understanding for the nitric oxide and sGC regulated enteric neuron migration, it would be of great importance to know the nature and developmental distribution of putative guidance cues on the locust midgut. Pharmacological perturbation of the bioactive molecule nitric oxide or its downstream effector sGC did not reveal a significant increase in pathfinding errors of midgut neurons (unpublished data/Knipp and Bicker, 2009). Nevertheless, the NO/cGMP signalling pathway may be involved in transduction of guidance cue signals to the cytoskeleton. Growth cone repulsion of *Xenopus* spinal cord neurons, that is caused by Semaphorin III can be converted by cGMP signalling (Song et al., 1998). Moreover, the NOS/sGC/PKG pathway is involved in neural cell adhesion molecule-mediated neurite outgrowth in rodent hippocampal neurons (Ditlevsen et al., 2007). Therefore, cell adhesion molecules and semaphorins seemed to be good candidates as possible guidance factors for locust enteric neuron migration. The semaphorin family of cell surface and secreted proteins are conserved from insects to humans. The first characterised member of the semaphorin family was the transmembrane protein Sema-1 (formerly Fasciclin-IV) (Kolodkin et al., 1992). Sema-1 acts as a permissive cue for axon outgrowth in the grasshopper limb bud (Wong et al., 1997) and semaphorin 3A and its receptor neuropilin are expressed in endothelial cells along the RSM in mice (Melendez-Herrera et al., 2008). Fasciclin-I and -II are membrane-associated glycoproteins that are among a large group of neuronal surface proteins expressing the carbohydrate that cross-reacts with antibodies to horseradish peroxidase (Snow et al., 1987; Snow et al., 1988). Fas-II was shown to play a key role in the migration and guidance of enteric plexus neurons (EP cells) in the developing ENS of the moth *Manduca sexta* (Wright et al., 1999; Wright and Copenhaver, 2000). This glycoprotein has structural and functional similarity to the vertebrate neural cell adhesion molecule N-CAM (Harrelson and Goodman, 1988). Interestingly,

polysialated neural cell adhesion molecule (PSA-N-CAM) is involved in neuroblast guidance and migration in the rostral migratory stream of mice (Rousselot et al., 1995; Hu, 2000). However, we were not able to detect a convincing labelling with anti-Sema-1 (DSHB mAb 6F8) or anti-Fas-II (DSHB mAb 8C6) on the locust midgut, although both antibodies produce specific staining in the CNS (data not shown). The developmental expression pattern of Fas-I, e.g. during early formation of the anterior commissure in the grasshopper embryonic CNS, suggests that it may play a role as pathway labels (Bastiani et al., 1987). On the locust midgut the Fas-I antibody 3B11 labelled selectively the migrating enteric neurons (Fig. 6C). However, detailed analysis of the cellular distribution of Fas-I labelling revealed that a guiding or pathfinding function for enteric neurons is quite unlikely (Fig. 6, 8). The neurites of the migratory pathway are brightly stained (Fig. 6D, E), as well as established lateral branches (Fig. 8C-F). The molecule can be detected close to leading neurons on the posterior migrating chain and also during lateral branching, but never on the neuronal soma or the growth cones of leading neurons (Fig. 6F, G, 8). Nevertheless, leading processes of following neurons can enwrap pioneering cells with neurites carrying Fas-I (Fig. 6F, G). Beside the cytoanatomical distribution of the epitope, revealed manipulation of Fas-I using blocking antibodies no effect on enteric neuron migration (Fig. 7). Thus, a guidance function of this cell surface glycoprotein is unlikely. The data rather suggest a function as adhesion molecule enabling enteric neuron fasciculation, thus guidance of following neurons.

Observation of leading neurons of enteric migratory chains in living preparations showed that not one single pioneering neuron is responsible for pathfinding, but that leading and following neurons at the migratory tip can frequently change place (data not shown), e.g. the neuron marked with an asterisk in fig. 4 may be heading to take the lead. This may hint to a group of pioneering neurons. In the wing development of the *Drosophila* pupa glial chain migration is lead by a discrete number of peripheral glia cells (Aigouy et al., 2008). But it is also quite likely that all migrating enteric neurons are able to follow specific guidance cues independent from the leading neurons. Leading enteric neurons frequently contact the bordering muscle fibres with their filopodia, immediately

retract them and steer back to a middle pathway (Fig. 4, left hand panels). Even if a neuron has incorrectly crossed a longitudinal muscle fibre during the phase of posterior migration, it turns again on a new path between two muscle fibres (data not shown). Enteric neurons of the migratory chain also contact the muscle fibres but mainly orient on the fibres of preceding neurons (Fig. 4, right hand panels). Whether the longitudinal musculature provides any guidance cues or if they simply provide a mechanical barrier for the enteric neurons remains unknown. Developing tissue may influence neuronal navigation by non-specific physical constraints as well as specific chemical signals (reviewed in Song and Poo, 2001). Also the detailed signalling cascades leading to lateral branching of enteric neurons remain unknown. But apparently muscle fibres or their extracellular composition play again a role, since enteric neurons branching from the posterior chain migration orient along the developing circular musculature (Fig. 9A-C) and the pattern of the mature enteric plexus is structured by the midgut musculature and innervating it (Fig. 9D-G). We like to conclude that during enteric midgut plexus development the main guidance molecules for pathfinding decisions of migrating enteric neurons may be expressed on the midgut musculature.

Experimental Procedures

Locust eggs (*Locusta migratoria*) were collected from our crowded animal culture, reared under standard conditions and kept in moist Petri dishes at 30°C prior to use. Embryos were staged by percentage of development (% E) according to Bentley et al. (1979) with additional criteria for later embryos (Ball and Truman, 1998). All chemicals were purchased from Sigma (St. Louis, MO, USA) unless stated otherwise.

Embryonic guts were dissected and collected as whole mount preparations in cooled Leibowitz 15 medium (L15, Gibco, Life Technologies, Paisley, UK). Some whole guts were dissected and prepared for “tissue blots” as previously described (Knipp and Bicker, 2009) to reduce the background staining caused by yolk inside guts. Preparations were fixed in 4% paraformaldehyde dissolved in phosphate-buffered saline (PBS, 10 mM sodium phosphate, 150 mM NaCl, pH 7.4) for 1–2 hours at room temperature or overnight at 4°C. In tissue blot-preparations the nerve cells were allowed to settle for at least 20 minutes at room temperature to ensure sufficient adherence ahead of fixation.

Time lapse video microscopy

For in situ video microscopy of living enteric midgut neurons we used embryos staged between 64% and 75% E. Dissected guts were prepared as “tissue blots” as already described (Knipp and Bicker, 2009). In short, the dissected gut was rolled carefully over a poly-D-Lysin (diluted 1:100) coated coverslip in a Petri dish containing L15 culture medium. During this procedure cells on the gut surface including neurons of the plexus, muscle fibres, and ganglia of the ENS adhered to the coated surface while the intact epithelium and yolk could be removed. Cells were allowed to settle for 20 minutes at room temperature. The tissue blots were then washed with sterile L15 supplemented with 1% penicillin-streptomycin solution (L15-PS) and incubated for at least one hour up to overnight at 30°C prior to time lapse imaging.

Cover slips with adjacent tissue blots were placed as bottom in an incubation chamber and covered with sterile L15-PS and an additional coverslip on top of the

incubation chamber. The incubation chamber was placed in a PTC-10npi warming heater (30°C) on the stage of a Zeiss Axiovert 200 microscope equipped with a Photometrics Cool Snap digital camera and associated MetaFluor Imaging software. Images were captured using phase contrast at 30 to 60 seconds intervals for a minimum of 40 minutes. Preparations were fixed either immediately after video imaging or following a subsequent preincubation for NO-induced cGMP-immunoreactivity and processed immunocytochemically.

Immunocytochemistry

All steps of immunocytochemistry were performed at room temperature and with smooth agitation for whole mount preparations unless stated otherwise.

For NO dependent cGMP immunocytochemistry preparations were preincubated for 20 minutes at room temperature prior to fixation in L15 containing the NO-donor sodium nitroprusside (SNP, 100 µM), the phosphodiesterase inhibitor IBMX (1 mM), and YC-1 ([3-(5-hydroxymethyl-2-furyl)-1-benzyl indazole], 25 µM), a sensitiser of soluble guanylyl cyclase (DeVente et al., 1987; Ott et al., 2004; Knipp and Bicker, 2009). IBMX and YC-1 were dissolved in DMSO, SNP in L15. Omitting the NO-source from the cGMP preincubation solution or adding sGC inhibitors, revealed no cGMP-IR at all.

Following fixation preparations were permeabilised in 0.3% Saponin in PBS for one hour, rinsed in PBS containing 0.5% Triton X-100 (PBS-T) and blocked for at least one hour in 5% normal serum/PBS-T (serum of animal in which secondary antibody was raised). The primary antibody was diluted in blocking solution and applied overnight at 4°C. Used primary antibodies and concentrations were: sheep anti-cGMP (1:10.000 – 1:20.000, Tanaka et al., 1997), monoclonal mouse anti-acetylated α -tubulin (1:500 – 1:1000), polyclonal goat anti-horseradish peroxidase (anti-HRP, 1:5000, Jackson Immunoresearch, West Grove, PA), and monoclonal mouse anti-Fas-I (3B11, 1:10 – 1:50, Bastiani et al. 1987). After rinsing several times in PBS-T, guts were exposed for at least two hours at room temperature or overnight at 4°C to biotinylated (Vector, Burlingame, CA, USA) or AlexaFluor-coupled (Molecular Probes, Eugene, OR, USA) secondary antibodies in blocking solution. After washing with PBS-T biotinylated secondary antibodies were

visualized using fluorescent streptavidin coupled dyes (Sigma, Molecular Probes). After washing in PBS-T and PBS, preparations were cleared in 50% glycerol (Roth, Karlsruhe, Germany)/PBS and mounted in 90% glycerol/PBS with 4% n-propyl-gallate. Some whole mount preparations and all tissue blot preparations were counterstained with DAPI (incubation for 60 seconds with 2µg/ml PBS) following visualization.

Phalloidin staining of actin cytoskeleton

For visualising the actin cytoskeleton of enteric neurons, F-actin was marked with AlexaFluor-488 or -568 coupled phalloidin (Molecular Probes). A subset of tissue blot preparations were processed immunocytochemically as described above and washed finally with PBS. The phalloidin staining solution was diluted in PBS according to the manufacturer instructions and applied for one hour at room temperature or overnight at 4°C in the dark. Preparations were rinsed in PBS and mounted in glycerol as described above.

In vivo culture experiments and statistical analysis

To test whether Fasciclin-I plays an essential role in pathfinding decisions and migration of locust embryonic enteric neurons we carried out some in vivo culturing experiments using a 3B11 antibody solution for specific blocking of Fas-I (Bastiani et al., 1987). Experiments and quantification of cell migration was carried out as already described (Knipp and Bicker, 2009). In brief, embryos staged between 62 and 65% E were used for the experiments. At this time point midgut neurons have just started their migration. Eggs of one clutch were sterilised in 70% ethanol and dissected in sterile L15 medium. A small incision in the dorsal epidermis above the foregut allowed access of compounds to the developing ENS during the in vivo culturing period. Following an incubation for 24 hours at 30°C, guts were dissected and prepared for anti-cGMP and anti-acetylated α -tubulin double immunocytochemistry.

To quantify the cell migration on the midgut surface, we measured the distance from the foregut-midgut boundary to the position of the leading enteric neuron (Wright et al., 1998; Knipp and Bicker, 2009) using NIH ImageJ (v. 1.35 – 1.39).

The obtained values were normalized with respect to the mean distance of migration of the control group. To test for possible misroutings of enteric neurons we compared the numbers migratory errors of enteric neurons on dorsal guts after *in vivo* culturing and calculated the mean average per gut. As a minimum criterium for a guidance error, counted the number of branchings from the main pathway. An error was counted if an enteric neuron had left the pathway for at least its diameter. A Wilcoxon Mann-Whitney test was employed for statistical comparisons of experimental and control groups using KyPlot (version 2.0 beta15). All significance levels are two-sided. Bar-graphs display mean values +/- standard error of the mean (s.e.m.).

Image acquisition and processing

Preparations were analysed and photographed using a Zeiss Axioscope equipped with an AxioCam3900 digital camera linked to a Zeiss image acquisition system (Zeiss Axiovision) or a Zeiss Axiovert 200 equipped with a Photometrics Cool Snap digital camera and associated MetaFluor Imaging software. Image quality was carefully enhanced by Adobe Photoshop or NIH ImageJ (Rasband, W.S., ImageJ, U.S. National Institutes of Health, Bethesda, MD, <http://rsb.info.nih.gov/ij/>) including arrangement, conversion to grayscale, inversion, adjusting evenness of illumination, brightness and contrast enhancement. Confocal images and z-stacks of selected preparations were taken with a Leica TCS SP5 confocal microscope using Leica LAS AF software and primarily processed with NIH ImageJ including the LOCI Bio-Formats library plugin.

Acknowledgement

The authors are grateful to Dr. J. DeVente for his kind gift of the cGMP antibody. The 3B11 antibody developed by C. Goodman was obtained from the Developmental Studies Hybridoma Bank developed under the auspices of the NICHD and maintained by The University of Iowa, Department of Biological Sciences, Iowa City, IA 52242. This work was supported by grants of the Deutsche Forschungsgemeinschaft (BI 262/10-5).

Figures

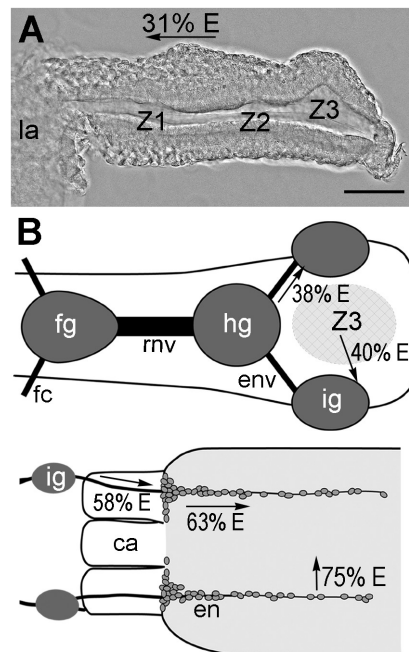


Figure 1: Timing and topology of neuronal migration on the developing locust alimentary canal.

Arrows illustrate main direction of cell migration and developmental onset of the particular migratory phase. See also text for details. Anterior is to the left. **(A)** Microphotograph using DIC optics of the locust stomodeum at around 38% E in a lateral view. The three neurogenic zones (Z1 to Z3) are clearly visible as evaginations of the dorsal epithelium. The first phase of active cell migration has started at around 31% E when neurons detached from the neurogenic zones migrate anteriorly (indicated by arrow). The labrum is still attached to the stomodeum. Scalebar indicates 100 μ m. **(B)** Schematic drawing of the developing locust ENS. Upper panel shows the layout of the foregut at around 45% E. Checked area denotes the still highly active posterior neurogenic zone Z3. Lower panel illustrates posterior foregut and midgut ENS at around 65% E. Ganglia are shown in dark grey, enteric neurons in midgrey, the midgut is shaded in light grey. ca, caecum; en, enteric neurons env, esophageal nerve; fc, frontal connective; fg, frontal ganglion; hg, hypocerebral ganglion; ig, ingluvial ganglion; la, labrum; rnv, recurrent nerve.

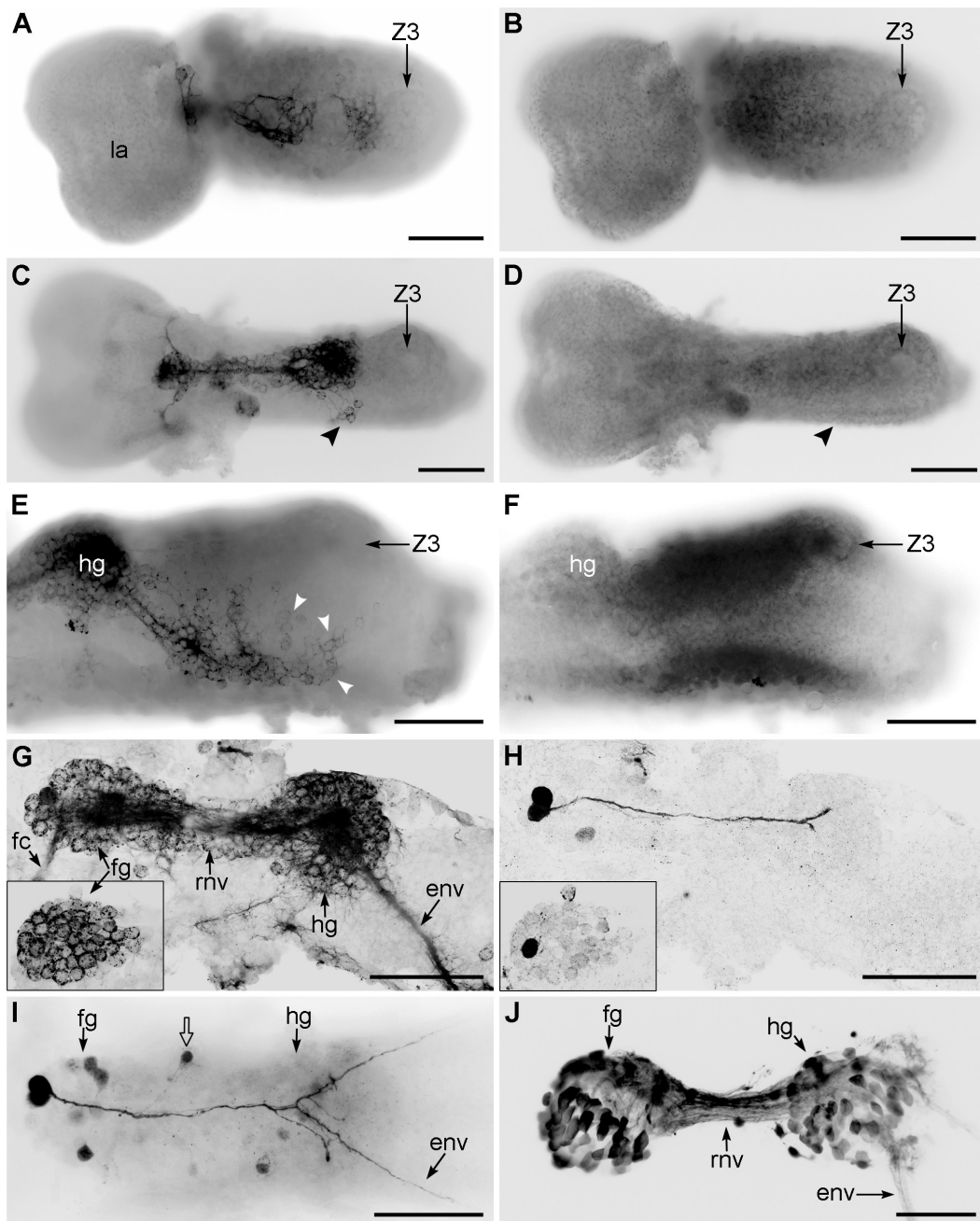


Figure 2: NO dependent cGMP immunoreactivity during ENS development on the foregut.

Figure 2: NO dependent cGMP immunoreactivity during ENS development on the foregut.

Immunofluorescence microphotographs of guts at different developmental timepoints stained for anti-HRP (left side, except image I) or anti-cGMP (right side). **(A), (B)** Dorsal view of the stomodeum and adhering labrum at 31-33%. **(C), (D)** Embryonic foregut at about 38% E. Black arrowhead points to the laterally migrated neurons beginning to form the future ingluvial ganglion. **(E), (F)** Lateral view of the posterior stomodeum at a stage between 40-45% E. White arrowheads point to some HRP-IR positive neurons migrating from Z3 to the caudal end of the prospective ingluvial ganglion. **(G), (H)** First cGMP-IR occurs at the timepoint of katatrepsis at 45% E quite sudden in two cells of the frontal ganglion (fg) and their axonal projections in the recurrent nerve. In some preparations only one single cell of the frontal ganglion shows cGMP-IR, illustrated in the small insets. Images are maximum projections of confocal z-stacks. **(I)** 50-55% E. Open arrow points to an exemplary neuron migrating on the foregut to build up the foregut plexus. **(J)** Close to hatching at around 85% E the foregut ganglia and nervous connections show strong cGMP immunoreactivity. Microphotographs in (C), (E), (H), and (I) are combined images of different focal planes. Anterior is to the left. Scalebars indicate 100 μ m. env, esophageal nerve; fc, frontal connective; fg, frontal ganglion; hg, hypocerebral ganglion; ig, ingluvial ganglion; la, labrum; rnv, recurrent nerve; Z1 to Z3, neurogenic Zones one to three.

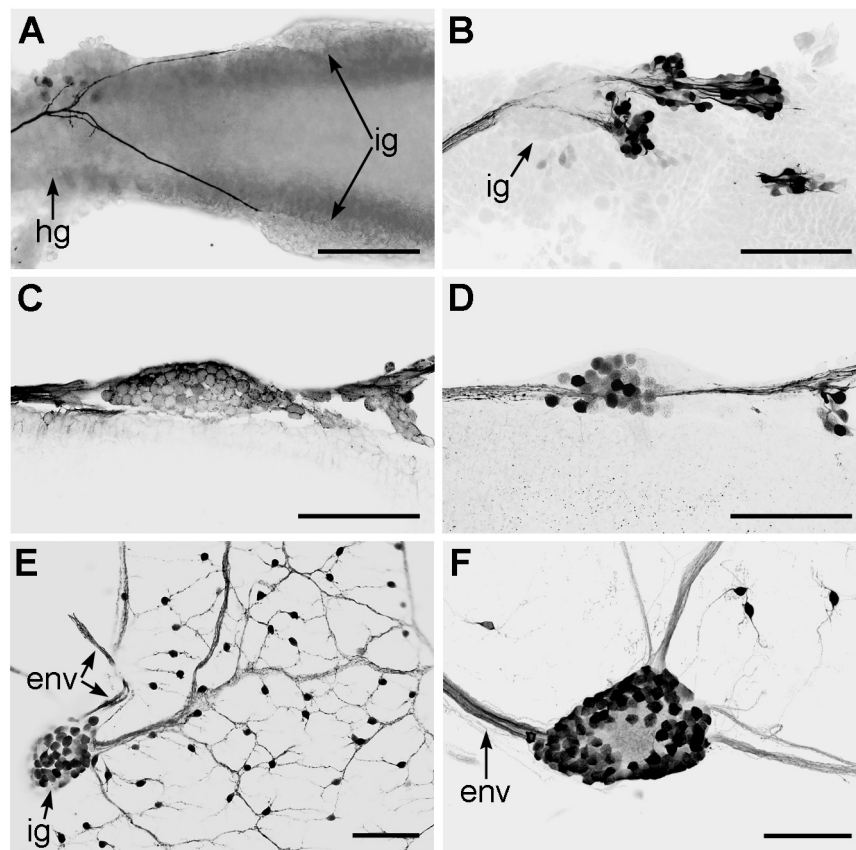


Figure 3: NO dependent cGMP immunoreactivity on the posterior foregut

(A) Dorsal view of the posterior embryonic foregut at 55% E. cGMP-IR is already present in the esophageal nerve (env) but not in the ingluvial ganglia (ig). Maximum projection of a confocal z-stack of cGMP immunofluorescence arranged together with a brightfield image of the foregut. **(B)** Maximum projection of a confocal z-stack of an ingluvial ganglion and caudal migrating prospective enteric neurons in a semi-lateral view at 58% E. **(C)** Confocal microphotograph of an ingluvial ganglion at around 60% E labelled with anti-HRP in a lateral view. **(D)** Maximum projection of a confocal z-stack from the same ingluvial ganglion as in (C) but labelled for cGMP. **(E)** Dorsal view of ingluvial ganglion and foregut nervous plexus at 90% E labelled for anti-cGMP. **(F)** Confocal z-stack of an ingluvial ganglion in a first instar larvae. Anterior is to the left, except (E): anterior is to the top. Scalebars indicate 100 µm. env, esophageal nerve; hg, hypocerebral ganglion; ig, ingluvial ganglion.

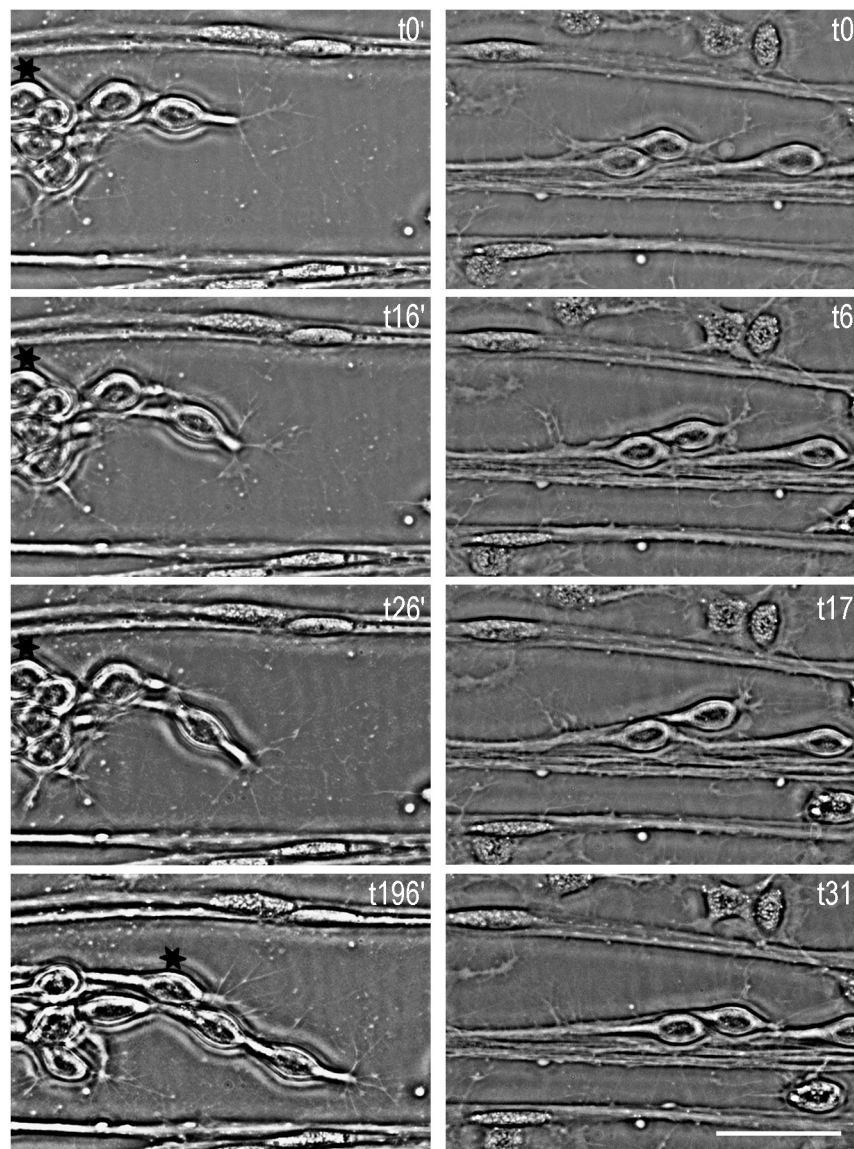


Figure 4: Time lapse video microscopy of living enteric midgut neurons.

Two examples of time lapse series taken from locust embryonic midguts in tissue blot preparations. Left hand panels show a leading group of migrating enteric neurons at 70% E. Right hand panels give an example of trailing migrating enteric neurons at 65% E. Numbers in upper right corner of each image indicate timepoint (t) in minutes. Muscle fibres are clearly discernable by their elongated nuclei. Hemocytes can be identified by their granular cytoplasm and multipolar cell shape, e.g. on the right hand panels. Anterior is to the left. Scalebars indicate 50 μm .

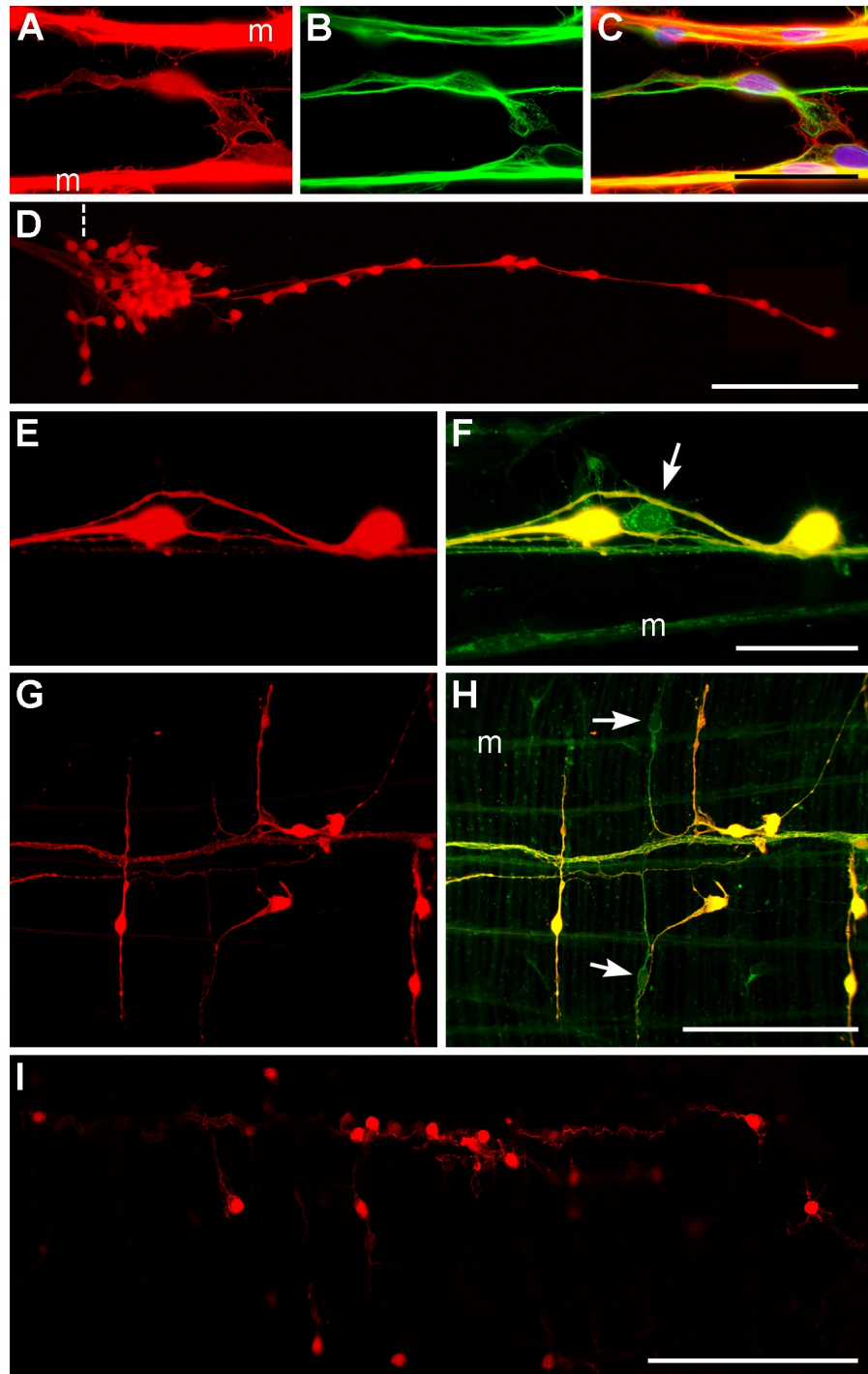


Figure 5: NO dependent cGMP immunoreactivity on the locust embryonic midgut.

Figure 5: NO dependent cGMP immunoreactivity on the locust embryonic midgut.

Tissue blot preparations of locust midguts at diverse developmental stages. **(A)**, **(B)** Cytoskeletal organisation of a migrating enteric neuron at 65% E. Actinfilaments are visualized with fluorescently labelled Phalloidin (red, A), microtubules by an antibody to acetylated α -tubulin (green, B). **(C)** RGB-Merged image of (A) and (B), with DAPI in blue as a nuclei marker. **(D)** Chain of migrating enteric neurons just after onset of midgut migration at 63% E. Neurons are labelled with an antibody to cGMP. Hatched line indicates foregut-midgut boundary. **(E)**, **(F)** Close up view of a migratory chain as shown in (D) at 65% E. The cGMP-IR is evenly distributed in the soma and neurites of enteric neurons (E). Counterstaining with anti-HRP reveals that not all enteric neurons exhibit a NO dependent cGMP-IR (arrow in F). **(G)** At 85-90% E the phase of lateral branching has culminated and formation of terminal processes on the midgut musculature has begun. Enteric neurons remain to show a strong cGMP-IR. **(H)** Same as in (G) but with additional anti-HRP labelling revealing cGMP negative neurons (arrows). **(I)** Anti-cGMP labelling of a whole mount preparation of the midgut from a freshly hatched first instar larvae. Anterior is to the left. Scalebars indicate 50 μ m, except (D) with 100 μ m. m, musculature.

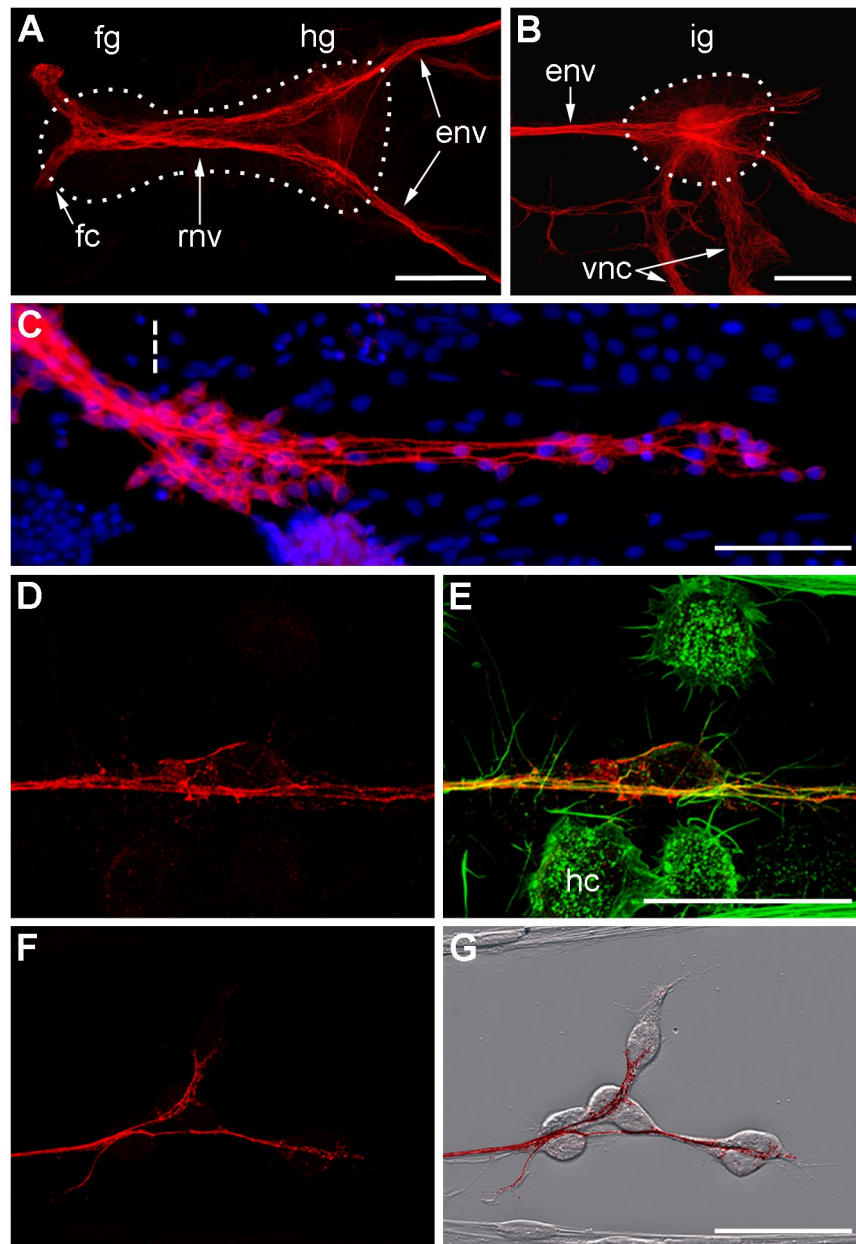


Figure 6: Fasciclin I in the locust enteric nervous system

Figure 6: Fasciclin I in the locust enteric nervous system

All preparations shown are labelled with an antibody against grasshopper fasciclin I (mAb 3B11). Tissue blot preparations of locust midguts at 63 to 65% E except (A) and (B) that are whole mount preparations of embryonic foreguts at 65% E. **(A)** Maximum projection of a confocal z-stack from a dorsal anterior foregut with frontal- and hypocerebral ganglion. **(B)** Confocal z-stack maximum projection of an ingluvial ganglion in a semi-lateral view. **(C)** Immunofluorescence image of enteric neurons on the midgut just after onset of the posteriorly directed cell migration. Cell nuclei were counterstained with DAPI (blue). Hatched line indicates foregut-midgut boundary. **(D)**, **(F)** Close up images of Fas-I labelled migrating enteric midgut neurons (red). **(E)**, **(G)** Merged images with counterstaining with fluorescently labelled phalloidin (E, green) or DIC-image (G) to illustrate overall morphology. (D) to (F) are maximum projections of confocal z-stacks. Anterior is to the left. Scalebars indicate 100 μm in (A) to (C) and 50 μm in (D) to (G). env, esophageal nerve; fc, frontal connective; fg, frontal ganglion; hc, hemocyte; hg, hypocerebral ganglion; ig, ingluvial ganglion; m, musculature; rnv, recurrent nerve; vcn, ventral nerve commissure.

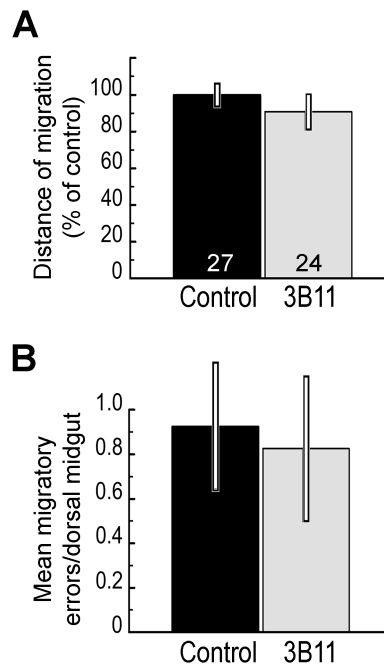


Figure 7: Effect of antigen absorption with mAb 3B11 on enteric neuron migration in the locust embryonic ENS.

For the in vivo culturing experiments hybridoma supernatant 3B11 from the Developmental Studies Hybridoma Bank was diluted in the same amount of sterile L15 cell culture medium. Sterile L15 medium was used as a control. (A) Bar plots show average migration distance covered by the leading enteric neurons during 24 hours of in vivo culture. Data are normalized to the mean of the corresponding control. (B) Mean of migratory errors averaged in respect to the number of analysed guts. Only the dorsal pathways were compared. The numbers of experimental gut preparations are indicated in the columns of (A). A Wilcoxon Mann-Whitney test revealed no significant difference in both experiments.

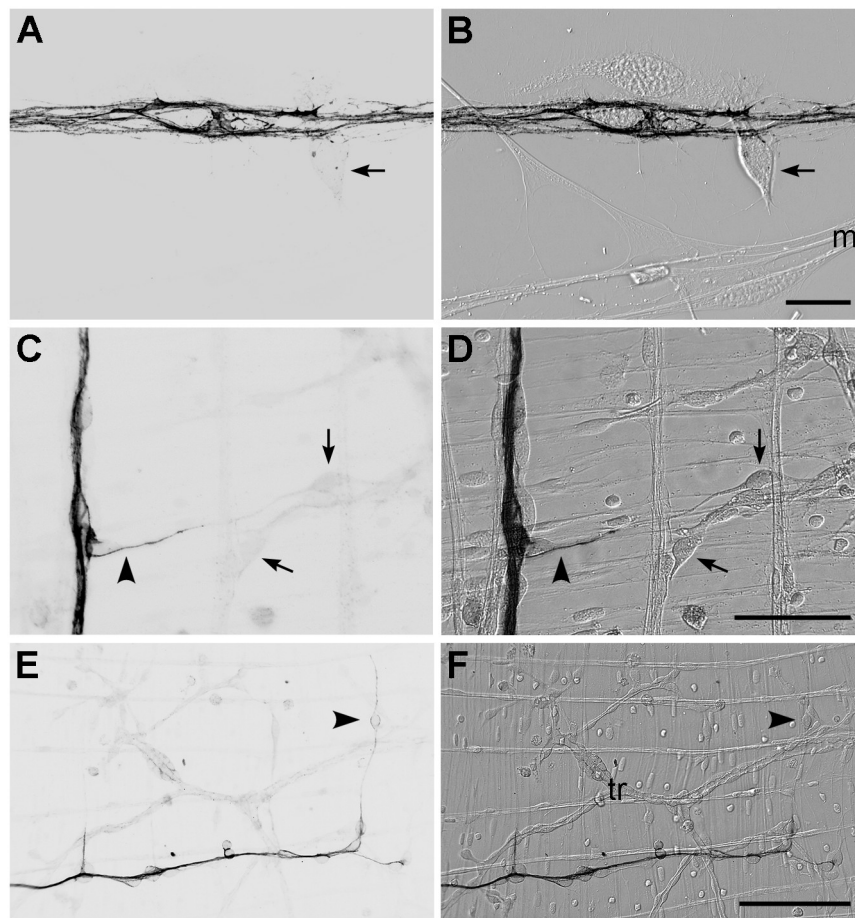


Figure 8: Late development of the midgut nervous plexus

Immunofluorescence images and confocal z-stack projection (A) of tissue blots labelled with Fas I were inverted and changed to greyscale (panels on the left). To clarify the layout of the midgut plexus and musculature, DIC-images were merged to respective fluorescence images (panels on the right). (A), (B) Anti-Fas I immunoreactivity at 80% E. (C) to (F) Developing midgut plexus at 85% E. See text for further details. Anterior is to the left except for (C) and (D) with anterior to the top. Scalebars indicate 20 μm in (A) and (B) and 100 μm in (C) to (F). m, musculature.

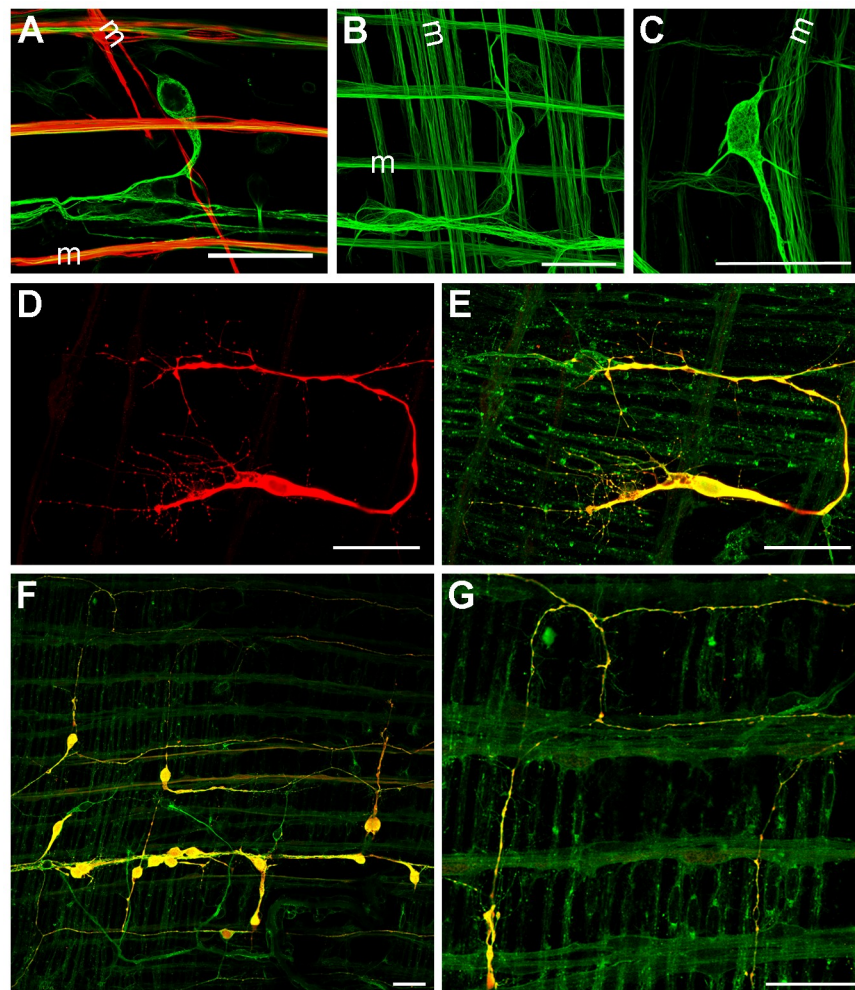


Figure 9: Confocal microphotographs of late midgut plexus development (A) to (C) Exemplary images from consecutive developmental stages: 80% E (A), 85% E (B) and 90-95% E (C). Lateral migrating enteric neurons and gut musculature were labelled for anti-acetylated α -tubulin (green). An additional counterstaining with rhodamin coupled phalloidin (red) was used in (A) to clarify the developing circular musculature. (D) Formation of terminal processes on the midgut musculature. Enteric neurons and neurites are labelled with anti-cGMP. (E) Merged image of (D) counterstained with anti-HRP (green). (F) Lay out of a midgut plexus at 90% E labelled with anti-HRP (green) and anti-cGMP (red). (G) Magnification of (D). Scalebar indicates 50 μ m.

4. Discussion

Due to its small cell number, simple behavioural output and easy accessibility, the mature ENS of arthropods has been used for many years as a model system to study the functioning of a neural network (Hartenstein, 1997; Ayali, 2004). The development of the insect ENS, especially of the midgut plexus, provides a useful model to study neural migration for comparable reasons (Ganfornina, 1996; Haase and Bicker, 2003; reviewed in Copenhaver, 2007).

Enteric neuron migration on the locust midgut takes place in a highly organised manner. This requires crucial pathfinding decisions but also an accurate timing for onset of migration and differentiation, intracellular signal transduction, and cytoskeletal rearrangement for enteric midgut neurons. I was able to demonstrate a developmental function of heme oxygenase and carbon monoxide, i.e. an autoregulatory role during enteric neuron migration. Furthermore, I obtained data from video microscopy of migrating enteric neurons together with immunocytochemical data, implying that especially anterior-posterior chain migration may be directed by the midgut musculature.

4.1 Localization of biosynthetic enzymes releasing gaseous modulators

The nitric oxide/cGMP/protein kinase G signalling pathway has been found to regulate neuronal migration (Wright et al., 1998; Haase & Bicker 2003; Boran and Garcia, 2007; Gutierrez-Mecinas et al., 2007), neurite outgrowth (Seidel and Bicker, 2000; Welshhans & Rehder 2005; Ditlevsen et al., 2007), and axonal regeneration (Stern and Bicker, 2008). In addition to NO, there is also increasing evidence for carbon monoxide as another gaseous messenger of vertebrate and invertebrate neural tissues (Verma et al., 1993; Ingi et al., 1996a,b; Gelperin et al., 2000; Boehning and Snyder, 2003; Christie et al., 2003; Zhang et al., 2004; Watanabe et al., 2007). Moreover, it has been shown to regulate cell migration in vertebrates (VanUffelen et al., 1996; Andersson et al., 2002; Freitas et al., 2006), but no neurodevelopmental functions of CO had emerged up to now.

Heme oxygenase enzymes are localised in enteric migrating neurons (Chapter 2.2, fig. 5, 6), thus providing an autocrine system. Even though I have used an

antibody that was prepared against the rat HO-2 enzyme, the staining in the grasshopper appears to be reliable. In the crustacean enteric nervous system, the same antibody labelled putative CO producing neurons (Christie et al., 2003). The antibody detects a protein in locust gut homogenates, that is of the same size like the purified rat HO-2 (Chapter 2.2, fig. 5A). What is more, preadsorption of the antibody with an excess of HO-2 protein abolishes HO-2 immunolabelling (Chapter 2.2, fig. 5B). Also, application of enzyme inhibitors or activators revealed a significant influence of HO activity on neuronal migration (Chapter 2.2, fig. 3, 4).

In contrast to this, NO synthesising enzymes are not specificity localised in the enteric neurons. The protein-biochemical data show that a nitric oxide synthase (NOS) is present in the developing midgut tissue (see chapter 2.2, fig. 2D). However, the detailed cellular localisation is not fully resolved. NADPH diaphorase (NADPHd) histochemistry detected stainings in a subset of the locust embryonic midgut cells (Haase and Bicker, 2003) as potential endogenous NO-producing cells. NADPHd histochemistry resulted in clearly stained neurons in the ingluvial ganglia, but not in the enteric midgut neurons. Nevertheless, some cells on the midgut exhibited quite distinct NADPHd positive staining (Knipp and Bicker, 2006). These cells possess the typical multipolar/fibroblast like shape of hemocytes, i.e. cells of the insect innate immune system. However, since the diaphorase reaction depends on fixation conditions (Ott and Burrows, 1999), it may quite often not completely resolve the expression pattern of NOS. An antibody against a consensus region of NOS-isoforms (universal NOS, see also chapter 2.2, pp. 29f) also labelled the hemocytes in a reproducible manner (Knipp and Bicker, 2006). The same result was obtained with an immunocytochemical labelling of L-citrulline (data not shown). These findings suggest hemocytes as a possible source for nitric oxide. However, the high NOS concentrations in the midgut probes as revealed by western blotting techniques (Chapter 2.2, fig. 2D), point towards an additional resource. This may be found in cells of the midgut epithelium, comparable to *Anopheles*, where a NOS gene was identified in the midgut epithelium (Akman-Anderson et al., 2007). Since scavenging of NO with extracellular acting hemoglobin results in a slowdown of enteric neuron migration comparable to inhibition of NOS, a transcellular signal transduction for NO seems quite plausible.

4.2 Regulation and guidance of enteric neuron migration

The results from pharmacological perturbation of enteric neuron migration, suggests that NO/cGMP promoted migration is slowed down by a carbon monoxide signal (discussed in chapter 2.2). Both gaseous messengers can bind to sGC and induce the formation of cGMP (Fig. 4.1) (e.g. Kharitonov et al., 1995, chapter 2.2) with about a hundredfold higher effectiveness after NO-binding above CO-binding. A likely mechanism for the observed effects would be a competitive inhibition by CO, although other mechanisms may be possible (discussed in detail in chapter 2.2, pp. 32f.). By reducing the cGMP concentration in the enteric neuron, carbon monoxide could shift the intracellular concentration ratio between cyclic nucleotides towards cyclic AMP (cAMP). Actually, artificial elevation of cAMP reduces enteric neuron migration (Haase and Bicker, 2003). It was convincingly demonstrated that growth cone response can be converted from attraction to repulsion by changing the concentration ratios of cyclic nucleotides (Song et al., 1998).

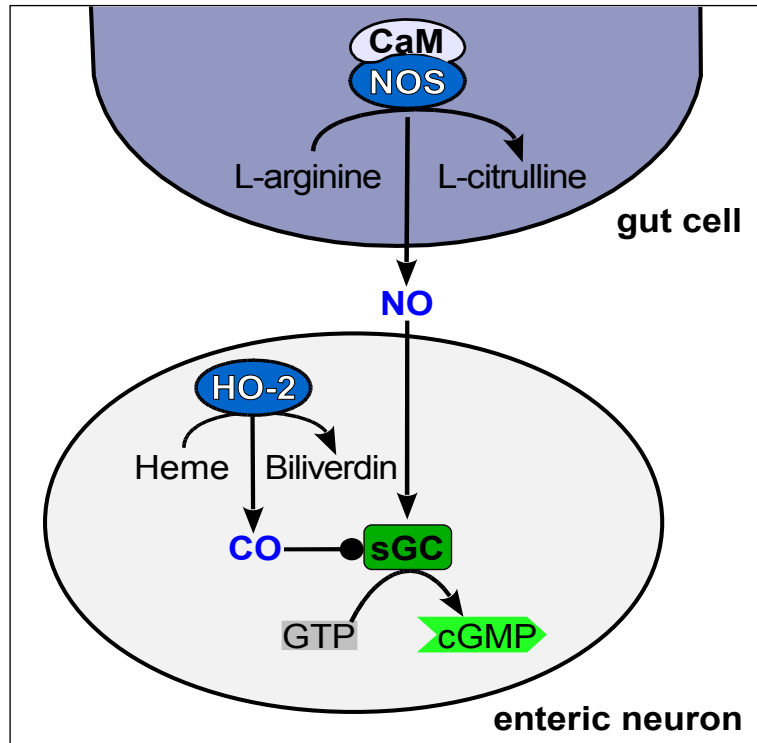


Figure 4.1: Proposed NO and CO signal transduction

NOS enzymes in midgut cells (shaded blue-grey) release freely diffusing NO that activates sGC (green) in the enteric neurons, thus cGMP (green arrow) is produced. Binding of intracellularly produced CO to sGC is less efficient.

Carbon monoxide signalling enables, that enteric neurons keep in close contact during their posterior migration. If CO release is inhibited, the distance between migrating neurons is enlarged significantly. In contrast, activation of HO activity, thus increased CO release, causes a more aggregated migratory chain. (Knipp and Bicker, 2008). Both effects can be observed independent of varying complete migratory distances. Considering, that CO can pass the cell membrane by diffusion, CO-releasing cells would provide an autocrine slowdown signal for themselves, but also a paracrine slowdown signal for neighbouring cells. Thus, by keeping the neurons close together, possible guidance errors of single neurons would be prevented.

Immunocytochemical data suggest, that the cell adhesion molecule Fasciclin-I supports fasciculation on the main migratory track and during lateral branching, thereby providing a guidance cue for neurons in the migratory chain. Many follower neurons may take advantage of the situation by adhering to trailing neurites via homophilic adhesion (Zheng and Poo, 2007). The neural adhesion molecules Fas-I and Fas-II have been shown to mediate fasciculation in grasshopper peripheral nervous system pioneers and to regulate migration of enteric plexus neurons in *Manduca* (Bastiani et al., 1987; Diamond et al., 1993; Wright and Copenhaver, 2000). The pioneering enteric neurons may be guided by extracellular matrix molecules on the surface of longitudinal muscle fibres.

4.3 Conclusions and Outlook

This study set out to analyse neuronal cell migration during development of a rather simple nervous system. Based on studies performed earlier (Haase and Bicker, 2003; Christie et al., 2003), I found a second gaseous molecule, carbon monoxide, to be a regulator of enteric neuron migration. Still, the temporal pattern of CO production and the actual identity of its downstream signalling remains uncertain. Further studies with varying compounds affecting HO and NOS in the preincubation solution for anti-cGMP staining may provide further insights. Detailed real-time analysis of CO production could be helpful too, but up to now a reliable CO sensitive indicator is missing. Further pharmacological manipulation of the CO-/cGMP signalling during enteric neuron migration would always interfere with the NO-/cGMP signalling cascade. Nevertheless, I was already able to show, that the gas carbon monoxide fulfils an important function for developmental neuronal migration. It would be of great interest to further investigate the properties of this modulator not only in insects, but also in vertebrate development.

The cell adhesion molecule Fasciclin I plays a role for fasciculation of the migratory chain on the locust midgut. The identity of guidance cues for the pathfinding decisions of chain leading neurons is not clear. The extracellular matrix of the gut musculature seems to be the place to look for such candidates. A screening for patterned distribution or possible gradients of glycoproteins with different lectins revealed no hopeful candidate up to now (data not shown). Possible guidance cues may be, for example, ephrin receptor tyrosine kinases and their ephrin receptors, that have been shown to play a role for enteric neuron migration in *Manduca* (Coate et al., 2007). Another candidate may be insect homologue of the receptor tyrosine kinase (RET). The RET/GFRa/GDNF signalling pathway has been demonstrated to direct enteric neuron migration during development of the vertebrate ENS (Burns, 2005) and a homologous RET gene is found in *Drosophila* (Hahn and Bishop, 2001).

One of the main neurotransmitters of the mature grasshopper ENS is serotonin (Klemm et al., 1986; Luffy and Dorn, 1992). Together with Michael Stern, I have studied the development and differentiation of serotonergic neurons in the embryonic ENS. Serotonin is known to play a vital role for gut motility and feeding

behaviour. Serotonergic neurons of the foregut ganglia grow descending neurites in all enteric ganglia and both plexus. Although this neurite outgrowth does not depend directly on NO/cGMP signalling, it is also affected, if enteric neuron migration is inhibited through perturbation of the NO/cGMP pathway.

Neurons of the enteric plexus exhibit no serotonergic phenotype (chapter 2.3). Also the neuropeptides dopamine and histamine are restricted to the enteric ganglia (M. Stern, personal communication). Acetylcholinesterase staining is found in the enteric ganglia on the foregut, but only in few enteric midgut cells in the larval grasshopper (Bicker et al., 2004). FMRFamide like immunoreactivity was found in endocrine cells and efferent fibres from the frontal ganglion on the larval and adult locust midgut (Hill and Orchard, 2003), but enteric neurons exhibited no labelling for FMRFamide like peptides during embryonic development (data not shown). Thus, the major neurochemical phenotype of locust enteric midgut neurons remains to be elucidated.

In the publications included in this thesis, I have provided evidences for yet unknown regulatory mechanisms for enteric neuron migration by carbon monoxide. Furthermore, I have supplied additional data for developmental distribution and differentiation of neuromodulators and guidance cues in the embryonic grasshopper ENS.

5. References

Aigouy B, Lepelletier L and Giangrande A. (2008). Glial chain migration requires pioneer cells. *J Neurosci* **28**, 11635-11641.

Akman-Anderson L, Olivier M and Luckhart S. (2007). Induction of nitric oxide synthase and activation of signaling proteins in *Anopheles* mosquitoes by the malaria pigment, hemozoin. *Infect Immun* **75**, 4012-4019.

Anderson RB, Turner KN, Nikonenko AG, Hemperly J, Schachner M and Young HM. (2006). The cell adhesion molecule L1 is required for chain migration of neural crest cells in the developing mouse gut. *Gastroenterology* **130**, 1221-1232.

Andersson JA, Uddman R and Cardell L-O. (2002). Hemin, a heme oxygenase substrate analog, both inhibits and enhances neutrophil random migration and chemotaxis. *Allergy* **57**, 1008-1012.

Appleton SD, Chretien ML, McLaughlin BE, Vreman HJ, Stevenson DK, Brien JF, Nakatsu K, Maurice DH and Marks GS. (1999). Selective inhibition of heme oxygenase, without inhibition of nitric oxide synthase or soluble guanylyl cyclase, by metalloporphyrins at low concentrations. *Drug Metab Dispos* **27**, 1214-1219.

Araújo SJ and Tear G. (2003). Axon guidance mechanisms and molecules: lessons from invertebrates. *Nat Rev Neurosci* **4**, 910-922.

Arendt D and Nübler-Jung K. (1999). Comparison of early nerve cord development in insects and vertebrates. *Development* **126**, 2309-2325.

Artinian LR, Ding JM and Gillette MU. (2001). Carbon monoxide and nitric oxide: interacting messengers in muscarinic signaling to the brain's circadian clock. *Exp Neurol* **171**, 293-300.

Ayali A. (2004). The insect frontal ganglion and stomatogastric pattern generator networks. *Neurosignals* **13**, 20-36.

Ayali A. (2009). The role of the arthropod stomatogastric nervous system in moulting behaviour and ecdysis. *J Exp Biol* **212**, e-pub ahead of print.

Ball EE and Truman JW. (1998). Developing grasshopper neurons show variable levels of guanylyl cyclase activity on arrival at their targets. *J Comp Neurol* **394**, 1-13.

Baranano DE and Snyder SH. (2001). Neural roles for heme oxygenase: contrasts to nitric oxide synthase. *Proc Natl Acad Sci USA* **98**, 10996-11002.

Barker EL, Perlman MA, Adkins EM, Houlihan WJ, Pristupa ZB, Niznik HB and Blakely RD. (1998). High affinity recognition of serotonin transporter

antagonists defined by species-scanning mutagenesis. *J Biol Chem* **273**, 19459-19468.

Bastiani MJ, Harrelson AL, Snow PM and Goodman CS. (1987). Expression of fasciclin I and II glycoproteins on subsets of axon pathways during neuronal development in the grasshopper. *Cell* **48**, 745-755.

Bentley D, Keshishian H, Shankland M and Toroian-Raymond A. (1979). Quantitative staging of embryonic development of the grasshopper, *Schistocerca nitens*. *J Embryol Exp Morphol* **54**, 47-74.

Bentley, D and Toroian-Raymond A. (1986). Disoriented pathfinding by pioneer neurone growth cones deprived of filopodia by cytochalasin treatment. *Nature* **323**, 712-715.

Benton JL and Beltz BS. (2001). Effects of serotonin depletion on local interneurons in the developing olfactory pathway of lobsters. *J Neurobiol* **46**, 193-205.

Benton JL, Sandeman DC and Beltz BS. (2007). Nitric oxide in the crustacean brain: regulation of neurogenesis and morphogenesis in the developing olfactory pathway. *Dev Dyn* **236**, 3047-3060.

Bernays EA and Chapman RF. (1973). The regulation of feeding in *Locusta migratoria*: internal inhibitory mechanisms. *Ent exp & appl* **16**, 329-342.

Bicker G, Naujock M and Haase A. (2004). Cellular expression patterns of acetyl-cholinesterase activity during grasshopper development. *Cell Tissue Res* **317**, 207-220.

Bicker G. (2001). Nitric oxide: an unconventional messenger in the nervous system of an orthopteroid insect. *Arch Insect Biochem Physiol* **48**, 100-110.

Bicker G. (2005). STOP and GO with NO: nitric oxide as a regulator of cell motility in simple brains. *Bioessays* **27**, 495-505.

Boehning D and Snyder SH. (2003). Novel neural modulators. *Annu Rev Neurosci* **26**, 105-131.

Boehning D, Moon C, Sharma S, Hurt KJ, Hester LD, Ronnett GV, Shugar D and Snyder SH. (2003). Carbon monoxide neurotransmission activated by CK2 phosphorylation of heme oxygenase-2. *Neuron* **40**, 129-137.

Boehning D, Sedaghat L, Sedlak TW and Snyder SH. (2004). Heme oxygenase-2 is activated by calcium-calmodulin. *J Biol Chem* **279**, 30927-30930.

Bräunig P. (2008). Neuronal connections between central and enteric nervous system in the locust, *Locusta migratoria*. *Cell Tissue Res* **333**, 159-168.

- Brooke NM, Garcia-Fernández J and Holland PW.** (1998). The ParaHox gene cluster is an evolutionary sister of the Hox gene cluster. *Nature* **392**, 920-922.
- Brüne B and Ullrich V.** (1987). Inhibition of platelet aggregation by carbon monoxide is mediated by activation of guanylate cyclase. *Mol Pharmacol* **32**, 497-504.
- Budnik V, Wu C-F and White K.** (1989). Altered branching of serotonin-containing neurons in *Drosophila* mutants unable to synthesize serotonin and dopamine. *J Neurosci* **9**, 2866-2877.
- Bullerjahn A and Pflüger HJ.** (2003). The distribution of putative nitric oxide releasing neurones in the locust abdominal nervous system: a comparison of NADPHd histochemistry and NOS-immunocytochemistry. *Zoology* **106**, 3-17.
- Burns AJ.** (2005). Migration of neural crest-derived enteric nervous system precursor cells to and within the gastrointestinal tract. *Int J Dev Biol* **49**, 143-150.
- Burrows M.** (1996). Development of the nervous system, in: *The Neurobiology of an Insect Brain*. Oxford University Press, Oxford.
- Buznikov GA, Nikitina LA, Voronezhskaya EE, Bezuglov VV, Willows AOD and Nezlin LP.** (2003). Localization of serotonin and its possible role in early embryos of *Tritonia diomedea* (Mollusca: Nudibranchia). *Cell Tissue Res* **311**, 259-266.
- Champlin DT and Truman JW.** (2000). Ecdysteroid coordinates optic lobe neurogenesis via a nitric oxide signaling pathway. *Development* **127**, 3543-3551.
- Chen CS, Tan J and Tien J.** (2004). Mechanotransduction at cell-matrix and cell-cell contacts. *Annu Rev Biomed Eng* **6**, 275-302.
- Chen J, Zacharek A, Zhang C, Jiang H, Li Y, Roberts C, Lu M, Kapke A and Chopp M.** (2005). Endothelial nitric oxide synthase regulates brain-derived neurotrophic factor expression and neurogenesis after stroke in mice. *J Neurosci* **25**, 2366-2375.
- Chen JJ, Tu YJ, Moon C, Matarazzo V, Palmer AM and Ronnett GV.** (2004). The localization of neuronal nitric oxide synthase may influence its role in neuronal precursor proliferation and synaptic maintenance. *Dev Biol* **269**, 165-182.
- Chitnis AB.** (1999). Control of neurogenesis--lessons from frogs, fish and flies. *Curr Opin Neurobiol* **9**, 18-25.
- Christie AE, Edwards JM, Cherny E, Clason TA and Graubard K.** (2003). Immunocytochemical evidence for nitric oxide- and carbon monoxide-producing neurons in the stomatogastric nervous system of the crayfish *Cherax quadricarinatus*. *J Comp Neurol* **467**, 293-306.

- Clarac F and Pearlstein E.** (2007). Invertebrate preparations and their contribution to neurobiology in the second half of the 20th century. *Brain Res Rev* **54**, 113-161.
- Clark L, Agricola H-J, Lange AB.** (2006). Proctolin-like immunoreactivity in the central and peripheral nervous systems of the locust, *Locusta migratoria*. *Peptides* **27**, 549-558.
- Coate TM, Swanson TL, Proctor TM, Nighorn AJ and Copenhaver PF.** (2007). Eph receptor expression defines midline boundaries for ephrin-positive migratory neurons in the enteric nervous system of *Manduca sexta*. *J Comp Neurol* **502**, 175-191.
- Coate TM, Wirz JA and Copenhaver PF.** (2008). Reverse signaling via a glycosyl-phosphatidylinositol-linked ephrin prevents midline crossing by migratory neurons during embryonic development in *Manduca*. *J Neurosci* **28**, 3846-3860.
- Colpaert EE, Timmermans JP and Lefebvre RA.** (2002). Investigation of the potential modulatory effect of biliverdin, carbon monoxide and bilirubin on nitrergic neurotransmission in the pig gastric fundus. *Eur J Pharmacol* **457**, 177-186.
- Condron BG.** (1999). Serotonergic neurons transiently require a midline-derived FGF signal. *Neuron* **24**, 531-540.
- Copenhaver PF and Taghert PH.** (1989a). Development of the enteric nervous system in the moth. I. Diversity of cell types and the embryonic expression of FMRFamide-related neuropeptides. *Dev Biol* **131**, 70-84.
- Copenhaver PF and Taghert PH.** (1989b). Development of the enteric nervous system in the moth. II. Stereotyped cell migration precedes the differentiation of embryonic neurons. *Dev Biol* **131**, 85-101.
- Copenhaver PF and Taghert PH.** (1990). Neurogenesis in the insect enteric nervous system: generation of premigratory neurons from an epithelial placode. *Development* **109**, 17-28.
- Copenhaver PF and Taghert PH.** (1991). Origins of the insect enteric nervous system: differentiation of the enteric ganglia from a neurogenic epithelium. *Development* **113**, 1115-1132.
- Copenhaver PF, Horgan AM and Combes S.** (1996). An identified set of visceral muscle bands is essential for the guidance of migratory neurons in the enteric nervous system of *Manduca sexta*. *Dev Biol* **179**, 412-426.
- Copenhaver PF.** (2007). How to innervate a simple gut: familiar themes and unique aspects in the formation of the insect enteric nervous system. *Dev Dyn* **236**, 1841-1864.

Davis NT. (1985). Serotonin-immunoreactive visceral nerves and neurohemal system in the cockroach *Periplaneta americana* (L.). *Cell Tissue Res* **240**, 593-600.

De Vente J, Steinbusch HWM and Schipper J. (1987). A new approach to immunocytochemistry of 3',5'-cyclic guanosine monophosphate: preparation, specificity and initial application of a new antiserum against formaldehyde fixed 3',5'-cyclic guanosine monophosphate. *Neurosci* **22**, 361-373.

Demyanenko GP, Halberstadt AI, Pryzwansky KB, Werner C, Hofmann F and Maness PF. (2005). Abnormal neocortical development in mice lacking cGMP-dependent protein kinase I. *Brain Res Dev Brain Res* **160**, 1-8.

Denninger JW and Marletta MA. (1999). Guanylate cyclase and the NO/cGMP signaling pathway. *Biochim Biophys Acta* **1411**, 334-350.

Diamond P, Mallavarapu A, Schnipper J, Booth J, Park L, O'Connor TP and Jay DG. (1993). Fasciclin I and II have distinct roles in the development of grasshopper pioneer neurons. *Neuron* **11**, 409-421.

Dickson BJ. (2002). Molecular mechanisms of axon guidance. *Science* **298**, 1959-964.

Diefenbach TJ, Sioley BD, Goldberg JI. (1995). Neurite branch development of an identified serotonergic neuron from embryonic *Helisoma*: evidence for autoregulation by serotonin. *Dev Biol* **167**, 282-293.

Ding Y, McCoubrey WK and Maines MD. (1999). Interaction of heme oxygenase-2 with nitric oxide donors. Is the oxygenase an intracellular 'sink' for NO? *Eur J Biochem* **264**, 854-861.

Ditlevsen DK, K hler LB, Berezin V and Bock E. (2007). Cyclic guanosine monophosphate signalling pathway plays a role in neural cell adhesion molecule-mediated neurite outgrowth and survival. *J Neurosci Res* **85**, 703-711.

Dormann D and Weijer CJ. (2003). Chemotactic cell movement during development. *Curr Opin Genet Dev* **13**, 358-364.

Duve H and Thorpe A. (2003). Neuropeptide co-localisation in the lepidopteran frontal ganglion studied by confocal laser scanning microscopy. *Cell Tissue Res* **311**, 79-89.

Elphick MR, Rayne RC, Riveros-Moreno V, Moncada S and O'Shea M. (1995). Nitric oxide synthesis in locust olfactory interneurons. *J Exp Biol* **198**, 821-829.

Enikolopov G, Banerji J and Kuzin B. (1999). Nitric oxide and *Drosophila* development. *Cell Death Differ* **6**, 956-963.

- Evgenov OV, Pacher P, Schmidt PM, Hasko G, Schmidt HHHW and Stasch J-P.** (2006). NO-independent stimulators and activators of soluble guanylate cyclase: discovery and therapeutic potential. *Nat Rev Drug Discov* **5**, 755-768.
- Fishman R B and Hatten ME.** (1993). Multiple receptor systems promote CNS neural migration. *J Neurosci* **13**, 3485-3495.
- Forscher P and Smith SJ.** (1988). Actions of cytochalasins on the organization of actin filaments and microtubules in a neuronal growth cone. *J Cell Biol* **107**, 1505-1516.
- Freitas A, Alves-Filho JC, Secco DD, Neto AF, Ferreira SH, Barja-Fidalgo C and Cunha FQ.** (2006). Heme oxygenase/carbon monoxide-biliverdin pathway down regulates neutrophil rolling, adhesion and migration in acute inflammation. *Br J Pharmacol* **149**, 345-354.
- Friebe A and Koesling D.** (1998). Mechanism of YC-1-induced activation of soluble guanylyl cyclase. *Mol Pharmacol* **53**, 123-127.
- Gallo G and Letourneau PC.** (2004) Regulation of growth cone actin filaments by guidance cues. *J Neurobiol* **58**, 92-102.
- Ganfornina MD, Sánchez D and Bastiani MJ.** (1996). Embryonic development of the enteric nervous system of the grasshopper *Schistocerca americana*. *J Comp Neurol* **372**, 581-596.
- Gelperin A, Flores J, Raccuia-Behling F and Cooke IR.** (2000). Nitric oxide and carbon monoxide modulate oscillations of olfactory interneurons in a terrestrial mollusk. *J Neurophysiol* **83**, 116-127.
- Gershon MD.** (2004). Review article: serotonin receptors and transporters – roles in normal and abnormal gastrointestinal motility. *Aliment Pharmacol Ther* **20** (Suppl. 7), 3-14.
- Gibbs SM and Truman JW.** (1998). Nitric oxide and cyclic GMP regulate retinal patterning in the optic lobe of *Drosophila*. *Neuron* **20**, 83-93.
- Gibson NJ and Nighorn A.** (2000). Expression of nitric oxide synthase and soluble guanylyl cyclase in the developing olfactory system of *Manduca sexta*. *J Comp Neurol* **422**, 191-205.
- Gilbert SF.** (1997). Chapter 8 Axonal specificity, in: *Developmental Biology*, 5th ed. Sinauer Associates, Sunderland, Massachusetts, USA.
- Godfrey EW, Longacher M, Neiswender H, Schwarte RC and Browning DD.** (2007). Guanylate cyclase and cyclic GMP-dependent protein kinase regulate agrin signaling at the developing neuromuscular junction. *Dev Biol* **307**, 195-201.

- Goldberg JI and Kater SB.** (1989). Expression and function of the neurotransmitter serotonin during development of the *Helisoma* nervous system. *Dev Biol* **131**, 483-495.
- Golden JA, Zitz JC, McFadden K and Cepko CL.** (1997). Cell migration in the developing chick diencephalon. *Development* **124**, 3525-3533.
- Gonzales-Gaitan M and Jäckle H.** (1995). Invagination centers within the *Drosophila* stomatogastric nervous system anlage are positioned by Notch-mediated signaling which is spatially. *Development* **121**, 2313-2325.
- Goodman CS and Bate M.** (1981). Neuronal development in the grasshopper. *Trends Neurosci* **4**, 163-169.
- Goodman CS.** (1996). Mechanisms and molecules that control growth cone guidance. *Annu Rev Neurosci* **19**, 341-377.
- Grundemar L and Ny L.** (1997). Pitfalls using metalloporphyrins in carbon monoxide research. *Trends Pharmacol Sci* **18**, 193-195.
- Gutierrez-Mecinas M, Crespo C, Blasco-Ibáñez JM, Nacher J, Varea E and Martínez-Guijarro FJ.** (2007). Migrating neuroblasts of the rostral migratory stream are putative targets for the action of nitric oxide. *Eur J Neurosci* **26**, 392-402.
- Haase A and Bicker G.** (2003). Nitric oxide and cyclic nucleotides are regulators of neuronal migration in an insect embryo. *Development* **130**, 3977-3987.
- Hahn M and Bishop J.** (2001) Expression pattern of *Drosophila* ret suggests a common ancestral origin between the metamorphosis precursors in insect endoderm and the vertebrate enteric neurons. *Proc Natl Acad Sci USA* **98**, 1053-1058.
- Hao MM, Anderson RB, Kobayashi K, Whittington PM and Young HM.** (2008). The migratory behavior of immature enteric neurons. *Dev Neurobiol* **69**, 22-35.
- Harrelson AL and Goodman CS.** (1988). Growth cone guidance in insects: fasciclin II is a member of the immunoglobulin superfamily. *Science* **242**, 700-708.
- Harris-Warrick RM and Marder E.** (1991). Modulation of neural networks for behaviour. *Annu Rev Neurosci* **14**, 39-57.
- Hartenstein V, Tepass U and Gruszynski-Defeo E.** (1994). Embryonic Development of the Stomatogastric Nervous System in *Drosophila*. *J Comp Neurol* **350**, 367-381.
- Hartenstein V.** (1997). Development of the insect stomatogastric nervous system. *Trends Neurosci* **20**, 421-427.

- Hatten ME.** (1999). Central nervous system neuronal migration. *Annu Rev Neurosci* **22**, 511-539.
- Hernández-Viadel M, Castoldi AF, Coccini T, Manzo L, Erceg S and Felipo V.** (2004). In vivo exposure to carbon monoxide causes delayed impairment of activation of soluble guanylate cyclase by nitric oxide in rat brain cortex and cerebellum. *J Neurochem* **89**, 1157-1165.
- Hess DT, Patterson SI, Smith DS and Skene HJP.** (1993). Neuronal growth cone collapse and inhibition of protein fatty acylation by nitric oxide. *Nature* **366**, 562-565.
- Hiki K, Hattori R, Kawai C and Yui Y.** (1992). Purification of insoluble nitric oxide synthase from rat cerebellum. *J Biochem (Tokyo)* **111**, 556-558.
- Hill SR and Orchard I.** (2003). FMRFamide-related peptides in the gut of *Locusta migratoria* L.: a comprehensive map and developmental profile. *Peptides* **24**, 1511-1524.
- Hu H.** (2000). Polysialic acid regulates chain formation by migrating olfactory interneuron precursors. *J Neurosci Res* **61**, 480-492.
- Ingi T, Cheng J and Ronnett GV.** (1996a). Carbon monoxide: an endogenous modulator of the nitric oxide-cyclic GMP signaling system. *Neuron* **16**, 835-842.
- Ingi T, Chiang G and Ronnett GV.** (1996b). The regulation of heme turnover and carbon monoxide biosynthesis in cultured primary rat olfactory receptor neurons. *J Neurosci* **16**, 5621-5628.
- Jan LY and Jan YN.** (1982). Antibodies to horseradish peroxidase as specific neuronal markers in *Drosophila* and in grasshopper embryos. *Proc Natl Acad Sci USA* **79**, 2700-2704.
- Kalil K and Dent EW.** (2005). Touch and go: guidance cues signal to the growth cone cytoskeleton. *Curr Opin Neurobiol* **15**, 521-526.
- Kharitonov VG, Sharma VS, Pilz RB, Magde D and Koesling D.** (1995). Basis of guanylate cyclase activation by carbon monoxide. *Proc Natl Acad Sci USA* **92**, 2568-2571.
- Kim HP, Ryter SW and Choi AMK.** (2006). CO as a cellular signaling molecule. *Annu Rev Pharmacol Toxicol* **46**, 411-449.
- Klemm N, Hustert R, Cantera R and Nässel DR.** (1986). Neurons reactive to antibodies against serotonin in the stomatogastric nervous system and in the alimentary canal of locust and crickets (Orthoptera, Insecta). *Neuroscience* **17**, 247-261.

- Knipp S and Bicker G.** (2006). The gaseous messenger molecules CO and NO regulate neuronal cell migration in an insect embryo. *FENS Abstr.* **3**, A122.14.
- Knipp S and Bicker G.** (2008). The messenger molecule carbon monoxide (CO) organises nitric oxide (NO)-dependent neuronal chain migration in an insect embryonic nervous system. *FENS Abstr.* **4**, 041.19.
- Knipp S and Bicker G.** (2009). Regulation of enteric neuron migration by the gaseous messenger molecules CO and NO. *Development* **136**, 85-93.
- Ko FN, Wu CC, Kuo SC, Lee FY and Teng CM.** (1994). YC-1, a novel activator of platelet guanylate cyclase. *Blood* **84**, 4226-4233.
- Koert CE, Spencer GE, van Minnen J, Li KW, Geraerts WPM, Syed NI, Smit AB and van Kesteren RE.** (2001). Functional implications of neurotransmitter expression during axonal regeneration: serotonin, but not peptides, auto-regulate axon growth of an identified central neuron. *J Neurosci* **21**, 5597-5606.
- Koesling D, Russwurm M, Mergia E, Mullershausen F and Friebe A.** (2004). Nitric oxide-sensitive guanylyl cyclase: structure and regulation. *Neurochem Int* **45**, 813-819.
- Kolodkin AL, Matthes DJ, O'Connor TP, Patel NH, Admon A, Bentley D and Goodman CS.** (1992). Fasciclin IV: sequence, expression, and function during growth cone guidance in the grasshopper embryo. *Neuron* **9**, 831-845.
- Kriegstein AR and Noctor SC.** (2004). Patterns of neuronal migration in the embryonic cortex. *Trends Neurosci* **27**, 392-399.
- Krumenacker JS and Murad F.** (2006). NO-cGMP signaling in development and stem cells. *Mol Genet Metab* **87**, 311-314.
- Kuzin B, Roberts I, Peunova N and Enikolopov G.** (1996). Nitric oxide regulates cell proliferation during *Drosophila* development. *Cell* **87**, 639-649.
- Labbe RF, Vreman HJ and Stevenson DK.** (1999). Zinc protoporphyrin: A metabolite with a mission. *Clin Chem* **45**, 2060-2072.
- Lambert de Rouvroit C and Goffinet AM.** (2001). Neuronal migration. *Mech Dev* **105**, 47-56.
- Lauffenburger DA and Horwitz AF.** (1996). Cell migration: a physically integrated molecular process. *Cell* **84**, 359-369.
- Lichtman JW and Fraser SE.** (2001). The neuronal naturalist: watching neurons in their native habitat. *Nat Neurosci* **4 (Suppl.)**, 1215-1220.
- Lin CH, Thompson CA and Forscher P.** (1994). Cytoskeletal reorganization underlying growth cone motility. *Curr Opin Neurobiol* **4**, 640-647.

- Lois C, García-Verdugo JM and Alvarez-Buylla A.** (1996). Chain migration of neuronal precursors. *Science* **271**, 978-981.
- Luffy D and Dorn A.** (1992). Immunohistochemical demonstration in the stomatogastric nervous system and effects of putative neurotransmitters on the motility of the isolated midgut of the stick insect, *Carausius morosus*. *J Insect Physiol* **37**, 287-299.
- Lundell MJ and Hirsh J.** 1998. *eagle* is required for the specification of serotonin neurons and other neuroblast 7-3 progeny in the *Drosophila* CNS. *Development* **125**, 463-472.
- Luo D and Vincent SR.** (1994). Metalloporphyrins inhibit nitric oxide-dependent cGMP formation in vivo. *Eur J Pharmacol* **267**, 263-267.
- Luo L.** (2000). Rho GTPases in neuronal morphogenesis. *Nat Rev Neurosci* **1**, 173-180.
- Ma N, Ding X, Doi M, Izumi N and Semba R.** (2004). Cellular and subcellular localization of heme oxygenase-2 in monkey retina. *J Neurocytol* **33**, 407-415.
- Maines MD.** (1981). Zinc protoporphyrin is a selective inhibitor of heme oxygenase activity in the neonatal rat. *Biochim Biophys Acta* **673**, 339-350.
- Maines MD.** (1988). Heme oxygenase: function, multiplicity, regulatory mechanisms, and clinical applications. *FASEB J* **2**, 2557-2568.
- Maines MD.** (1997). The heme oxygenase system: a regulator of second messenger gases. *Annu Rev Pharmacol Toxicol* **37**, 517-554.
- Marín O, Valdeolmillos M and Moya F.** (2006). Neurons in motion: same principles for different shapes? *Trends Neurosci* **29**, 655-661.
- Mazer C, Muneyyirci J, Taheny K, Raio N, Borella A and Whitaker-Azmitia P.** (1997). Serotonin depletion during synaptogenesis leads to decreased synaptic density and learning deficits in the adult rat: a possible model of neurodevelopmental disorders with cognitive deficits. *Brain Res* **760**, 68-73.
- Melendez-Herrera E, Colin-Castelan D, Varela-Echavarria A and Gutierrez-Ospina G.** (2008). Semaphorin-3A and its receptor neuropilin-1 are predominantly expressed in endothelial cells along the rostral migratory stream of young and adult mice. *Cell Tissue Res* **333**, 175-184
- Miller SM, Reed D, Sarr MG, Farrugia G and Szurszewski JH.** (2001). Haem oxygenase in enteric nervous system of human stomach and jejunum and co-localization with nitric oxide synthase. *Neurogastroenterol Motil* **13**, 121-131.
- Moiseiwitsch JRD and Lauder JM.** (1995). Serotonin regulates mouse cranial

neural crest migration. *Proc Natl Acad Sci USA* **92**, 7182-7186.

Molaei G and Lange AB. (2003). The association of serotonin with the alimentary canal of the african migratory locust, *Locusta migratoria*: distribution, physiology and pharmacological profile. *J Insect Physiol* **49**, 1073-1082.

Mortimer D, Fothergill T, Pujic Z, Richards LJ and Goodhill GJ. (2008). Growth cone chemotaxis. *Trends Neurosci* **31**, 90-98.

Motterlini R, Clark JE, Foresti R, Sarathchandra P, Mann BE and Green CJ. (2002). Carbon monoxide-releasing molecules: characterization of biochemical and vascular activities. *Circ Res* **90**, E17-E24.

Müller U and Bicker G. (1994). Calcium-activated release of nitric oxide and cellular distribution of nitric oxide-synthesizing neurons in the nervous system of the locust. *J Neurosci* **14**, 7521-7528.

Oess S, Icking A, Fulton D, Govers R and Müller-Esterl W. (2006). Subcellular targeting and trafficking of nitric oxide synthases. *Biochem J* **396**, 401-409.

Ott SR and Burrows M. (1999). NADPH diaphorase histochemistry in the thoracic ganglia of locusts, crickets, and cockroaches: species differences and the impact of fixation. *J Comp Neurol* **410**, 387-397.

Ott SR, Delago A and Elphick MR. (2004). An evolutionarily conserved mechanism for sensitization of soluble guanylyl cyclase reveals extensive nitric oxide-mediated upregulation of cyclic GMP in insect brain. *Eur J Neurosci* **20**, 1231-1244.

Park HT, Wu J and Rao Y. (2002). Molecular control of neuronal migration. *Bioessays* **24**, 821-827.

Park SK, George R, Cai Y, Chang HY, Krantz DE, Friggi-Grelin F, Birman S and Hirsh J. (2006). Cell-type-specific limitation on in vivo serotonin storage following ectopic expression of the *Drosophila* serotonin transporter, dSERT. *J Neurobiol* **66**, 452-462.

Peunova N, Scheinker V, Cline H and Enikolopov G. (2001). Nitric oxide is an essential negative regulator of cell proliferation in *Xenopus* brain. *J Neurosci* **21**, 8809-8818.

Polleux F, Morrow T and Ghosh A. (2000). Semaphorin 3A is a chemoattractant for cortical apical dendrites. *Nature* **404**, 567-573.

Radwan WA, Granger NA and Lauder JM. (1989). Development and distribution of serotonin in the central nervous system of *Manduca sexta* during embryogenesis. I. The brain and frontal ganglion. *Int J Devl Neuroscience* **7**, 27-41.

- Regulski M and Tully T.** (1995). Molecular and biochemical characterization of dNOS: a *Drosophila* Ca²⁺/calmodulin-dependent nitric oxide synthase. *Proc Nat Acad Sci USA* **92**, 9072-9076.
- Regulski M, Stasiv Y, Tully T and Enikolopov G.** (2004). Essential function of nitric oxide synthase in *Drosophila*. *Curr Biol* **14**, R881-R882.
- Richards KS, Simon DJ, Pulver SR, Beltz BE and Marder E.** (2003). Serotonin in the developing stomatogastric system of the lobster, *Homarus americanus*. *J Neurobiol* **54**, 380-392.
- Rousselot P, Lois C and Alvarez-Buylla A.** (1995). Embryonic (PSA) N-CAM reveals chains of migrating neuroblasts between the lateral ventricle and the olfactory bulb of adult mice. *J Comp Neurol* **351**, 51-61.
- Schmidt H, Werner M, Heppenstall PA, Henning M, More MI, Kuhbandner S, Lewin GR, Hofmann F, Feil R and Rathjen FG.** (2002). cGMP-mediated signaling via cGKI alpha is required for the guidance and connectivity of sensory axons. *J Cell Biol* **159**, 489-498.
- Schmidt JT.** (2004). Activity-driven sharpening of the retinotectal projection: the search for retrograde synaptic signaling pathways. *J Neurobiol* **59**, 114-133.
- Scholz NL, de Vente J, Truman JW and Graubard K.** (2001). Neural network partitioning by NO and cGMP. *J Neurosci* **21**, 1610-1618.
- Seidel C and Bicker G** (2000). Nitric oxide and cGMP influence axonogenesis of antennal pioneer neurons. *Development* **127**, 4541-4549.
- Serfass L and Burstyn JN.** (1998). Effect of heme oxygenase inhibitors on soluble guanylyl cyclase activity. *Arch Biochem Biophys* **359**, 8-16.
- Settembrini BP, Coronel MF, Nowicki S, Nighorn AJ and Villar MJ.** (2007). Distribution and characterization of nitric oxide synthase in the nervous system of *Triatoma infestans* (Insecta: Heteroptera). *Cell Tissue Res* **328**, 421-430.
- Snow PM, Patel NH, Harrelson AL and Goodman CS.** (1987). Neural-specific carbohydrate moiety shared by many surface glycoproteins in *Drosophila* and grasshopper embryos. *J Neurosci* **7**, 4137-4144.
- Snow PM, Zinn K, Harrelson AL, McAllister L, Schilling J, Bastiani MJ, Makk G and Goodman CS.** (1988). Characterization and cloning of fasciclin I and fasciclin II glycoproteins in the grasshopper. *Proc Natl Acad Sci USA* **85**, 5291-5295.
- Song H, Ming G, He Z, Lehmann M, McKerracher L, Tessier-Lavigne M and Poo M.** (1998). Conversion of neuronal growth cone responses from repulsion to attraction by cyclic nucleotides. *Science* **281**, 1515-1518.

- Song H and Poo M.** (2001). The cell biology of neuronal navigation. *Nat Cell Biol* **3**, E81-E88.
- Stern M and Bicker G.** (2008). Nitric oxide regulates axonal regeneration in an insect embryonic CNS. *Dev Neurobiol* **68**, 295-308.
- Stern M, Knipp S and Bicker G.** (2007). Embryonic differentiation of serotonin-containing neurons in the enteric nervous system of the locust (*Locusta migratoria*). *J Comp Neurol* **501**, 38-51.
- Sullivan JM, Benton JL, Beltz BS.** (2000). Serotonin depletion *in vivo* inhibits the branching of olfactory projection neurons in the lobster deutocerebrum. *J Neurosci* **20**, 7716-7721.
- Sun Y, Rotenberg MO and Maines MD.** (1990). Developmental expression of heme oxygenase isozymes in rat brain. Two HO-2 mRNAs are detected. *J Biol Chem* **265**, 8212-8217.
- Sykes PA and Condron BG.** (2005). Development and sensitivity to serotonin of *Drosophila* serotonergic varicosities in the central nervous system. *Dev Biol* **286**, 207-216.
- Taghert PH, Goodman CS.** (1984). Cell determination and differentiation of identified serotonin-immunoreactive neurons in the grasshopper embryo. *J Neurosci* **4**, 989-1000.
- Tamagnone L and Comoglio PM.** (2004). To move or not to move? Semaphorin signalling in cell migration. *EMBO Rep* **5**, 356-361.
- Tanaka J, Markerink-van Ittersum M, Steinbusch HW and De Vente J.** (1997). Nitric oxide-mediated cGMP synthesis in oligodendrocytes in the developing rat brain. *Glia* **19**, 286-297.
- Tenhunen R, Marver HS and Schmid R.** (1968). The enzymatic conversion of heme to bilirubin by microsomal heme oxygenase. *Proc Natl Acad Sci USA* **61**, 748-755.
- Tessier-Lavigne M and Goodman CS.** (1996). The molecular biology of axon guidance. *Science* **274**, 1123-1133.
- Tornieri K and Rehder V.** (2007). Nitric oxide release from a single cell affects filopodial motility on growth cones of neighboring neurons. *Dev Neurobiol* **67**, 1932-1943.
- Trimm KR and Rehder V.** (2004). Nitric oxide acts as a slow-down and search signal in developing neurites. *Eur J Neurosci* **19**, 809-818.
- Truman JW, De Vente J and Ball EE.** (1996). Nitric oxide-sensitive guanylate

cyclase activity is associated with the maturational phase of neuronal development in insects. *Development* **122**, 3949-3958.

Trumm P and Dorn A. (2000). Effects of azadirachtin on the regulation of midgut peristalsis by the stomatogastric nervous system in *Locusta migratoria*. *Phytoparasitica* **28**, 7-26.

Tsai LH and Gleeson JG. (2005). Nucleokinesis in neuronal migration. *Neuron* **46**, 383-388.

Valles AM and White K. (1988). Serotonin-containing neurons in *Drosophila melanogaster*: development and distribution. *J Comp Neurol* **268**, 414-428.

Van Vactor DV and Lorenz JL. (1999). Introduction: invertebrate axons find their way. *Cell Mol Life Sci* **55**, 1355-1357.

Van Wagenen S and Rehder V. (2001). Regulation of neuronal growth cone filopodia by nitric oxide depends on soluble guanylyl cyclase. *J Neurobiol* **46**, 206-219.

VanUffelen BE, de Koster BM, VanSteveninck J and Elferink JG. (1996). Carbon monoxide enhances human neutrophil migration in a cyclic GMP-dependent way. *Biochem Biophys Res Commun* **226**, 21-26.

Verma A, Hirsch DJ, Glatt CE, Ronnett GV and Snyder SH. (1993). Carbon monoxide: a putative neural messenger. *Science* **259**, 381-384.

Watanabe T, Kikuchi M, Hatakeyama D, Shiga T, Yamamoto T, Aonuma H, Takahata M, Suzuki N and Ito E. (2007). Gaseous neuromodulator-related genes expressed in the brain of honeybee *Apis mellifera*. *Dev Neurobiol* **67**, 456-473.

Watanabe Y, Nishio M, Hamaji S, Hayashi Y, Hu Y and Hidaka H. (1998). Neuronal nitric oxide synthase-membrane phospholipid interactions. *Arch Biochem Biophys* **358**, 68-73.

Welshhans K and Rehder V. (2005). Local activation of the nitric oxide/cyclic guanosine monophosphate pathway in growth cones regulates filopodial length via protein kinase G, cyclic ADP ribose and intracellular Ca²⁺ release. *Eur J Neurosci* **22**, 3006-3016.

Wichterle H, Garcia-Verdugo JM and Alvarez-Buylla A. (1997). Direct evidence for homotypic, glia-independent neuronal migration. *Neuron* **18**, 779-791.

Wildemann B, Reichert H and Bicker G. (1997). Embryonic brain tract formation in *Drosophila melanogaster*. *Dev Genes Evol* **206**, 536-540

Wong JT, Yu WT and O'Connor TP. (1997). Transmembrane grasshopper Semaphorin I promotes axon outgrowth in vivo. *Development* **124**, 3597-3607.

- Wright JW and Copenhaver PF.** (2000). Different isoforms of Fasciclin II play distinct roles in the guidance of neuronal migration during insect embryogenesis. *Dev Biol* **225**, 59-78.
- Wright JW, Schwinof KM, Snyder MA and Copenhaver PF.** (1998). A delayed role for nitric oxide-sensitive guanylate cyclases in a migratory population of embryonic neurons. *Dev Biol* **204**, 15-33.
- Wright JW, Snyder MA, Schwinof KM, Combes S and Copenhaver PF.** (1999). A role for fasciclin II in the guidance of neuronal migration. *Development* **126**, 3217-3228.
- Wu W, Wong K, Chen J, Jiang Z, Dupuis S, Wu JY and Rao Y.** (1999). Directional guidance of neuronal migration in the olfactory system by the protein Slit. *Nature* **400**, 331-336.
- Xue L, Farrugia G, Miller SM, Ferris CD, Snyder SH and Szurszewski JH.** (2000). Carbon monoxide and nitric oxide as coneurotransmitters in the enteric nervous system: evidence from genomic deletion of biosynthetic enzymes. *Proc Natl Acad Sci USA* **97**, 1851-1855.
- Yeh J-RJ and Crews CM.** (2003). Chemical genetics: adding to the developmental biology toolbox. *Dev Cell* **5**, 11-19.
- Young HM, Anderson RB and Anderson CR.** (2004). Guidance cues involved in the development of the peripheral autonomic nervous system. *Auton Neurosci* **112**, 1-14.
- Zhang X, Sato M, Sasahara M, Migita CT and Yoshida T.** (2004). Unique features of recombinant heme oxygenase of *Drosophila melanogaster* compared with those of other heme oxygenases studied. *Eur J Biochem* **271**, 1713-1724.
- Zheng JQ and Poo M.** (2007). Calcium signaling in neuronal motility. *Annu Rev Cell Dev Biol* **23**, 375-404.
- Zufall F and Leinders-Zufall T.** (1997). Identification of a long-lasting form of odor adaptation that depends on the carbon Monoxide/cGMP second-messenger system. *J Neurosci* **17**, 2703-2712.

Abbreviations

5-HT	5-hydroxytryptamine (serotonin)
7-NI	7-nitroindazole
% E	% of embryonic development
BSA	bovine serum albumin
CO	carbon monoxide
CORM II	tricarbonyldichlororuthenium (II) dimer
cGMP	cyclic guanosine-monophosphate
ca	caeca
CaM	calcium-calmodulin
cAMP	cyclic adenosine-monophosphate
CNS	central nervous system
DMSO	dimethyl-sulfoxide
en	enteric neuron
ENS	enteric nervous system
env	esophageal nerve
Fas-I/-II	Fasciclin I/II
fc	frontal connective
FG	foregut
fg	frontal ganglion
hg	hypocerebral ganglion
HO	heme oxygenase
HRP	horse radish peroxidase
ICC	immunocytochemistry
ig	ingluvial ganglion
IR	immunoreactivity
la	labrum
m	musculature
MG	midgut
MG-M	membrane fraction of midgut homogenate
NADPHd	NADPH diaphorase
N-CAM	neural cell adhesion molecule

NO	nitric oxide
NOS	nitric oxide synthase
PBS	phosphate buffered saline
PBS-T	PBS with triton X-100
PBS-TW	PBS with TWEEN
PFA	paraformaldehyd
PNS	peripheral nervous system
PSA-N-CAM	polysialated N-CAM
RMS	rostral migratory stream
rnv	recurrent nerve
sGC	soluble guanylate cyclase
Sema-1	Semaphorin 1
SERT	serotonin uptake transporter
SNS	stomatogastric nervous system
SVZ	subventricular zone
uNOS	universal NOS
YC-1	3-(5'-hydroxymethyl-2'-furyl)-1-benzyl Indazole
Z1-3	neurogenic zone 1-3
ZnBG	zincdeuteroporphyrin-IX 2,4 bis glycol
ZnPP-IX	zinc protoporphyrin-IX

Appendix

Summary of the measured migratory distances after 24 h in vivo culturing.

L-arginine

iv 08-08-06 65% E (embryonic age at start of in vivo culture)					
Kontrolle L15			2 mM L-Arginin		
max./Darm [mm]	[%] von Mittelwert Kontrolle		max./Darm [mm]	[%] von Mittelwert Kontrolle	
1,640	68,305		0,714	29,738	
3,319	138,234		2,992	124,615	
1,604	66,805		2,989	124,490	
1,171	48,771		3,196	133,111	
3,119	129,904		1,861	77,509	
2,765	115,160		3,328	138,609	
3,217	133,986		1,804	75,135	
2,374	98,875		3,318	138,192	
			3,030	126,197	
2,401	100,005	Mittelwert	2,581	107,511	Mittelwert
2,570	107,018	Median	2,992	124,615	Median

iv 21-08-06 65% (embryonic age at start of in vivo culture)					
Kontrolle L15			2 mM L-Arginin		
max./Darm [mm]	[%] von Mittelwert Kontrolle		max./Darm [mm]	[%] von Mittelwert Kontrolle	
2,068	96,953		1,957	91,749	
1,724	80,825		3,082	144,491	
2,043	95,781		2,699	126,535	
2,228	104,454		1,782	83,544	
2,876	134,834		3,091	144,913	
2,078	97,421		3,492	163,713	
2,579	120,910		2,764	129,583	
2,282	106,985		2,575	120,722	
1,156	54,196		2,879	134,974	
2,743	128,598		1,836	86,076	
2,728	127,895		1,972	92,452	
1,839	86,217				
2,357	110,502				
2,244	105,204				
1,761	82,560				
1,665	78,059				
1,883	88,279				
2,133	99,981	Mittelwert	2,557	119,887	Mittelwert
2,078	97,421	Median	2,699	126,535	Median

iv 01-02-07 63% (embryonic age at start of in vivo culture)					
Kontrolle L15			2 mM L-Arginin		
max./Darm [mm]	[%] von Mittelwert Kontrolle		max./Darm [mm]	[%] von Mittelwert Kontrolle	
1,953	115,085		2,249	132,528	
1,807	106,482		0,945	55,687	
2,064	121,626		1,577	92,929	
1,315	77,490		1,442	84,973	
2,103	123,925		1,080	63,642	
0,889	52,387		1,679	98,939	
1,493	87,979		0,987	58,161	
1,970	116,087		2,526	148,851	
1,678	98,880		1,924	113,377	
1,697	99,993	Mittelwert	1,601	94,343	Mittelwert
1,807		Median	1,577		Median

iv 14-02-07-I 63% (embryonic age at start of in vivo culture)					
Kontrolle L15			2 mM L-Arginin		
max./Darm [mm]	[%] von Mittelwert Kontrolle		max./Darm [mm]	[%] von Mittelwert Kontrolle	
0,468	87,151		1,302	242,458	
0,681	126,816		0,856	159,404	
0,293	54,562		0,268	49,907	
0,462	86,034		0,215	40,037	
0,389	72,439		0,784	145,996	
0,855	159,218		0,308	57,356	
0,254	47,300		0,412	76,723	
0,924	172,067		0,533	99,255	
0,707	131,657		0,488	90,875	
0,337	62,756		0,376	70,019	
0,537	100,000	Mittelwert	0,554	103,203	Mittelwert
0,465		Median	0,450		Median

CORM-II

iv 12-03-08-I 63% E (embryonic age at start of in vivo culture)								
Kontrolle L15 + 0,1% DMSO			20 µM iCORM-II		20 µM CORM-II			
max./Darm [mm]	[%] von Mittelwert Kontrolle		max./Darm [mm]	[%] von Mittelwert Kontrolle		max./Darm [mm]	[%] von Mittelwert Kontrolle	
0,847	75,423		1,192	106,144		0,730	65,004	
1,841	163,936		1,321	117,631		1,078	95,993	
1,002	89,225		2,560	227,961		0,464	41,318	
0,911	81,122		0,781	69,546		0,674	60,018	
2,052	182,725		1,639	145,948		1,658	147,640	
1,176	104,720		0,868	77,293		0,649	57,792	
1,173	104,452		1,383	123,152		0,873	77,738	
0,848	75,512		0,828	73,731		1,012	90,116	
1,452	129,297		0,743	66,162		0,861	76,670	
0,459	40,873		0,975	86,821		0,710	63,224	
0,769	68,477		1,136	101,158		0,836	74,443	
0,942	83,882		1,036	92,253		1,067	95,013	
			0,729	64,915		0,748	66,607	
1,123	99,970	Mittelwert	1,169	104,055	Mittelwert	0,874	77,814	Mittelwert
0,972		Median	1,036		Median	0,836		Median

iv 12-03-08-II 63% E (embryonic age at start of in vivo culture)					
Kontrolle L15 + 0,1% DMSO			20 µM CORM-II		
max./Darm [mm]	[%] von Mittelwert Kontrolle		max./Darm [mm]	[%] von Mittelwert Kontrolle	
1,018	173,424		0,413	70,358	
0,262	44,634		0,370	63,032	
0,604	102,896		0,521	88,756	
0,703	119,761		0,244	41,567	
0,769	131,005		0,172	29,302	
0,855	145,656		0,392	66,780	
0,496	84,497		0,401	68,313	
0,323	55,026		0,150	25,554	
0,502	85,520		0,262	44,634	
0,342	58,262		0,222	37,819	
			0,460	78,365	
			0,107	18,228	
0,587	100,068	Mittelwert	0,310	52,726	Mittelwert
0,553		Median	0,316		Median

iv 13-03-08 63% E (embryonic age at start of in vivo culture)					
Kontrolle L15 + 0,1% DMSO			20 µM iCORM-II		
max./Darm [mm]	[%] von Mittelwert Kontrolle		max./Darm [mm]	[%] von Mittelwert Kontrolle	
0,679	147,930		0,073	15,904	
0,288	62,745		0,176	38,344	
0,514	111,983		0,267	58,170	
0,174	37,908		0,339	73,856	
0,307	66,885		0,350	76,253	
0,637	138,780		0,479	104,357	
0,369	80,392		1,580	344,227	
0,844	183,878		0,485	105,664	
0,397	86,492		0,731	159,259	
0,686	149,455		0,547	119,172	
0,359	78,214		0,186	40,523	
0,249	54,248		0,158	34,423	
0,459	99,909	Mittelwert	0,448	97,513	Mittelwert
0,383		Median	0,345		Median

Hemin

iv 08-02-07 63%					
Kontrolle L15 + 1% DMSO			100 µM Hemin (ausgefallen)		
max. länge [mm]	% von Mittelwert Kontrolle		max. länge [mm]	% von Mittelwert Kontrolle	
2,384	133,259		1,655	92,510	
1,743	97,429		1,676	93,684	
1,059	59,195		2,432	135,942	
2,280	127,446		0,642	35,886	
2,362	132,029		1,785	99,776	
1,314	73,449		1,166	65,176	
3,059	170,989		1,310	73,225	
0,889	49,693		0,916	51,202	
0,750	41,923		1,099	61,431	
0,953	53,270		1,572	87,870	
1,430	79,933		2,390	133,594	
2,033	113,639		1,091	60,984	
1,095	61,207		1,218	68,083	
3,689	206,205		2,743	153,326	
1,79	99,976	Mittelwert	1,550	86,621	Mittelwert
1,59		Median	1,441		Median

iv 14-02-07-II 63% +					
Kontrolle L15 + 1% 0,1M NaOH			100 µM Hemin		
max. länge [mm]	% von Mittelwert Kontrolle		max. länge [mm]	% von Mittelwert Kontrolle	
0,942	81,913		0,073	6,348	
2,772	241,043		0,390	33,913	
0,358	31,130		0,862	74,957	
1,034	89,913		0,847	73,652	
0,855	74,348		1,812	157,565	
3,054	265,565		1,178	102,435	
0,774	67,304		0,018	1,565	
0,329	28,609		0,552	48,000	
0,534	46,435		1,099	95,565	
0,852	74,087		0,957	83,217	
			0,433	37,652	
			0,363	31,565	
			0,257	22,348	
1,150	100,035	Mittelwert	0,680	59,14	Mittelwert
0,854		Median	0,55		Median

iv 14-03-07		63% +			
Kontrolle L15 + 1% 0,1M NaOH		100 µM Hemin			
max. länge [mm]	% von Mittelwert Kontrolle	max. länge [mm]	% von Mittelwert Kontrolle		
0,439	44,209	1,625	163,646		
1,089	109,668	1,355	136,455		
0,463	46,626	1,325	133,434		
1,556	156,697	1,174	118,228		
1,048	105,539	0,252	25,378		
0,721	72,608	0,195	19,637		
1,303	131,219	1,153	116,113		
0,444	44,713	1,985	199,899		
1,242	125,076	1,084	109,164		
1,383	139,275	0,517	52,064		
0,546	54,985	1,205	121,349		
1,043	105,035	0,948	95,468		
0,548	55,186	1,237	124,572		
0,605	60,926	1,088	109,567		
1,605	161,631	1,527	153,776		
0,838	84,391	0,696	70,091		
1,514	152,467	0,743	74,824		
0,749	75,428	1,197	120,544		
0,977	98,389	1,715	172,709		
1,742	175,428	0,526	52,971		
		1,137	114,502		
		0,521	52,467		
0,993	99,975	Mittelwert	1,05	106,221	Mittelwert
1,010		Median	1,15		Median

iv 07-08-07-I		63% +			
Kontrolle L15 + 1% 0,1M NaOH		100 µM Hemin			
max. länge [mm]	% von Mittelwert Kontrolle	max. länge [mm]	% von Mittelwert Kontrolle		
1,050	94,424	0,765	68,795		
0,935	84,083	1,137	102,248		
1,409	126,709	1,340	120,504		
1,626	146,223	1,259	113,219		
0,791	71,133	1,336	120,144		
1,602	144,065	1,596	143,525		
1,470	132,194	1,673	150,450		
0,776	69,784	0,647	58,183		
0,640	57,554	1,077	96,853		
1,172	105,396	0,885	79,586		
0,766	68,885				
1,112	100,041	Mittelwert	1,172	105,351	Mittelwert
1,050		Median	1,198		Median

Hemoglobin

iv 19-07-05 63% E (embryonic age at start of in vivo culture)			
Kontrolle L15		500 µM Hämoglobin	
max./Darm [mm]	[%] von Mittelwert Kontrolle	max./Darm [mm]	[%] von Mittelwert Kontrolle
0,724	54,273	0,844	63,268
0,979	73,388	0,673	50,450
1,193	89,430	0,169	12,669
1,252	93,853	0,466	34,933
1,473	110,420	1,121	84,033
3,253	243,853	0,217	16,267
0,579	43,403	0,648	48,576
1,978	148,276	0,747	55,997
0,575	43,103	1,142	85,607
		0,777	58,246
		0,723	54,198
1,334	100,000	0,684	51,295
1,193		0,723	
	Mittelwert		Mittelwert
	Median		Median

iv 21-03-07 65% E (embryonic age at start of in vivo culture)			
Kontrolle L15		500 µM Hämoglobin	
max./Darm [mm]	[%] von Mittelwert Kontrolle	max./Darm [mm]	[%] von Mittelwert Kontrolle
1,516	106,461	1,319	92,626
1,417	99,508	1,092	76,685
1,330	93,399	1,224	85,955
2,172	152,528	0,987	69,312
1,714	120,365	1,839	129,143
1,310	91,994	1,176	82,584
1,087	76,334	1,25	87,781
2,072	145,506	1,391	97,683
0,81	56,882	1,177	82,654
1,424	100	1,076	75,562
1,323	92,907	1,557	109,340
0,913	64,115	1,304	91,573
1,424	100	1,283	90,075
1,374		1,237	
	Mittelwert		Mittelwert
	Median		Median

YC-1

iv-17-08-06 62% +			
Kontrolle 1,8% DMSO		65 µM YC-1	
max. länge [mm]	% von Mittelwert Kontrolle	max. länge [mm]	% von Mittelwert Kontrolle
0,695	82,936	0,240	28,640
0,187	22,315	3,294	393,079
2,643	315,394	0,798	95,227
0,243	28,998	0,426	50,835
0,688	82,100	0,845	100,835
0,323	38,544	0,728	86,874
2,053	244,988	1,119	133,532
0,897	107,041	1,019	121,599
0,477	56,921	0,530	63,246
0,445	53,103	0,932	111,217
0,866	103,341	0,647	77,208
0,544	64,916		
0,838	100,050	0,962	114,754
0,616		0,798	
	Mittelwert		Mittelwert
	Median		Median

iv-14-09-06		63% +	
Kontrolle 0,65% DMSO		65 μM YC-1	
max. Länge [mm]	% von Mittelwert Kontrolle	max. Länge [mm]	% von Mittelwert Kontrolle
1,408	138,719	1,327	130,739
1,095	107,882	0,277	27,291
1,096	107,980	1,575	155,172
0,941	92,709	0,760	74,877
1,329	130,936	1,153	113,596
0,573	56,453	0,935	92,118
0,754	74,286	1,468	144,631
1,288	126,897	1,827	180,000
1,147	113,005	1,618	159,409
0,115	11,330	1,507	148,473
0,981	96,650	0,564	55,567
0,975	96,059	0,614	60,493
1,750	172,414	1,336	131,626
0,753	74,187	0,719	70,837
		1,290	127,094
		1,360	133,990
1,015	99,96 Mittelwert	1,15	112,87 Mittelwert
1,038	Median	1,309	Median

ZnBG

iv 13-09-06-I		63% +	
Kontrolle		5 μM ZnBG	
max. Länge [mm]	% von Mittelwert Kontrolle	max. Länge [mm]	% von Mittelwert Kontrolle
0,851	79,384	1,765	164,646
1,005	93,750	2,217	206,810
0,821	76,586	1,690	157,649
0,780	72,761	2,228	207,836
0,811	75,653	2,329	217,257
0,741	69,123	1,457	135,914
1,046	97,575	1,676	156,343
1,422	132,649	2,456	229,104
0,778	72,575	0,881	82,183
1,353	126,213	0,765	71,362
2,186	203,918	1,039	96,922
		0,969	90,392
		1,454	135,634
		0,992	92,537
		1,262	117,724
		1,905	177,705
		1,15	107,369
		1,51	140,392
		1,18	110,354
1,07	100,017 Mittelwert	1,52	142,007 Mittelwert
0,85	Median	1,46	Median

iv 15-02-07		62% +	
Kontrolle		5 μM ZnBG	
max. Länge [mm]	% von Mittelwert Kontrolle	max. Länge [mm]	% von Mittelwert Kontrolle
0,453	81,038	0,565	101,073
1,186	212,165	0,238	42,576
0,633	113,238	0,369	66,011
0,451	80,680	0,492	88,014
0,692	123,792	0,567	101,431
0,236	42,218	1,282	229,338
0,109	19,499	0,470	84,079
0,640	114,490	1,241	222,004
0,545	97,496	0,781	139,714
0,648	115,921	1,287	230,233
0,56	100,054 Mittelwert	0,73	130,45 Mittelwert
0,59	Median	0,57	Median

iv 20-02-07-I		64% +	
Kontrolle		5 μM ZnBG	
max. Länge [mm]	% von Mittelwert Kontrolle	max. Länge [mm]	% von Mittelwert Kontrolle
1,468	92,502	1,471	92,691
1,708	107,624	1,840	115,942
1,219	76,812	2,271	143,100
1,664	104,852	2,315	145,873
1,001	63,075	1,996	125,772
0,824	51,922	1,698	106,994
1,531	96,471	2,886	181,853
1,391	87,650	1,695	106,805
1,431	90,170	1,811	114,115
1,241	78,198	2,555	160,996
2,727	171,834	1,598	100,693
1,594	100,441	0,961	60,555
1,763	111,090	1,530	96,408
2,047	128,986	1,839	115,879
1,059	66,730	2,169	136,673
2,739	172,590	2,163	136,295
1,573	99,118	2,159	136,043
1,59	100,004 Mittelwert	1,94	122,158 Mittelwert
1,53	Median	1,840	Median

iv 20-02-07-III		63% +	
Kontrolle		5 μM ZnBG	
max. Länge [mm]	% von Mittelwert Kontrolle	max. Länge [mm]	% von Mittelwert Kontrolle
0,936	110,769	1,249	147,811
0,918	108,639	0,822	97,278
1,698	200,947	0,449	53,136
0,782	92,544	2,287	270,651
0,115	13,609	0,844	99,882
0,891	105,444	1,212	143,432
1,346	159,290	0,605	71,598
1,063	125,799	1,247	147,574
0,227	26,864	0,887	104,970
0,475	56,213	1,126	133,254
0,85	100,012 Mittelwert	1,07	126,959 Mittelwert
0,9	Median	1,01	Median

7-NI

iv 22-03-07 64% E (embryonic age at start of in vivo culture)					
Kontrolle L15			500 µM 7-NI		
max./Darm [mm]	[%] von Mittelwert Kontrolle		max./Darm [mm]	[%] von Mittelwert Kontrolle	
2,270	205,059		0,632	51,888	
0,815	73,622		2,430	199,507	
1,541	139,235		0,639	52,463	
1,068	96,477		0,711	58,374	
1,033	93,315		0,744	61,084	
1,136	102,620		1,168	95,895	
0,922	83,288		1,175	96,470	
0,909	82,114		0,525	43,103	
1,370	123,758		0,932	76,519	
0,68	61,427		0,725	59,524	
1,206	108,943		0,894	73,399	
0,59	53,297		1,469	120,608	
0,855	77,236		1,069	87,767	
1,107	100,03	Mittelwert	1,009	82,815	Mittelwert
1,033		Median	0,894		Median

iv 05-06-07 64% E (embryonic age at start of in vivo culture)					
Kontrolle L15			500 µM 7-NI		
max./Darm [mm]	[%] von Mittelwert Kontrolle		max./Darm [mm]	[%] von Mittelwert Kontrolle	
1,113	82,322		0,781	57,766	
1,173	86,760		0,748	55,325	
1,702	125,888		1,075	79,512	
0,859	63,536		0,609	45,044	
2,737	202,441		1,221	90,311	
1,226	90,680		0,926	68,491	
1,407	104,068		0,568	42,012	
1,388	102,663		0,995	73,595	
0,990	73,225		0,182	13,462	
1,058	78,254		0,841	62,204	
1,221	90,311		0,659	48,743	
1,352	100,013	Mittelwert	0,782	57,86	Mittelwert
1,221		Median	0,781		Median

3B11

iv 03-06-08 63% E (embryonic age at start of in vivo culture)					
Kontrolle L15			3B11 50% in L15		
max./Darm [mm]	[%] von Mittelwert Kontrolle		max./Darm [mm]	[%] von Mittelwert Kontrolle	
0,907	139,753		0,554	85,362	
0,591	91,063		0,520	80,123	
0,541	83,359		0,709	109,245	
0,594	91,525		0,670	103,236	
0,577	88,906		0,933	143,760	
0,668	102,928		0,535	82,435	
0,369	56,857		0,542	83,513	
0,388	59,784		0,368	56,703	
0,728	112,173		0,353	54,391	
0,340	52,388		0,474	73,035	
0,981	151,156				
1,107	170,570				
0,649	100,039	Mittelwert	0,566	87,180	Mittelwert
0,593		Median	0,539		Median

iv 03-06-08		63% E (embryonic age at start of in vivo culture)			
Kontrolle L15		3B11 50% in L15			
max./Darm [mm]	[%] von Mittelwert Kontrolle	max./Darm [mm]	[%] von Mittelwert Kontrolle		
0,907	139,753	0,554	85,362		
0,591	91,063	0,520	80,123		
0,541	83,359	0,709	109,245		
0,594	91,525	0,670	103,236		
0,577	88,906	0,933	143,760		
0,668	102,928	0,535	82,435		
0,369	56,857	0,542	83,513		
0,388	59,784	0,368	56,703		
0,728	112,173	0,353	54,391		
0,340	52,388	0,474	73,035		
0,981	151,156				
1,107	170,570				
0,649	100,039	Mittelwert	0,566	87,180	Mittelwert
0,593		Median	0,539		Median

Acknowledgement

I like to thank Prof. Gerd Bicker for supervising and reviewing my thesis. Thanks for all the patience, encouragement, and time. Thank you very much for open doors and ears at any time, not only for problems concerning my dissertation.

Thanks to Michael Stern for sharing knowledge and enthusiasm with me, for countless ideas, and sometimes lively discussions. I will give the receipt for Schoko-Kipferl to your family, promised.

Saime Tan and all other members of the lab group, now and former ones, for providing help and encouragement. Thank you all for having such a good time in science and social life.

Thanks to Ina Fischer for introducing me to western blotting tricks.

To Deborah, Ina, Kirsten, Markus, Yvonne, and Zeynep many thanks for having a good time in Hannover – although it wasn't Bremen.

Lots of thanks to my family. I could not have done all this without your help and confidence. Thanks to Harald, that I did not become a vet.

Last but not least, many thanks to Arndt.

Lebenslauf

PERSÖNLICHE DATEN

Name: Knipp, Sabine
Adresse: Daimlerstr. 18, 30165 Hannover
Telefon: 0511-1673796
Staatsangehörigkeit: deutsch
Geburtsdaten: 14. 11. 1972 in Siegen

Schulische Ausbildung/Studium

August/1979 – Juni/1983 **Grundschule Oberdielfen / Wilnsdorf-Niederdielfen**

August/1983 - Juni/1992 **Gymnasium am Löhrtor / Siegen**
Abitur, Note: 2,5

Oktober/1992 - März/1993 **Philipps Universität Marburg / Biologie, Diplom**

April/1993 - Januar/2003 **Universität Bremen / Biologie, Diplom**
Abschluss: Diplom, Gesamtnote: 1 -Sehr gut-

Thema der Diplomarbeit

Ontogenetische Untersuchung zur Darstellung und Auswertung proliferierender Zellen im embryonalen und frühen postembryonalen Gehirn des Zebrafischlings *Danio rerio* durch den immunohistochemischen Nachweis des Proteins PCNA.

Betreuer: PD Dr. Mario F. Wullimann, Institut für Hirnforschung (jetzt LMU München)

Oktober/1996 - März/2003 **Universität Bremen / Geologie, Diplom**
Zweitstudium

Beruflicher Werdegang

Januar/2004 - Mai/2009 **Tierärztliche Hochschule Hannover**, Physiologisches Institut, Abt. Zellbiologie (Prof. G. Bicker)

Mai/2003 - September/2003 **MPI für Experimentelle Endokrinologie (AG Bauer) / Hannover**
Laborpraktikum: experimentelle Neuroentwicklung bei Mäusen

September/2000 - April/2003 **MPI für Marine Mikrobiologie (Bio-Geochemie) / Bremen**
Studentische Hilfskraft Sedimentlabor

1995 - 2002 **Universität Bremen**
Studentische Hilfskraft in der Praktikumsbetreuung, Tutorien für Erstsemester

Präsentationen

Knipp, S. und Bicker, G. 2009. Carbon monoxide organises NO-dependent neuronal chain migration. Posterpräsentation auf dem 8. Treffen der Neurowissenschaftlichen Gesellschaft, Göttingen.

Knipp, S. und Bicker, G. 2008. The messenger molecule CO organises NO-dependent neuronal chain migration in an insect embryonic nervous system. Posterpräsentation auf dem 6. FENS Forum 2008, Genf, Fens Forum Abstr., vol. 4, 041.19, 2008.

Knipp, S. und Bicker, G. 2007. Neuronal cell migration in an insect embryo. Posterpräsentation auf 7. Treffen der Neurowissenschaftlichen Gesellschaft, Göttingen.

Knipp S. und Bicker G. 2006. The gaseous messenger molecules CO and NO regulate neuronal cell migration in an insect embryo. Posterpräsentation auf dem 5. FENS Forum 2006, Wien, FENS Forum Abstracts A122.14.

Publikationen

Knipp, S. and Bicker, G. 2009. Regulation of enteric neuron migration by the gaseous messenger molecules CO and NO. *Development* 136, pp. 85-93.

Stern, M., Knipp, S., Bicker, G. 2007. Embryonic differentiation of serotonin-containing neurons in the enteric nervous system of the locust (*Locusta migratoria*). *J. Comp. Neurol.* 501, pp. 38-51.

Wullimann, M.F. and Knipp, S. 2000. Proliferation pattern changes in the zebrafish brain from embryonic through early postembryonic stages. *Anat. Embryol.* 202, pp. 385-400.

Hannover, 13. Mai 2009

Eidesstattliche Erklärung

Erklärung zur Dissertation

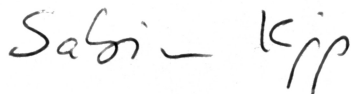
Hierdurch erkläre ich, dass die Dissertation

Neuronal migration and differentiation in the developing locust enteric nervous system.

selbstständig verfasst und alle benutzten Hilfsmittel sowie evtl. zur Hilfeleistung herangezogene Institutionen vollständig angegeben wurden.

Die Dissertation wurde nicht schon als Diplom- oder ähnliche Prüfungsarbeit verwendet.

Hannover, den 13. 05. 2009



(Unterschrift)

Name: Sabine Knipp